Synergistic roles of Aquaporin 5 and Intra- and Extracellular Carbonic Anhydrases in promoting CO_2 Diffusion across the *Xenopus* Oocyte Plasma Membrane

Deng-Ke Wang[1], Fraser J. Moss[1], and Walter F. Boron[1-3‡]

[1]Department of Physiology and Biophysics, [2]Department of Medicine, and
[3]Department of Biochemistry
Case Western Reserve University School of Medicine,
Cleveland, OH 44106, USA

Key words: intracellular pH, cell-surface pH, pH-sensitive microelectrodes, Fick's law, gas channels

Running Head: AQP5 and CA synergism in transmembrane CO_2 diffusion

For submission to: *The Journal of Physiology*

‡ **Address correspondence to: Walter F. Boron**

Department of Physiology and Biophysics
Case Western Reserve University School of Medicine
10900 Euclid Ave. Robbins Building E524
Cleveland, OH 44106-4970
Tel: 216-368-3400
E-mail: walter.boron@case.edu

Key Points

- According to Fick's law, transmembrane CO_2 flux (J_{CO_2}) is the product of membrane permeability (P_{M,CO_2}) and transmembrane concentration gradient ($\Delta[CO_2]$): $J_{CO_2}=P_{M,CO_2}\times\Delta[CO_2]$. Previous work separately showed that (1) human aquaporin-5 (hAQP5) enhances P_{M,CO_2}, and (2) intracellular and (3) extracellular carbonic anhydrases (CAs) enhance $\Delta[CO_2]$ by consuming accumulated or replenishing lost CO_2. We now examine interactions among #1–#3.
- We assess CO_2 fluxes—produced by addition/removal of extracellular CO_2/HCO_3^-—using microelectrodes to monitor extracellular-surface pH (pH_S) and intracellular pH (pH_i) of *Xenopus* oocytes heterologously expressing hAQP5, injected with human CA II (hCA II), and/or exposed to extracellular bovine CA (bCA).
- Enhancing effects on CO_2 fluxes are synergistic among hAQP5, hCA II, and bCA, any of which can become rate limiting, depending on the status of the other two.
- CO_2/HCO_3^- addition transiently increases pH_S (ΔpH_S), hCA II augments ΔpH_S ($\Delta\Delta pH_S$), and hAQP5 enhances $\Delta\Delta pH_S$ ($\Delta\Delta\Delta pH_S$)—a novel tool to assess potential CO_2 channels.

Abstract

CO_2 diffusion across plasma membranes depends on both membrane CO_2 permeability (P_{M,CO_2}) and transmembrane CO_2 concentration gradient ($\Delta[CO_2]$)—Fick's law. Human aquaporin-5 (hAQP5) accelerates CO_2 diffusion by increasing P_{M,CO_2}, whereas carbonic anhydrases (CAs) accelerate CO_2 diffusion by enhancing CO_2 consumption/production and thus $\Delta[CO_2]$. Here, we systematically assess functional interactions among a gas channel and intra-/extracellular CAs. On Day 1, we inject *Xenopus* oocytes with cRNA encoding hAQP5 (control: H_2O). On Day 4, we inject hCA II protein in "Tris" buffer (control: "Tris"). We assess CO_2 fluxes by introducing extracellular 1.5% CO_2/10 mM HCO_3^- and using microelectrodes to measure (1) maximal extracellular-surface pH increase ΔpH_S, (2) maximal rate of pH_S relaxation $(dpH_S/dt)_{Max}$, and (3) maximal rate of intracellular-pH decrease $(dpH_i/dt)_{Max}$. By itself, hCA II minimally increases ΔpH_S—measured "trans" to added cytosolic CA (CA_i)—even at highest doses (100 ng/oocyte). However, hAQP5 alone triples ΔpH_S, an effect further doubled by increasing hCA II. By itself, bovine erythrocyte CA (bCA) in the extracellular fluid doubles $(dpH_i/dt)_{Max}$ magnitude—measured "trans" to added extracellular CA (CA_o)—an effect further doubled by hAQP5. Note: pH measurements "cis" to added CAs—pH_S for bCA, $(dpH_i/dt)_{Max}$ for hCA II—are overwhelmed by enzymatically-produced/consumed H^+, and cannot provide intuitive insight into CO_2 fluxes. Our "trans" pH measurements: (1) confirm synergy between CA_o and CA_i; establish synergy between hAQP5 and both (2) CA_o and (3) CA_i; and show that enhancement of ΔpH_S by CA_i ($\Delta\Delta pH_S$) is a useful tool for assessing CO_2 permeability of membrane proteins (e.g., hAQP5).

Introduction

Aquaporins (AQPs) are integral membrane proteins named for their ability to conduct H_2O across biological membranes. The AQPs occur ubiquitously across all kingdoms of life (King *et al.*, 2004; Maurel *et al.*, 2015; Ishibashi *et al.*, 2017; Ni *et al.*, 2017). To date, the cDNAs encoding 13 human AQPs have been cloned and characterized (for review, see Li and Wang, 2017). One can divide them into three groups, based on whether or not they can conduct glycerol in addition to H_2O. The first group—the classical aquaporins—comprises AQP0, 1, 2, 4, 5, 6, and 8. Although some classical aquaporins are also permeable to urea (AQP6 and AQP8) or ions (AQP6), all of them have a high permeability to H_2O. The second group—the aquaglyceroporins—includes AQP3, 7, 9 and 10 (Ishibashi *et al.*, 1997; Heymann & Engel, 1999; Michalek, 2016; Zhang *et al.*, 2019; Moss *et al.*, 2020). Besides H_2O, they can mediate the diffusion of glycerol, urea, and other non-volatile solutes. Finally, the third group consists of AQP11 and AQP12, which have the lowest homologies to the other aquaporins, and uncertain functions (Ishibashi, 2009; Calvanese *et al.*, 2013).

In addition to conducting H_2O, glycerol, urea, and other small solutes, some AQPs serve as conduits for the highly volatile solutes CO_2 and NH_3 (for review, see Boron, 2010), and probably O_2 (Moss *et al.*, 2025; Occhipinti *et al.*, 2025; Zhao *et al.*, 2025). Nakhoul *et al.*, (1998) and Cooper & Boron, (1998) used the rate of intracellular acidification (dpH_i/dt) to examine the effects of expressing human AQP1 on CO_2 diffusion across the plasma membrane of *Xenopus laevis* oocytes. They were the first to observe that a membrane protein can act as a channel for a dissolved gas. Later, Endeward *et al.*, (2006) confirmed the CO_2 permeability of AQP1 in human red blood cells, using mass spectrometry to monitor the disappearance of $C^{18}O^{16}O$. As part of the Endeward study, Musa-Aziz introduced the technique of using the rapid, transient increase of surface-pH (pH_S)—during the application of CO_2/HCO_3^-—as a semiquantitative index of the CO_2 influx across the oocyte membrane. This pH_S approach is technically simpler than the others, and its use led to the elucidation of the roles that several other AQPs—including AQP5—play as CO_2 channels (Musa-Aziz *et al.*, 2009; Geyer *et al.*, 2013). Mathematical modeling has

provided quantitative insight into the events surrounding CO_2 influx, including the time course of pH_S (Somersalo *et al.*, 2012; Musa-Aziz *et al.*, 2014*a*, 2014*b*; Occhipinti *et al.*, 2014; Calvetti *et al.*, 2020).

Raina *et al.*, (1995) were the first to clone the cDNA encoding AQP5, obtaining the clone from a library of rat submandibular gland. Others localized AQP5 to the apical membrane of acinar cells in secretory glands, such as salivary glands (Nielsen *et al.*, 1997; Ma *et al.*, 1999; Steinfeld *et al.*, 2001; Gresz *et al.*, 2001; Larsen *et al.*, 2011; Yoshimura *et al.*, 2016) and lacrimal glands (Ishida *et al.*, 1997; Tsubota *et al.*, 2001). AQP5 also is present in the apical membranes of secretory cells of pyloric glands and duodenal glands (Parvin *et al.*, 2002; Matsuzaki *et al.*, 2003), as well as sweat glands (Nejsum *et al.*, 2002). In the lung, AQP5 in rats and humans is localized to apical membrane of alveolar type I pneumocytes, but not type II pneumocytes (Nielsen *et al.*, 1997; Funaki *et al.*, 1998; Kreda *et al.*, 2001). However, in mice, AQP5 is present in the apical membranes of both type I and type II pneumocytes (Krane *et al.*, 2001; Matsuzaki *et al.*, 2009). In the kidney, AQP5 co-localizes with pendrin at the apical membrane of β-intercalated cells (β-ICs) that secrete HCO_3^- into the lumen of cortical collecting duct (Procino *et al.*, 2011). In the aforementioned cells, AQP5 presumably plays an important role in transepithelial fluid and electrolyte transport either because of its role as a H_2O channel or, perhaps in the case of β-intercalated cells, as a CO_2 channel that promotes HCO_3^- secretion.

Besides the above glandular tissues, AQP5 is present in astrocytes, where it may play a role during metabolic and traumatic injuries (Chai *et al.*, 2013). In the eye, AQP5 is present in the epithelia layer (Funaki *et al.*, 1998) and stromal keratocytes (Kumari *et al.*, 2012) of the cornea, as well as in the epithelial and fiber cells of the lens (Kumari *et al.*, 2012). In the palmar epidermis, AQP5 is expressed in keratinocytes (Blaydon *et al.*, 2013). In the aforementioned cells and elsewhere in the body, AQP5 could play a role in cell-volume regulation and osmo-sensing.

Governing CO_2 diffusion across a membrane is Fick's law, a simplified and integrated form of which was introduced by Wroblewski (1879):

$$J_{CO_2} = P_{M,CO_2} \cdot \left([CO_2]_o - [CO_2]_i\right) \ . \qquad \textbf{(1)}$$

Here, J_{CO_2} is flux across the membrane, the P_{M,CO_2} is the macroscopic membrane CO_2 permeability, and the term in parentheses indicates the transmembrane CO_2 concentration gradient expressed in terms of bulk extracellular and intracellular.

For our purposes, it is more informative to consider events immediately adjacent to the membrane:

$$J_{CO_2} = P_{M*,CO_2} \cdot \left([CO_2]_{os} - [CO_2]_{is}\right) , \quad \textbf{(2)}$$

where $[CO_2]_{os}$ refers to a thin film of aqueous solution on the outer surface of the plasma membrane, $[CO_2]_{is}$ refers to a thin film on the inner surface, and P_{M*,CO_2} (with an *) is the corresponding permeability.

Eqn (2) better reflects the reaction-diffusion mathematical models to which we refer above. Stated simply, J_{CO_2} depends both on P_{M*,CO_2}, which can be augmented by certain AQPs and other protein channels, and factors that can influence the nanoscopic concentration gradient near the membrane. Among these latter factors are the carbonic anhydrases (CAs), enzymes that reversibly catalyze the hydration of CO_2 and the dehydration of H_2CO_3 (for review, see Boone et al., 2014). Among the 12 enzymatically active human (h) α-carbonic anhydrases (hCA), hCA II has one of the highest catalytic rates (see Purkerson and Schwartz, 2007). It is expressed broadly throughout the body, and is especially abundant in cells that engage in substantial CO_2/HCO_3^- transport, including red blood cells, the renal proximal tubule, and alveolar type I cells (Chen *et al.*, 2008). Moreover, CA II appears to play a role in CO_2 elimination by the lung (Heming *et al.*, 1986; Lien & Lai, 1998; Taki *et al.*, 1999).

A long-established role of CAs is in the facilitated diffusion of CO_2 within a single compartment (for review, see Occhipinti and Boron, 2019). In the case of transmembrane CO_2 diffusion, when CA is present on both sides of an artificial membrane, the CA can replenish depleted CO_2 on the membrane surface from which CO_2 departs, and consume newly arriving CO_2 on the opposite surface. The result is a magnification of the transmembrane CO_2 concentration gradient on a nano-scale (see Eqn (2)), and thus an increase in transmembrane CO_2 diffusion (Gutknecht *et al.*, 1977). Work from our group on *Xenopus* oocytes—in the absence of exogenously expressed CO_2 channels—has shown that hCA II (in the cytosol) and CA IV (mainly on the extracellular surface) each can enhance transmembrane CO_2 fluxes, and that, together, the

two enzymes produce a supra-additive stimulation (Musa-Aziz *et al.*, 2014*a*, 2014*b*; Occhipinti *et al.*, 2014)—synergism. Moreover, the group quantitatively accounted for these effects using computer simulations based on three-dimensional reaction-diffusion models. Left unanswered is the question of whether CAs can enhance the effect of CO_2 channels (the P_{M*,CO_2} term in Eqn (2)), and vice versa, on transmembrane CO_2 fluxes. In the present study, we use simultaneous measurements of pH_S and intracellular pH (pH_i) to ask whether hAQP5, cytosolic hCA II, and extracellular bovine CA (bCA; from erythrocytes) augment each other's effects in accentuating CO_2 fluxes across *Xenopus* oocyte plasma membranes. We find that the effects of expressing hAQP5 are supra-additive (i.e., synergistic) to those of adding CA to either the intra- or extracellular fluid. Moreover, in experiments in which we measure the increase in cell-surface pH (ΔpH_S) caused by the influx of CO_2, the introduction of CA to the cytosol augments the pH_S increase—a $\Delta\Delta pH_S$—by an amount that CO_2 channels further augment—a $\Delta\Delta\Delta pH_S$. Thus, this $\Delta\Delta\Delta$ approach could be a diagnostic tool for identifying candidate CO_2 channels.

Methods

Ethical approval and animal procedures

The Institutional Animal Care and Use Committee at Case Western Reserve University approved all procedures for the housing and handling of *Xenopus laevis*. Housing, anesthesia and euthanasia were as described by Moss & Boron, (2020).

Physiological solutions

Our ND96 solution comprises 93.5 mM NaCl, 2 mM KCl, 1 mM $MgCl_2$, 1.8 mM $CaCl_2$ and 5 mM HEPES (including ~2.5 mM Na-HEPES after titration of solution pH to 7.50 using NaOH). We adjusted the osmolality to 195±5 mOsm by adding NaCl or H_2O. Our 1.5% CO_2/10 mM $NaHCO_3$ solution was identical to ND96, except that 10 mM $NaHCO_3$ replaced 10 mM NaCl, and we bubbled the solution with 1.5% CO_2/balance O_2. Our ND48—identical to ND96, except contained only 48 mM NaCl—was a hypotonic solution (~100 mOsm) for the osmotic water permeability coefficient (P_f) assay. The 0 Ca^{2+}-normal saline (NRS) solution used during oocyte isolation was as described by Musa-Aziz *et al.*, (2010).

To study the effect of extracellular carbonic anhydrase on CO_2 diffusion, we dissolved bCA purified from bovine erythrocytes (Cat#C3934, Sigma-Aldrich, St. Louis, MO, USA)—a mixture of CA I and CA II—in both the ND96 and 1.5% CO_2/10 mM $NaHCO_3$ solutions of an experiment to achieve a concentration of 0.1 mg/ml (Musa-Aziz *et al.*, 2014*b*).

OR3 medium as described by Musa-Aziz *et al.*, (2010), comprises one sachet of Leibovitz L-15 (Cat#41300, ThermoFisher, Waltham, MA, USA), 100 ml Penicillin-Streptomycin (Cat#15140, ThermoFisher), and 1.785 g HEPES, all dissolved in ~1.6 L of deionized H_2O (dH_2O), with pH titrated to 7.50 and osmolality adjusted to 195±5 mOsm by adding an appropriate volume of dH_2O.

We confirmed all solution osmolalities with a Wescor model 5520 osmometer.

Oocyte preparation

For a description of our approach, see Musa-Aziz et al. (2010) and Parker et al. (2008). Briefly, on Day 0, we anesthetized a frog (female *Xenopus laevis*, NASCO, Fort Atkinson, WI, USA) in 0.2% Tricaine (Cat#A5040, Sigma-Aldrich), surgically removed an ovary from the ventral side of the frog, cut the ovary into small pieces (~0.5 × 0.5 × 0.5 cm), and washed the pieces ×3 with 0 Ca^{2+}-NRS in a 50-ml Falcon tube, using a benchtop end-over-end rotator. We then digested the extracellular matrix of the follicles with 2 mg/ml collagenase (Cat#C5138, Sigma-Aldrich) dissolved in 0 Ca^{2+}-NRS, washed ×3 in 0 Ca^{2+}-NRS, carefully selected stage V and VI oocytes from the processed batch, and then cultured in OR3 medium in an incubator at 18 °C for subsequent injection of complementary RNA (cRNA).

cDNA construct encoding human AQP5

The cDNA encoding human AQP5 (GenBank# NM_001651.4), subcloned into pGH19 vector, was the same construct as used by Qin and Boron (2012). After confirming the sequence, we linearized the cDNA using Xho I (Cat# R0146, New England Biolabs, Ipswich, MA, USA), transcribed it *in vitro* using a mMESSAGE mMACHINE™ T7 capped RNA transcription kit (Cat#AM1344, ThermoFisher). We purified the cRNA using an RNeasy MinElute Cleanup Kit (Cat#74204, QIAGEN, Hilden, Germany), eluted the resulting cRNA with DNase/RNase-free H_2O, quantified the cRNA concentration by measuring peak absorbance at λ=260 nm (A_{260}) and assessed its purity by measuring the ratio of the λ=260 nm vs. λ=280 nm absorbance ($A_{260/280}$) using a NanoDrop 2000 UV spectrophotometer (ThermoFisher), and diluted the cRNA into 1000 ng/µl aliquots, which we stored at –80°C.

Expression in *Xenopus* oocytes

On Day 1, we injected oocytes with 25 ng (25 nl) of cRNA encoding hAQP5, or 25 nl of H_2O as a control. On Day 4, we separated both cRNA-injected and H_2O-injected oocytes into two subgroups, one pair of subgroups for injection with 25 nl containing 1 ng, 10 ng, or 100 ng of hCA II protein purified from human erythrocytes (Cat #C6165, Sigma-Aldrich) dissolved in "Tris" (i.e., 50 mM Tris base, titrated with HCl) at pH 7.40, and the other pair of subgroups for injection with 25 nl of "Tris" as a control.

Electrophysiological measurements

Solution delivery to the chamber

At room temperature, we put each solution into two 140-ml piston syringes (Cat#8881114030, Covidien, Dublin, Ireland) and delivered the solution using a dual syringe pump (Cat#55-2226, Harvard Apparatus, Holliston, MA, USA) at a constant total flow of 4 ml/min. The solutions flowed through Tygon® tubing (4.76 mm OD × 1.59 mm ID, Cat#ACF00003, Saint-Gobain, Courbevoie, France) to minimize the leak of CO_2. We used custom-manufactured 5-way valves (Clippard, Cincinnati, OH, USA) actuated by nitrogen pressure to switch solutions between ND96 and 1.5% CO_2/10 mM $NaHCO_3$. We controlled the nitrogen pressure using electrically activated 4-way solenoid valves (R481, Clippard).

Construction of microelectrodes

We made V_m electrodes from borosilicate tubing (2.00 mm OD × 1.56 mm ID, with filament; Cat#BF200-156-10, Sutter Instrument, Novato, CA, USA), which we pulled on a Sutter puller (model P-97, Sutter Instrument), and filled with 3 M KCl, to achieve a resistance of 0.5 to 1.0 MΩ. For pH_i electrodes, after pulling, we dried the micropipettes at 270°C overnight, treated with *bis*-di-(methylamino)-dimethylsilane (Cat#14755, Sigma-Aldrich) for 20 min, vented the silane vapors, maintained the silanized micropipettes at 270°C overnight, removed them from the oven, filled the tip with H^+ ionophore I-cocktail B (Cat#95293, Sigma-Aldrich), and then filled with backfill solution (see Musa-Aziz et al., 2010). We made pH_S electrodes in a fashion as pH_i electrodes, except that, after pulling the tubing (2.00 mm OD × 1.16 mm ID, without filament; Cat#B200-116-10, Sutter Instrument), we used a microforge to break the micropipette tip to give a final inner diameter of 30 μm. The thicker wall for the pH_S electrodes produces a better tip break, and the lack of the filament stabilizes the H^+ cocktail.

Measurement of pH_S and pH_i

We measured pH_S and pH_i as previously described (Musa-Aziz *et al.*, 2010). Briefly, with all electrodes (see below) in place in the plastic chamber, we placed an oocyte in the chamber, with flowing ND96; X-shaped nylon fibers downstream of the oocyte held the cell in place. We connected the V_m electrode to an OC-725C oocyte clamp (Warner Instruments, Hamden, CT, USA), and the pH_i and pH_S

electrodes to a HiZ-223 amplifier (Warner Instruments). The electrical ground of the chamber was a bath clamp in which the same OC-725C as above connected to (a) a platinum wire in the chamber and (b) a reference electrode (identical to a V_m electrode, but with its tip broken by dragging on paper) that contacted the ND96 downstream from the oocyte. The reference electrode for the pH_S measurements was a longer version of a V_m microelectrode, but with a carefully broken tip, placed downstream from the oocyte, and connected via a plastic electrode holder and calomel half-cell to a model 750 amplifier (WPI, Sarasota, FL, USA). All of the primary electrical signals fed into custom data-acquisition hardware "Ribbit Box" built in-house by Dale Huffman around a LabJack U6Pro device (LabJack, Lakewood, CO, USA) and connected to a Windows-based computer, controlled by custom software "The Frog Whisperer," written in house by Dale Huffman.

Our sampling frequency was 3/s. We obtained the pH_i value by digitally subtracting (in the computer) the V_m signal (voltage) from the pH_i-electrode signal (voltage), and converted the difference to a pH_i value using the electrode-calibration data (see below). We similarly obtained the pH_S value by subtracting the signal of pH_S reference (calomel) from that of the pH_S electrode. The above custom software performed the calculations and displayed the record of all electrical parameters vs. time on a computer monitor.

Calibration of pH electrodes

The first time we used a new pH_S or pH_i electrode—we never used an electrode for more than 1 day—we obtained the electrode slope by using the solution-delivery system (see above) to flow sequentially a pH 6.00 or pH 8.00 buffer (Certified, Cat#SB104-1 and SB112-1, ThermoFisher) through the chamber—before adding the oocyte—and measuring the voltage signal as described above. We accepted an electrode only if it had a slope of at least 55 mV/pH. We flushed the chamber with ND96 before adding the oocyte, and then performed a one-point calibration for each electrode in the ND96 (i.e., we assigned to the subtracted pH_S or pH_i electrode voltage the pH value of 7.50 in the ND96, and used the slope previously measured).

Recording of electrophysiological data

In consecutive fashion, with ND96 flowing in the chamber, we impaled the oocyte with a V_m electrode and a pH_i electrode, and then positioned the tip of the pH_S electrode ~300 μm from the oocyte surface using a precision remote-controlled micro-manipulator (Cat#ROE200, Sutter Instrument), all as previously described (Musa-Aziz *et al.*, 2014*a*). While maintaining the flow of ND96, we advanced the pH_S electrode tip ~300 μm to touch the oocyte surface, and an additional 40 μm to create a slight dimple on the oocyte surface. After 1 min, we switched the solution from ND96 to 1.5% CO_2/10 mM $NaHCO_3$. After several minutes, we retracted the pH_S electrode 340 μm from the oocyte surface for 1 min, in order to obtain a 1-point calibration of the pH_S electrode in the bulk 1.5% CO_2/10 mM $NaHCO_3$ solution. We then re-advanced the pH_S electrode 340 μm to resume pH_S measurements, before switching back to ND96. Finally, after pH_S had stabilized, we retracted the pH_S electrode 340 μm again, to obtain a 1-point calibration in the bulk ND96 solution at the end of the experiment.

Calculation of ΔpHs

With its tip in the bulk ND96 solution, the pH_S electrode detected, by definition, a pH of 7.50 (i.e., the initial ND96 calibration). Once dimpling the membrane with the oocyte exposed to ND96, the pH_S electrode—calibrated for ND96—detected pH_S. The average pH_S over at least the final 30 s—when pH_S was stable—we took as $pH_S(ND96_{Init})$. From the moment that we switched the chamber solution to 1.5% CO_2/10 mM $NaHCO_3$, the initial ND96 calibration of the pH_S electrode was no longer valid, which is why we obtained a new 1-point calibration in 1.5% CO_2/10 mM $NaHCO_3$ (see above); we applied this second CO_2/HCO_3^- calibration to all pH_S data obtained during the CO_2/HCO_3^- exposure, as pH_S rises to a peak and then decays downward. Using this second calibration, we computed the peak pH_S after the switch to CO_2/HCO_3^-, that is, $pH_S(CO_{2,Peak})$. We define the "upward" ΔpH_S for CO_2 addition as $pH_S(CO_{2,Peak}) - pH_S(ND96_{Init})$. At the end of the CO_2/HCO_3^- exposure, the average pH_S over at least the final 30 s—when pH_S was stable—we took as $pH_S(CO_{2,Tail})$. From the moment that we switched the chamber solution to ND96, the previous 1.5% CO_2/10 mM $NaHCO_3$ calibration of the pH_S electrode was no longer valid, which is why we obtained a final (i.e., third) 1-point calibration in ND96 (see above); we applied this final

ND96 calibration to all pH_S data obtained during the final ND96 exposure, as pH_S falls to a trough and then decays upward. Using this third calibration, we computed the lowest pH_S after the switch to ND96, namely, $pH_S(ND96_{Nadir})$. We define the "downward" ΔpH_S for CO_2 removal as $pH_S(ND96_{Nadir}) - pH_S(CO_{2,Tail})$, which is a negative number.

Calculation of "maximal" dpH_S/dt

During CO_2/HCO_3^- addition (e.g., see Figure 1*C*), pH_S rises rapidly from around 7.50 to a peak (where $dpH_S/dt \cong 0$) and then begins to decline, at first slowly (dpH_S/dt is slightly negative), later rapidly (dpH_S/dt reaches a maximally negative value), and finally more slowly again (dpH_S/dt gradually becomes less and less negative) as pH_S relaxes towards an asymptotic value around 7.50. During CO_2/HCO_3^- removal, the changes are in the opposite direction. Here we describe the analysis for CO_2/HCO_3^- addition, but the approach is similar for CO_2/HCO_3^- removal. Using software written in house by Dale Huffman, we obtain a running linear fit of (pH_S, time) data points to generate a plot of $(dpH_S/dt)_{Running}$ vs. time, which allows us to identify the time (which we define as local time: $t_{Local} = 0$) of the maximally negative dpH_S/dt (i.e., minimal dpH_S/dt). We then obtain a double-exponential (DExp) fit of the (pH_S, time) data points, beginning at $t_{Local} = 0$ and extending to the time when we removed the pH_S electrode from the cell surface to the bECF (for calibration). Finally, we evaluate the derivative of the DExp function at $t_{Local} = 0$, and take this value as $(dpH_S/dt)_{Max}$. During CO_2/HCO_3^- addition, this value is negative (i.e., maximal rate of pH_S descent), and during CO_2/HCO_3^- removal (e.g., see Figure 1*C*), this value is positive (i.e., maximal rate of pH_S rise).

Calculation of "maximal" dpH_i/dt

After either the addition or removal of CO_2/HCO_3^-, we define $(dpH_i/dt)_{Max}$ as the fastest change of pH_i, which occurs several seconds after the new solution reaches the oocytes (Musa-Aziz *et al.*, 2014*a*). For CO_2/HCO_3^- addition, pH_i decreases and thus the "downward" $(dpH_i/dt)_{Max}$ is a negative number; upon CO_2/HCO_3^- removal the "upward" $(dpH_i/dt)_{Max}$ is positive. After identifying, by eye, the time of fastest pH_i change (i.e., corresponding to the most extreme local value of dpH_i/dt), we used Origin 2024 to obtain $(dpH_i/dt)_{Max}$ by a linear fit over the next ~10 s of (pH_i, time) data.

Calculation of intrinsic intracellular buffering power

We define initial pH_i in ND96 solution—$pH_i(ND96_{Init})$—as the average of at least 90 data points over a period (i.e., 30 s) when the experimenter (in real experimental time) judged pH_i to be stable, just before switching from ND96 to the CO_2/HCO_3^- solution. Similarly, we defined the final pH_i in the CO_2/HCO_3^- solution—$pH_i(CO_{2,Tail})$—as the average of at least 90 data points over a period when the experimenter (in real experimental time) judged pH_i appeared stable, just before switching from the CO_2/HCO_3^- solution to ND96. During CO_2/HCO_3^- application, we define ΔpH_i (a negative number) as $pH_i(CO_{2,Tail}) - pH_i(ND96_{Init})$.

Based on the decrease in steady-state pH_i produced by the aforementioned application of CO_2/HCO_3^-, we calculated the intrinsic intracellular buffering (Boron, 1977) power β_I (mM/pH) of oocytes using the following equation:

$$\beta_I = -\frac{\Delta[HCO_3^-]_i}{\Delta pH_i} \quad .$$

Here, the negative sign arises because we are observing a pH_i decrease produced by an intracellular, CO_2-induced acid load. Because we impose the acid load by the introduction of CO_2/HCO_3^-, followed by the intracellular reaction $CO_2 + H_2O \rightarrow H^+ + HCO_3^-$, the magnitude of the acid load is $\Delta[HCO_3^-]_i$ (for a discussion, see Roos and Boron, 1981). Because we assume that $[HCO_3^-]_i$ is 0 before the exposure to CO_2/HCO_3^-, $\Delta[HCO_3^-]_i$ (a positive number) is the same as the final $[HCO_3^-]_i$ after the introduction of CO_2/HCO_3^-, determined at a time when pH_i is stable. Because we observed no pH_i recovery during the CO_2/HCO_3^- exposure, nor a pH_i overshoot after the removal of CO_2/HCO_3^-, we can conclude that net acid extrusion during the CO_2/HCO_3^- exposure was negligible (Boron & De Weer, 1976). Thus, we computed the final $[HCO_3^-]_i$ using $pH_i(CO_{2,Tail})$. Because we used 1.5% CO_2/10 mM HCO_3^- at a pH of 7.5,

$$[HCO_3^-]_i = [CO_2]_i \cdot 10^{pH_i - 7.50} \quad .$$

Here we assume that $[CO_2]_i = [CO_2]_o$, where the subscript "o" denotes the bulk extracellular fluid, and that the pK_a in the intracellular fluid is the same as in the extracellular fluid.

Measurement of P_f

After recording the pH_S and pH_i, we saved the oocyte, equilibrated it in ND96 for at least 10 min, transferred it to a petri dish containing the hypotonic solution ND48 and a 1.6-mm diameter steel sphere (i.e., a ball bearing), placed the dish under a dissecting microscope (model Stemi 508, ZEISS, Oberkochen, Germany) equipped with a video camera (OptixCam summit series, Microscope LLC , Roanoke, VA, USA) connecting to a computer running proprietary software, and recorded 1 image/s of the swelling oocyte and the nearby steel sphere for 1 min. We used Image J software (U. S. National Institutes of Health, Bethesda, Maryland, USA, https://imagej.nih.gov/ij) to determine the perimeter of the oocyte at each time point, computed the projection area (using the steel sphere as an area standard), computed the oocyte volume (assuming the oocyte to be a sphere), and used the following equation to calculate osmotic water permeability:

$$P_f = \frac{V_0 \cdot \frac{d(V/V_0)}{dt}}{S \cdot \Delta Osm \cdot V_w}$$

Here, V_0 is the initial oocyte volume, $d(V/V_0)/dt$ is the rate of volume increase during the first minute, ΔOsm is the osmotic gradient across the membrane (i.e., 195 mOsm – 100 mOsm), V_W is the molar volume of water (18 ml/molar), and S is the oocyte surface area, assumed to be 8-fold greater than the idealized area (Chandy *et al.*, 1997).

Statistical analysis

We present data as mean ± SD. To compare the difference between 2 or more groups, we use a one-way ANOVA followed by the Tukey post-hoc analysis. We perform the analyses using Origin 2024, considering $P<0.05$ as significant.

To compare means of analyzed parameters of oocytes exposed to bECF lacking bCA (gray, black, light- and dark-blue bars in Figure 3 *A–D*) with oocytes for which the bECF contained bCA (Figure 8*A–D*), we perform a one-way ANOVA with Tukey's means comparisons. In Statistics Tables 8*E–H*, we

present descriptive statistics and means comparisons to determine the statistical significance of bCA-dependent differences.

To compare mean values of various other parameters—initial pH_i, ΔpH_i, β_I, and P_f—from oocytes not exposed to bCA (gray, black, light- and dark-blue bars in Figure 6*A–D*) with their counterparts exposed to bCA (Figure 10*A–D* (bECF +bCA), we use the same approach described in the previous paragraph. In Statistics Tables 10*E–H*, we present descriptive statistics and means comparisons to determine the statistical significance of bCA-dependent differences.

In Figure 11 we determine the mean $\Delta\Delta pH_{S,Base}$ by subtracting the mean ΔpH_S for –hAQP5/–hCA II oocytes from each measured ΔpH_S of –hAQP5/+hCA II oocytes. We determine the mean $\Delta\Delta pH_{S,hAQP5}$ by subtracting the mean (ΔpH_S) for +hAQP5/–hCA II oocytes from each measured ΔpH_S of +hAQP5/+hCA II oocytes. We then performed a one-way ANOVA followed by the Tukey post-hoc analysis on the data for $\Delta\Delta pH_{S,Base}$ vs. $\Delta\Delta pH_{S,hAQP5}$.

In Figure 12 we determine the mean $\Delta(dpH_i/dt)_{Max,Base}$ by subtracting the mean $(dpH_i/dt)_{Max}$ for –hAQP5/–bCA oocytes from each measured $(dpH_i/dt)_{Max}$ of –hAQP5/+bCA oocytes. We determine the mean $\Delta(dpH_i/dt)_{Max,hAQP5}$ by subtracting the mean $\Delta(dpH_i/dt)_{Max}$ for +hAQP5/–bCA oocytes from each measured $\Delta(dpH_i/dt)_{Max}$ of +hAQP5/+bCA oocytes. We then perform a one-way ANOVA followed by the Tukey post-hoc analysis on the data for $\Delta(dpH_i/dt)_{Max,Base}$ vs. $\Delta(dpH_i/dt)_{Max,hAQP5}$.

Results

General protocol

Figure 1*A* and *B* are schematic representations suggesting how hAQP5, cytosolic hCA II, and extracellular bCA, would affect the influx (panel *A*) or efflux of CO_2 (panel *B*) and thus pH_S and pH_i of an *Xenopus* oocyte. Imagine that we switch the solution—the bulk extracellular fluid (bECF[1])—that flows through our chamber from one that nominally lacks, to one that contains CO_2/HCO_3^-. Imagine also that we have a cell whose membrane is initially impermeable to CO_2 and HCO_3^-. Thus, a short time after we switch solutions, CO_2 and HCO_3^- will have diffused throughout the system so that $[CO_2]$ and $[HCO_3^-]$ will be uniform through the bECF (an "infinite reservoir") and extracellular unconvected fluid (EUF), including a thin layer of fluid at the oocyte surface (S). Suddenly, we now increase P_{M,CO_2}, which is where Figure 1*A* picks up the narrative. Now CO_2 diffuses into the cell (Figure 1*A*), leading to the depletion of CO_2 at the cell surface. The replenishment of this surface CO_2 occurs via both CO_2 diffusion from bECF and—especially adjacent to the cell surface—the reaction $HCO_3^- + H^+ \rightarrow CO_2 + H_2O$. The reaction causes a rise in pH_S, the maximum magnitude of which is ΔpH_S; assuming that cell-surface CA activity is fixed, ΔpH_S is a semiquantitative index of the CO_2 influx (see Eqn (2)). Meanwhile, beneath the membrane, the CO_2 that has entered the cell undergoes the reaction $CO_2 + H_2O \rightarrow H^+ + HCO_3^-$, thus causing a fall in pH_i. The maximal rate of intracellular acidification—assuming that cytosolic CA activity is fixed—is also an index of the CO_2 influx. However, $(dpH_i/dt)_{Max}$ is a far less sensitive measure than ΔpH_S (Musa-Aziz *et al.*, 2014*b*).

If we nominally remove CO_2/HCO_3^- from the solution flowing through the chamber, all of the above processes, including pH_S and pH_i changes reverse (Figure 1*B*).

Figure 1*C* shows typical pH_S and pH_i records of a control oocyte—that is, one injected with H_2O (rather than cDNA dissolved in H_2O encoding hAQP5) on Day 1, and then "Tris" (rather than hCA II

[1] For simplicity, we refer to concentrations in the bECF using the subscript "o".

dissolved in "Tris") on Day 4—during the application and removal of CO_2/HCO_3^-. No bCA is present in the bECF. The shaded vertical bars represent periods of time during which the pH_S electrode is ~300 µm from the cell surface, in the bECF, for electrode calibration. At other times (i.e., between shaded bars), the electrode tip dimples the oocyte surface. Switching the solution from ND96 to 1.5% CO_2/10 mM $NaHCO_3$ causes an upward pH_S transient that soon reaches a maximum (left upward red arrow), and a pH_i decrease, the maximum rate of which is indicated by the left dashed line. The pH_S signal (after the pH_S peak) relaxes and pH_i signal declines with similar time constants (Musa-Aziz *et al.*, 2014*a*, 2014*b*; Occhipinti *et al.*, 2014). Later, we switch the solution back to ND96, which elicits a reversal of the previous events. In Methods and the figure legend, we define the red and green labels shown in Figure 1*C*.

In the following eight sections, we describe the effects—on various parameters measured during our standard protocol in Figure 1*C*—of various combinations of human AQP5 expressed or not (±hAQP5), human CA II injected or not (±hCA II), and bovine CA added to the bulk extracellular fluid or not (±bCA). In the first four sections, we examine oocytes in the absence of bCA, but with various combinations of ±hAQP5 and ±hCA II. In the second group of four, we study oocytes in the presence of extracellular bCA.

±hAQP5[2] in absence of exogenous CAs: Effects on ΔpH_S & $(dpH_i/dt)_{Max}$

Our overall goal is to investigate the relative roles of hAQP5, cytosolic hCA II, and extracellular bCA in promoting CO_2 fluxes across the plasma membrane of a *Xenopus* oocyte. In this first section, we begin by verifying previous data that addressed the role of hAQP5 in promoting CO_2 diffusion in the absence of added CAs. We injected oocytes on Day 1 with either "H_2O" or H_2O + cRNA encoding "hAQP5" and then, on Day 4, with "Tris" (as a control for "Tris + hCA II").

pH_S The red record in Figure 2*A* shows the pH_S data for a representative "H_2O + Tris" oocyte. The red record in Figure 2*B* shows the comparable data for an "hAQP5 + Tris" oocyte. Consistent with

[2] Here, ±hAQP5 indicates that experiments in this section compare pH responses in the absence vs. presence of hAQP5.

previous results (Musa-Aziz *et al.*, 2009; Geyer *et al.*, 2013), the expression of hAQP5 leads to pH_S transients that are substantially greater in magnitude—both with the addition of CO_2/HCO_3^- (0.101 vs. 0.028) and with the removal of CO_2/HCO_3^- (–0.129 vs. –0.032)—than the mere injection of H_2O into the oocytes (red records in Figure 2*A* vs. *B*).

Summary. For a larger number of these oocytes studied in the absence of both hCA II and bCA, the bars in Figure 3*A* provide the mean ΔpH_S data for CO_2/HCO_3^- addition in the absence (gray) and presence (black) of hAQP5, respectively. The gray and black bars in Figure 3*B* summarize the corresponding data for CO_2/HCO_3^- removal.

Conclusions. From the statistical analysis of the data summarized in Figure 3*A,B*, we conclude that—in the absence of both hCA II and bCA, both for CO_2/HCO_3^- addition and removal—expression of hAQP5 increases the magnitude of ΔpH_S.

Interpretation: ΔpH_S (gray vs. black bars) in Figure 3A,B; ±hAQP5, –hCA II, –bCA. Expression of hAQP5 increases P_{M,CO_2} in Eqn (1).

dpH_i/dt The green records in Figure 2*A* and *B* show the pH_i data that correspond to the pH_S data presented above. The expression of hAQP5 does not produce a remarkable change in either the downward or upward $(dpH_i/dt)_{Max}$.

Summary. The gray and black bars in Figure 3*C* show the mean downward $(dpH_i/dt)_{Max}$ for CO_2/HCO_3^- addition, ±hAQP5—in the absence of both hCA II and bCA. The bars in Figure 3*D* show the analogous data for CO_2/HCO_3^- removal.

Conclusions. With either CO_2/HCO_3^- addition or removal—in the absence of injected hCA II and extracellular bCA—the expression of hAQP5 does not significantly affect $(dpH_i/dt)_{Max}$.

Interpretation: $(dpH_i/dt)_{Max}$ (gray vs. black bars) in Figure 3C,D; ±hAQP5, –hCA II, –bCA. (1) Expression of hAQP5, even though it markedly increases P_{M,CO_2} as indicated by the ΔpH_S signals in Figure 3*A,B*, does not increase the magnitude of $(dpH_i/dt)_{Max}$. The reason, in part, is that—without hCA II—the cytosolic CO_2 hydration reaction (during CO_2 influx) and dehydration reaction (during CO_2 efflux) are

rate limiting, thereby limiting the transmembrane CO_2 gradient and choking the CO_2 fluxes (see Eqn (2)). In the second half of Results, we will see that the availability of CO_2 on the outer surface of the cell (replenished/consumed by bCA) also is rate limiting under the conditions of Figure 2*A,B*. (2) Thus, $(dpH_i/dt)_{Max}$ is a relatively insensitive indicator of CO_2 fluxes in the absence of bCA in the bECF. And (3) a contributing factor may be the large diameter of oocytes (~1.2 mm); a prolonged time for diffusion to/from the center of the cell limits the dynamic range of $(dpH_i/dt)_{Max}$. Note that, in the hands of Nakhoul et al. (1998) and Cooper & Boron, (1998), AQP1 expression did not produce a statistically significant effect on $(dpH_i/dt)_{Max}$ under similar experimental conditions (i.e., in the absence of injected CA enzyme, and with vitelline membrane intact).

±hAQP5, ΔhCA II, –bCA[3]: Effects on ΔpH_S & $(dpH_i/dt)_{Max}$

To explore the interaction between hAQP5 and intracellular CA (CA_i) in the diffusion of CO_2, we injected oocytes on Day 1 with either "H_2O" or "H_2O + cRNA encoding hAQP5" and then, on Day 4, we injected oocytes with either "Tris" as a control, or "Tris + hCA II" at hCA II levels of 1, 10 or 100 ng.

pHs The red record in Figure 2*C* shows the pH_S data for a representative "H_2O + 1 ng hCA II" oocyte and, in Figure 2*D*, the comparable data for an "hAQP5 + 1 ng hCA II" oocyte. Comparing the pH_S records between Figure 2*C* vs. Figure 2*A*, we see that—in the absence of hAQP5—the addition of 1 ng hCA II appears to increase the magnitude of the pH_S transient slightly. Musa-Aziz et al. (2014a) had previously observed that hCA II—presumably with a higher specific activity—significantly increases the magnitude of ΔpH_S with both CO_2/HCO_3^- addition and removal. If we compare Figure 2*D* vs. Figure 2*B*, we see that—in the presence of hAQP5—the injection of 1 ng hCA II has a much larger effect on the pH_S transient. Finally, comparing Figure 2*D* vs. Figure 2*C*, and Figure 2*B* vs. Figure 2*A*, we see that the hAQP5

[3] Here, "Δ" indicates that, in this section, we compare a series of injected doses of hCA II; "–bCA" indicates that extracellular bCA was absent in all experiments.

expression has a far greater effect on augmenting the magnitude of ΔpH_S—both with CO_2/HCO_3^- addition and removal—with the injection of 1 ng hCA II than with no added hCA II.

Note that, in the above comparisons, the pH_S electrode is "trans"—or on the opposite side of the membrane—with respect to the hCA II that we added to the cytosol, a concept developed by Musa-Aziz et al. (2014a, 2014b) and Occhipinti et al. (2014). In such cases, one can conclude by intuition—but supported by mathematical simulations—that the trans-side increase in ΔpH_S is indicative of an increased CO_2 flux when hCA II is present in the cytosol. Thus, based on Figure 2*A–D*, we can conclude that both the expression of hAQP5 alone (a large effect) and the injection of hCA II alone (a small effect), and especially the two in combination, increase CO_2 fluxes into/out of oocytes.

Examining the effects of injecting larger amounts of hCA II, we continue to see—in the absence of hAQP5—very little effect on the pH_S transients (Figure 2*E,G*) compared to the "Tris" control (Figure 2*A*). In the presence of hAQP5, the higher levels of injected hCA II (Figure 2*F,H*) continue to enhance the pH_S transients greatly compared to the "AQP5 + Tris" control (Figure 2*B*), but the stimulatory effect is little more than with our 1 ng dose of hCA II (Figure 2*D*).

In their earlier work, Musa-Aziz et al. (2014a) observed a baseline ΔpH_S (i.e., no injected CA) of slightly more than 0.04, whereas in the present study, our baseline ΔpH_S is only ~0.03. Thus, the baseline values of CO_2 permeability, surface CA activity, or cytosolic CA activity in that previous study may have been somewhat greater than in the present study. Moreover, Musa-Aziz et al. (2014a) found that injecting 300 ng of recombinant hCA II approximately doubled the ΔpH_S, whereas in the present study injecting 100 ng hCA II enzyme (a dose at which the ΔpH_S seemingly had already plateaued) increased ΔpH_S only by about 1/3 (compare Figure 2*G* vs. *A*). We presume that our commercially obtained hCA II, purified from red blood cells (RBCs), had a lower specific activity than the recombinant hCA II in the previous study. We abandoned attempts at injecting >100 ng/oocyte because these higher doses seemed to have deleterious effects on the oocytes, perhaps because of contaminants.

Summary. The lighter-colored blue, red and green bars in Figure 3*A* display the mean ΔpH_S data for CO_2/HCO_3^- addition with increasing doses of hCA II, all in the absence of hAQP5 and bCA. The darker

bars in Figure 3*A* summarize comparable data, but in the presence of hAQP5. For CO_2/HCO_3^- removal, Figure 3*B* reveals patterns that are similar to those in Figure 3*A*.

Conclusions. For oocytes examined in the absence of bCA, both for the addition and removal of CO_2/HCO_3^-: (a)[4] Expressing hAQP5 (darker vs. lighter bars) increases the magnitude of ΔpH_S at every level of injected hCA II. (b) In the absence of hAQP5 (lighter bars), injecting oocytes with increasing amounts of hCA II, despite a modest upward trend, does not have a statistically significant effect on ΔpH_S magnitudes, neither for CO_2/HCO_3^- addition nor removal. And (c) in the presence of hAQP5 (darker bars), injection of increasing amounts of hCA II tends to cause graded increases of ΔpH_S magnitudes, both for CO_2 influx and efflux. Relative to no injected hCA II, the effects reach statistical significance at all three levels of injected hCA II, although these three bars are not significantly different from each other.

Interpretation: ΔpH_S (colorful bars) in Figure 3A,B; ±hAQP5, ΔhCA II, –bCA. (1) In the absence of hAQP5 (4 lighter bars), P_{M,CO_2} is the major rate-limiting factor in both directions of CO_2 diffusion, and at all hCA II levels. Expression of hAQP5 augments P_{M,CO_2} and thereby increases ΔpH_S (4 darker bars). (2) During CO_2/HCO_3^- addition in control cells (–hAQP5, –hCA II; gray bars), disposal of incoming CO_2 (in this case by cytosolic CA) is borderline rate limiting (i.e., with greater CA_i activity, the flux would have been modestly greater), as noted previously by Musa-Aziz et al. (2014a). Conversely, during the subsequent CO_2/HCO_3^- removal, replenishment of outgoing CO_2 (here, by hCA II), likewise, is borderline rate limiting. And (3) as we will see below in our presentation of data on bCA in the bECF, for control cells (gray bars), the replenishment of CO_2 on the extracellular surface is also rate limiting during CO_2 influx. Conversely, disposal of exiting CO_2 at the cell surface during CO_2 efflux is also rate limiting. (4)

[4] In lists of points in the Summary and Conclusion, we use (a), (b), (c) … . The (a) in one list corresponds to the (a) in another list, etc. However, in the Interpretation, we list points as (1), (2), (3) … because the interpretations do not necessarily correspond to lettered points in a one-to-one fashion.

The greater effect of expressing hAQP5 in oocytes injected with 1 ng of hCA II (light- vs. dark-blue bars) than in oocytes injected only with "Tris" (gray vs. black bars) is an example of synergism.

dpH_i/dt The green records in Figure 2*C,E,G* and *D,F,H* show the pH_i data that correspond to the pH_S data presented above, with incremental amounts of injected hCA II, without hAQP5 (left side of Figure 2) and with hAQP5 (right side). We observe that injecting even 1 ng hCA II into the cytosol produces a striking increase in $(dpH_i/dt)_{Max}$, both for CO_2/HCO_3^- application and removal. Increasing the injected hCA II to 10 ng further increases the downward $(dpH_i/dt)_{Max}$ but has only a modest effect on the upward $(dpH_i/dt)_{Max}$ in this example. Increasing injected hCA II to 100 ng has no additional effect. Comparing the left and right sides of Figure 2, we see that hAQP5 expression seemingly has little effect on downward or upward $(dpH_i/dt)_{Max}$, regardless of the amount of injected hCA II.

Note that, in the above $(dpH_i/dt)_{Max}$ analyses, the pH_i electrode is "cis"—or on the same side of the membrane—with respect to the hCA II that we added to the cytosol, again, a concept developed by Musa-Aziz et al. (2014a, 2014b) and Occhipinti et al. (2014). In such cases, one cannot use intuition to arrive at conclusions that the cis-side acceleration of a pH_i change by hCA II is indicative of an increased CO_2 flux. The reason is that—near the intracellular surface of the plasma membrane—the added hCA II greatly accelerates H^+ formation during CO_2 influx, and H^+ consumption during CO_2 efflux. The pH_i electrode directly senses the changes in $[H^+]$, which only indirectly reflect CO_2 fluxes. However, previous mathematical simulations predict that the CO_2 fluxes must have increased under these conditions (Musa-Aziz et al. (2014a) and Occhipinti et al. (2014).

Summary. The lighter/darker pairs of bars (–/+ hAQP5) in Figure 3*C,D* précis the mean $(dpH_i/dt)_{Max}$ data for CO_2/HCO_3^- addition and removal.

Conclusions. Both for CO_2/HCO_3^- addition and removal: (a) Expression of hAQP5 does not significantly affect $(dpH_i/dt)_{Max}$ at any level of injected hCA II (4 sets of lighter vs. darker bars). And (b) in the absence of hAQP5 (4 lighter bars), increasing amounts of injected hCA II cause $(dpH_i/dt)_{Max}$ values to trend toward greater magnitudes. However, the effects do not reach statistical significance (vs. 0 ng) until 10 and 100 ng; the lighter blue, red, and green bars are not significantly different from one another.

Interpretation: $(dpH_i/dt)_{Max}$ (colorful bars) in Figure 3C,D; ±hAQP5, ΔhCA II, –bCA. (1) Because the injected hCA II is "cis" to the pH_i electrode, we cannot draw intuitive conclusions about CO_2 fluxes as we compare the gray $(dpH_i/dt)_{Max}$ bar (i.e., –hAQP5) to the other three light-colored bars (i.e., increasing amounts of hCA II), or as we compare the black bar (i.e., +hAQP5) to the other three darker-colored bars. (2) Expression of hAQP5 (compare lighter- vs. darker-blue, red, and green bars) does not increase $(dpH_i/dt)_{Max}$ magnitudes. As noted in our interpretation of ΔpH_S data immediately above[5], this lack of effect probably reflects limited availability of CO_2 at the extracellular surface during influx and disposal of CO_2 at the extracellular surface during efflux. Such choking could be mitigated by introducing an extracellular carbonic anhydrase (CA_o), as we will see below as we discuss the gray vs. black bars in Figure 8*C*. Also already mentioned[6], a compounding factor may be the large diameter of the oocyte. (3) Nevertheless, we know that expression of hAQP5 leads to a sizeable increase of P_{M,CO_2} because of the parallel ΔpH_S data summarized by the lighter/darker pairs of bars in Figure 3*A,B*.

±hAQP5, ΔhCA II, –bCA: Effects on pH_S relaxation

Theoretical considerations. Let us assume that the oocyte is a sphere, containing only an aqueous pH buffer, surrounded by a membrane permeable only to CO_2, and initially devoid of CO_2/HCO_3^-. If we now expose the oocyte to a CO_2/HCO_3^- solution, we could compute—given $[CO_2]_o$, initial pH_i, buffering power, and cell volume—the net number of CO_2 molecules that would diffuse into the cell before the system came into equilibrium. The speed of this equilibration depends on the parameters that contribute to the description of Fick's law in Eqns (1) and (2), including $[CO_2]_{os}$, $[CO_2]_{is}$, and P_{M*,CO_2}.

---

[5] See "Results" > "±hAQP5, ΔhCA II, –bCA: Effects on ΔpH_S & $(dpH_i/dt)_{Max}$" > "ΔpH_S" > "Interpretation: ΔpH_S (colorful bars) in Figure 3A,B; ±hAQP5, ΔhCA II, –bCA".

[6] See "Results" > "±hAQP5 in absence of exogenous CAs: Effects on ΔpH_S & $(dpH_i/dt)_{Max}$" > "$(dpH_i/dt)_{Max}$" > "Interpretation: $(dpH_i/dt)_{Max}$ (gray vs. black bars) in Figure 3*C,D*; ±hAQP5, –hCA II, –bCA".

In their study of the impact of cytosolic CA II and CA IV (predominantly extracellular) on CO_2 equilibration, Musa-Aziz et al. (2014a, 2014b) noted that, following the rapid upswing in pH_S triggered by CO_2/HCO_3^- application (or the rapid downswing in pH_S triggered by CO_2/HCO_3^- removal), (1) pH_S decayed following an approximately single-exponential (SExp) time course, and that the time constant (τ) of this decay decreased markedly either with (2) injection of recombinant hCA II into the cytosol (see fig. 13 in Musa-Aziz et al. (2014a) or (3) expression of hCA IV (see fig. 21 in Musa-Aziz et al. (2014b). Moreover, mathematical simulations based on a reaction-diffusion model (Somersalo *et al.*, 2012) corroborated nearly all of the essential observations (Occhipinti *et al.*, 2014). In other words, CA II and CA IV increased the speed (reflected by the rate constant = $1/\tau$) of CO_2 equilibration, and thus $1/\tau$ is an indirect measure of the transmembrane CO_2 flux.

In the present study, we note that the pH_S relaxations do not so nearly approximate an SExp decay as in the work by Musa-Aziz et al. (2014a, 2014b), probably due to (1) minor differences in the tip of the pH_S electrodes, (2) the angles with which the pH_S electrode contacted the cell surface, and (3) the precise location of the pH_S electrode on the oocyte surface (see figure 1 insets in Musa-Aziz et al. (2014a). Note also that the mathematical simulations suggest that the pH_S decays should not be perfectly exponential in the first place (Musa-Aziz *et al.*, 2014*a*, 2014*b*; Occhipinti *et al.*, 2014). Therefore, in the present study, as a surrogate for $1/\tau$, we chose to use the maximal initial rate of pH_S relaxation.

Exemplar data. Figure 4*A* reproduces the pH_S time course for CO_2/HCO_3^- addition in Figure 2*B* (i.e., "hAQP5 + Tris"). The jittery black record in Figure 4*B* shows the time course of the actual pH_S relaxation, beginning at a local time (t_{Local}) of 0, which we judged by eye to be time of fastest pH_S decay. The smooth orange curve is the result of a double-exponential (DExp) curve fit. The dashed orange line is the tangent to the DExp function, evaluated at $t_{Local} = 0$. The blue curve in Figure 4*C* is a plot of dpH_S/dt, computed as the derivative of the best-fit DExp function, versus pH_S. Here, time flows from right to left. The break in slopes at $pH_S \cong 7.54$ is the result of the second, slower exponential process. The dashed blue line is the derivative of the DExp function, again calculated at $t_{Local} = 0$, but now plotted as a function of pH_S. Although the choice of $t_{Local} = 0$ is subject to human error, the effect of misjudgment is likely to be minimal

inasmuch as the DExp fit encompasses so many points, and because both the initial time course and the initial plot of dpH_S/dt vs. pH_S are nearly linear.

Figure 4*D–F* are analogous to the top row of panels, except that here we analyze the CO_2/HCO_3^--removal step in Figure 2*B*. Note that all of the pH_S records are inverted, and that, in Figure 4*F*, time runs from left to right.

Summary. The layout of the synopses in Figure 5*A,B* for $(dpH_S/dt)_{Max}$ data—CO_2 addition/removal, ±hAQP5, with increasing amounts of injected hCA II—are the same as in Figure 3*A* for the ΔpH_S data.

Conclusions. Both for CO_2/HCO_3^- addition and removal: (a) In the absence of hCA II, expression of hAQP5 (gray vs. black bars) increases the magnitude of $(dpH_S/dt)_{Max}$, and the difference in mean values is statistically significant. The same is true for the expression of hAQP5 at each of the increasing hCA II levels (compare light- vs. dark-blue, red, and green bars). (b) In the absence of hAQP5, injecting hCA II in ever-greater amounts (lighter bars) causes $(dpH_S/dt)_{Max}$ to trend upward, but is without a statistically significant effect on $(dpH_S/dt)_{Max}$. And (c) in the presence of hAQP5, injecting increasing amounts of hCA II tends to produce ever-greater magnitudes of $(dpH_S/dt)_{Max}$, with several of the differences reaching statistical significance, especially for CO_2/HCO_3^- addition. And (d) the effects on $(dpH_S/dt)_{Max}$ are in the same direction but statistically more robust than for ΔpH_S in Figure 3*A,B*.

Interpretation: $(dpH_S/dt)_{Max}$ in Figure 5A,B; ±hAQP5, ΔhCA II, –bCA. Our analysis of these data is similar to those for ΔpH_S in sections above .[7]

---

[7] See Results > "±hAQP5 in absence of exogenous CAs: Effects on ΔpH_S & $(dpH_i/dt)_{Max}$" > "pH_S" > "Interpretation: ΔpHS (gray vs. black bars) in Figure 3A,B; ±hAQP5, − hCA II, − bCA".

Also see Results > "±hAQP5, ΔhCA II,[7] –bCA: Effects on ΔpH_S & $(dpH_i/dt)_{Max}$" > "pH_S" > "*Interpretation: ΔpH_S (colorful bars) in* Figure 3*A,B; ±hAQP5, –hCA II, –bCA*".

±hAQP5, ΔhCA II, –bCA: Effects on other oocyte parameters

Initial pH_i Figure 6*A* summarizes the initial pH_i values of oocytes subjected to the eight protocols of Figure 2. All of the mean values are within 0.1 pH units of each other. Statistical analyses reveal no significant differences.

ΔpH_i Figure 6*B* summarizes the ΔpH_i values—that is, the decreases in pH_i—elicited by application of 1.5% $CO_2/NaHCO_3$ for the eight protocols. These values are all well within 0.1 of each other, and statistical analyses shows no statistically significant differences among the eight ΔpH_i mean values.

β_I Figure 6*C* summarizes the intrinsic buffering power values of the eight groups of oocytes. Statistical analyses show no significant differences among the groups. The modest downward trend from the leftmost bars to the rightmost bars may reflect a faster equilibration of CO_2 within oocytes with higher injected levels of hCA II, especially with hAQP5 expression. With a slower CO_2 equilibration (see Figure 2*A*), the measured ΔpH_i would tend to underestimate the value that we would have obtained at $t = \infty$, and thus lead to an artificially elevated computed β_I value.

P_f After monitoring pH_S and pH_i, we performed the P_f assay with each oocyte. Figure 6*D* summarizes our P_f data. The injection of cRNA encoding hAQP5 significantly increases P_f for each of the four groups of oocytes previously injected with no or increasing amounts of hCA II (compare lighter vs. darker bars in blue, red, and green). Thus, we can conclude that the oocytes express hAQP5 that traffics normally to the plasma membrane. Because the increase in P_f induced by hAQP5 was virtually the same for the four doses of hCA II, it is most likely that the CA has no effect on the monomeric pores that are responsible for the osmotic water permeability of hAQP5.

±hAQP5, –hCA II, +bCA: Effects on ΔpH_S & $(dpH_i/dt)_{Max}$

In the final four sections of Results, we examine oocytes studied in the presence of extracellular bCA and thereby explore the functional interaction between hAQP5 and CA_o in the transmembrane diffusion of CO_2.

In this first of the final four sections, we study oocytes in the absence of injected hCA II. On Day 1, we injected oocytes with either "H_2O" or "H_2O + cRNA" encoding "hAQP5" and then, on Day 4, we injected all oocytes with "Tris". During the experiment, we augment the extracellular solutions with 0.1 mg/ml of bCA, the same level as used previously by Musa-Aziz *et al.* (2014*b*). This protocol is identical to that of Figure 2*AB* (–bCA) except for the presence of bCA.

pHs The red record in Figure 7*A* shows the pH_S data for a representative "H_2O + Tris" oocyte and, in Figure 7*B*, the comparable data for an "hAQP5 + Tris" oocyte. Notice that the pH_S transients in Figure 7*A* (+bCA, extracellular) are many fold larger—both with CO_2/HCO_3^- addition and removal—than their counterparts in Figure 2*A* (–bCA). Musa-Aziz et al. (2014b) had previously made a similar observation with extracellular hCA II (compare their figs. 13g and 15g).

Theoretical considerations. Note that in comparing pH_S transients in Figure 7*A* vs. Figure 2*A*, the pH_S electrode is "cis" to the added bCA in Figure 7. A major reason that bCA increases the magnitude of ΔpH_S is that—near the extracellular surface of the plasma membrane—the added bCA greatly accelerates H^+ consumption during CO_2 influx (see Figure 1*A*), and H^+ production during CO_2 efflux (see Figure 1*B*). Although the pH_S electrode directly senses changes in $[H^+]_S$, these only indirectly reflect CO_2 fluxes. Thus, by comparing ±bCA, we can reach no intuitive conclusions about the possible effect of bCA on transmembrane CO_2 fluxes from pH_S data. However, previous mathematical simulations predict that the CO_2 fluxes must have increased under these conditions (Musa-Aziz *et al.*, 2014*b*; Occhipinti *et al.*, 2014), even though in some cases the effects may be too small to measure.

Exemplar data in Figure 7A vs. B. The pH_S records show that—in the presence of extracellular bCA—the expression of hAQP5 does not produce an apparent increase in the magnitudes of the pH_S transients. This apparent lack of effect is quite different from the large fractional increases in ΔpH_S magnitudes that we observed in the absence of extracellular bCA (i.e., Figure 2*B* vs. Figure 2*A*), where the ΔpH_S magnitudes are so much smaller.

Summary. The gray and black bars in Figure 8*A* show the mean ΔpH_S data for CO_2/HCO_3^- addition, ±hAQP5, all in the absence of hCA II but presence of extracellular bCA. Figure 8*B* shows corresponding data for CO_2/HCO_3^- removal.

Conclusions. Considering oocytes examined in the presence of bCA: In the absence of hCA II, expression of hAQP5 (black vs. gray bars) does not significantly affect ΔpH_S, either for CO_2/HCO_3^- addition or removal.

Interpretation: ΔpH_S (gray vs. black bars) in Figure 8A,B: ±hAQP5, –hCA II, +bCA. (1) bCA promotes large transmembrane CO_2 gradients. During CO_2/HCO_3^- addition, bCA maintains relatively high CO_2 levels near the extracellular face of the membrane and markedly increases CO_2 influxes. During the subsequent CO_2/HCO_3^- removal, bCA maintains relatively low CO_2 levels at the cell surface. Thus, even in the absence of hAQP5 (gray bars), the CO_2 fluxes enabled by bCA are very high. (2) In parallel, in a "cis-side" effect, bCA greatly increases the magnitudes of ΔpH_S, as we can see by comparing Figure 8*A,B* vs. Figure 3*A,B*. Thus, during CO_2/HCO_3^- addition, bCA enhances H^+ consumption, whereas during CO_2/HCO_3^- removal, bCA enhances H^+ production. (3) With expression of hAQP5 (black bars)—combining an increased P_{M,CO_2} with the capacity of bCA to replenish/consume cell-surface CO_2—cytosolic CA activity becomes rate limiting. Thus, during CO_2 addition, CO_2 rapidly builds up near the inner surface of the membrane, limiting the transmembrane gradient, and choking CO_2 influx—especially as assessed by a pH_S electrode that is "cis" to the bCA. The same is true in reverse during CO_2/HCO_3^- removal. (4) The evidence that hAQP5 does indeed increase P_{M,CO_2} will come below in our analysis of Figure 8*C*.

dpH_i/dt The green records in Figure 7*A* and *B* show the pH_i data collected simultaneously with the red pH_S transients (presented above) in these same panels. Note that $(dpH_i/dt)_{Max}$ values in Figure 7*A* (+bCA) are substantially greater—both with CO_2/HCO_3^- addition and removal—than their counterparts in Figure 2*A* (–bCA). Musa-Aziz et al. (2014b) had previously made a similar observation with extracellular hCA II (compare their figures 13e and 15e). Note that in comparing pH_i changes in Figure 7*A* vs. Figure 2*A*, the pH_i electrode is "trans" to the bCA that we add to the bECF. During CO_2/HCO_3^- addition, bCA

accelerates extracellular CO_2 formation and thus maintains a relatively high [CO_2] near the extracellular surface of the membrane. Similarly, during CO_2/HCO_3^- removal, bCA accelerates CO_2 consumption and thus maintains a relatively low [CO_2] at the extracellular membrane surface. The greater transmembrane CO_2 gradients lead to greater CO_2 fluxes and thus faster "trans-side" pH_i changes. Thus, comparing Figure 7*A* vs. Figure 2*A*, we can conclude that bCA increases transmembrane CO_2 fluxes.

If we now compare the pH_i records in Figure 7*A* and Figure 7*B*, we see that hAQP5 expression produces a substantial acceleration in the rate of pH_i decrease during CO_2/HCO_3^- addition, consistent with an hAQP5-dependent increase in CO_2 influx. During CO_2/HCO_3^- removal, the presence of hAQP5 does not substantially speed the pH_i increase.

Summary. The gray and black bars in Figure 8*C* summarize the downward $(dpH_i/dt)_{Max}$ for CO_2/HCO_3^- addition, ±hAQP5, all in the presence of extracellular bCA but absence of hCA II. Figure 8*D* summarizes the corresponding data for CO_2/HCO_3^- removal.

Conclusions. Considering oocytes examined in the absence of hCA II but presence of bCA (Figure 8*C,D*): During CO_2/HCO_3^- addition, expression of hAQP5 (black vs. gray bars) significantly increases the magnitude of $(dpH_i/dt)_{Max}$. During CO_2/HCO_3^- removal, expression of hAQP5 causes $(dpH_i/dt)_{Max}$ to trend faster, although the difference is not statistically significant.

Interpretation: $(dpH_i/dt)_{Max}$ (gray vs. black bars) in Figure 8C,D; ±hAQP5, –hCA II, +bCA. See our ΔpH_S "Interpretation" immediately above.[8] (1) bCA promotes large transmembrane CO_2 gradients. (2) In a "trans-side" effect, bCA greatly increases the magnitudes of $(dpH_i/dt)_{Max}$, as we can see by comparing gray and black bars in Figure 8*C,D* (+bCA) vs. Figure 3*C,D* (–bCA)—consequences of the gradient effect in point #1. (3) Here in Figure 8*C* (+bCA), hAQP5 increases the magnitude of $(dpH_i/dt)_{Max}$ during

[8] See Results > "±hAQP5, –hCA II, +bCA: Effects on ΔpH_S & $(dpH_i/dt)_{Max}$" > *"pH_S"* > *"Interpretation: ΔpH_S (gray vs. black bars) in Figure 8A,B: ±hAQP5, –hCA II, +bCA".*

CO_2/HCO_3^- addition, demonstrating the hAQP5 increases P_{M,CO_2}. In Figure 3*C* (–bCA), the effect of expressing hAQP5 was nil because the limited availability of extracellular CO_2 choked influx.

±hAQP5, +hCA II, +bCA: Effects on ΔpH_S & $(dpH_i/dt)_{Max}$

To continue our exploration of the functional interaction of hAQP5 with CAs in the diffusion of CO_2, in this next series of experiments, we not only augment the extracellular solutions with 0.1 mg/ml bCA, but also inject hCA II. On Day 1, we injected all oocytes with either "H_2O" or "H_2O + cRNA" encoding "hAQP5" and then, on Day 4, we injected all oocytes with 1 ng hCA II.

pH_S The red records in Figure 7*C* (–hAQP5, +hCA II, +bCA) and Figure 7*D* (+hAQP5, +hCA II, +bCA) are analogous to those in panels *A* and *B*, except for the injection of hCA II. We now make three sets of comparisons:

(a) Comparing the red pH_S records between Figure 7*C* (+hCA II) vs. Figure 7*A* (–hCA II)—having in common –hAQP5, +bCA—we see that addition of 1 ng hCA II increases the magnitudes of the pH_S transients—both with CO_2/HCO_3^- addition and removal. Recall that Musa-Aziz et al. (2014a) made similar ΔpH_S observations ±cytosolic hCA II, though in the absence of added CA_o. Because the pH_S electrode is "trans" to the added hCA II (in comparing Figure 7*C* vs. Figure 7*A*), we can conclude that the hCA II has increased the transmembrane CO_2 flux in the continued presence of extracellular bCA.

(b) Comparing the pH_S records in Figure 7*D* (+hCA II) vs. Figure 7*B* (–hCA II)—having in common +hAQP5, +bCA—we see that addition of 1 ng hCA II again increases the magnitudes of the pH_S transients.

(c) Comparing Figure 7*D* (+hAQP5) vs. Figure 7*C* (–hAQP5), we see that—on a background of injected hCA II and extracellular bCA—hAQP5 expression has limited effect.

(d) Note that the pH_S transients here in Figure 7*C,D* (±hAQP5, +hCA II, +bCA) are much larger than their counterparts in Figure 2*C,D* (±hAQP5, +hCA II, –bCA).

Summary. (a) The gray vs. light-blue bars in Figure 8*A* show the mean ΔpH_S data for CO_2/HCO_3^- addition, ± hCA II, all in the absence of hAQP5 but presence of bCA. Figure 8*B* shows the corresponding

data for CO_2/HCO_3^- removal. (b) The black vs. dark-blue bars compare ±hCA II, but in the presence of both hAQP5 and bCA. (c) The light-blue vs. dark-blue bars compare ±hAQP5, all in the presence of both hCA II and bCA.

Conclusions. (a) The difference in mean values represented by the gray and light-blue bars (±hCA II in the absence of hAQP5) is statistically significant, as is (b) the difference between the black and dark-blue bars (±hCA II in the presence of hAQP5). Note that the effects in 'a' and 'b' correspond to the previously described synergistic effects of CA_i and CA_o (Musa-Aziz *et al.*, 2014*a*, 2014*b*; Occhipinti *et al.*, 2014). (c) The difference between the light- vs. dark-blue bars (±hAQP5 in the presence of hCA II and bCA) is not significant. (d) The statistical analysis summarized in Statistics Tables 8*E,F* compares ΔpH_S amplitudes summarized in Figure 8*A,B* (+bCA) vs. the gray/black/light-blue/dark-blue bars in Figure 3*A,B* (–bCA). The result is that the effect of bCA is significant.

Interpretation: ΔpH_S (colorful bars) in Figure 8A,B; ±hAQP5, +hCA II, +bCA. See "Interpretation" for ΔpH_S in the previous section.[9] Namely: (1) the bCA enhances transmembrane CO_2. (2) The ΔpH_S data summarized by the light/dark-blue bars in Figure 8*A,B* (+bCA) are in stark contrast to the analogous data in Figure 3*A,B* (–bCA)—note that this is a "cis" comparison (i.e., ±bCA→pH_S)—where the ΔpH_S values are only about ⅛ to ½ as large during CO_2/HCO_3^- addition. (3) Expression of hAQP5 in the presence of 1 ng injected hCA II (light- vs. dark-blue bars), even with the increase in P_{M,CO_2}, does not increase ΔpH_S magnitudes because CO_2 fluxes are choked by insufficient cytosolic CA activity (i.e., insufficient transmembrane CO_2 gradient). And (4) recall that hAQP5 does indeed increase P_{M,O_2} (see Figure 8*C*, below). In addition to points #1 – #4, which are analogous to the corresponding points made in the previous section: (5) in a "trans-side" effect, injection of 1 ng of hCA II—either in the absence of hAQP5 (gray vs.

[9] See Results > "±hAQP5, –hCA II, +bCA: Effects on ΔpH_S & $(dpH_i/dt)_{Max}$" > *"pH_S"* > *"Interpretation: ΔpH_S (gray vs. black bars) in Figure 8A,B: ±hAQP5, –hCA II, +bCA"*.

light-blue bars) or the presence of hAQP5 (black vs. dark-blue bars)—increases the ΔpH_S magnitudes because the hCA II is able to increase transmembrane CO_2 gradients sufficiently under these conditions.

dpH_i/dt The green records in Figure 7*C* and *D* show the pH_i data that correspond to the pH_S data presented above, and lead to three comparisons:

(a) Comparing the pH_i records between Figure 7*C* (+hCA II) vs. Figure 7*A* (–hCA II)—both in the absence of hAQP5—we see that addition of 1 ng hCA II substantially increases the rates of pH_i changes, both with CO_2/HCO_3^- addition and removal. Musa-Aziz et al. (2014a) made similar $(dpH_i/dt)_{Max}$ observations ±hCA II, though in the absence of added CA_o.

(b) Comparing the pH_i records in Figure 7*D*(+hCA II) vs. Figure 7*B* (–hCA II)—now both in the presence of hAQP5—we again see that addition of 1 ng hCA II again increases the magnitudes of $(dpH_i/dt)_{Max}$.

(c) Comparing the pH_i records in Figure 7*D* (+hAQP5) vs. Figure 7*C* (–hAQP5), we see that—on a background of injected hCA II and extracellular bCA—hAQP5 expression has little effect.

(d) Finally, the magnitudes of $(dpH_i/dt)_{Max}$ here Figure 7*C,D* are modestly larger than their Figure 2*C,D* counterparts.

Summary. The layout and meaning of the bars in Figure 8*C,D* are the same as in Figure 8*A,B*.

Conclusions. As we saw for the ΔpH_S data, the differences between (a) the two lighter-colored bars (– hAQP5, ±hCA II,) as well as (b) the two darker-colored bars (+hAQP5, ±hCA II) are statistically significant. (c) The difference between the light- and dark-blue bars (±hAQP5, + hCA II, +bCA) is not.

(d) The statistical analysis summarized in Statistics Tables 8*G,H* compares $(dpH_i/dt)_{Max}$ magnitudes from Figure 8*C,D* (+bCA) vs. the gray/black/light-blue/dark-blue bars in Figure 3*C,D* (–bCA). The result is that the effect of bCA is significant.

Interpretation: $(dpH_i/dt)_{Max}$ (colorful bars) in Figure 8C,D; ±hAQP5, +hCA II, +bCA. See "Interpretation" for ΔpH_S immediately above.[10] Namely: (1) bCA magnifies transmembrane CO_2 gradients. (2) In a "trans" effect, the magnitudes of the light- and dark-blue bars in Figure 8*C,D* (+hCA II, +bCA) are modestly larger than their counterparts in Figure 3*C,D* (+hCA II, –bCA)—a specific example of enhanced transmembrane CO_2 gradients noted in point #1. (3) The light- and dark-blue bars (i.e., ±hAQP5, +hCA II, +bCA) are not significantly different, presumably because, 1 ng injected hCA II does not raise cytosolic CA activity sufficiently to prevent choking the dominant effects of hAQP5 ($\uparrow P_{M,O_2}$) and bCA ($\uparrow CO_2$ gradient). We predict that, greater CA_i activities (e.g., 100 ng) would have alleviated the choke and revealed a much taller +hAQP5 bar. And (4) hAQP5 does indeed increase P_{M,O_2} as evidenced by the comparison of gray vs. black bars in Figure 8*C*, above. In addition to points #1 – #4 (analogous to those made in previous section), (5) we note that—because of a "cis" effect—we cannot intuitively interpret the effects of injecting hCA II on $(dpH_i/dt)_{Max}$, either in the absence of hAQP5 (gray vs. light-blue bars) or the presence of hAQP5 (black vs. dark-blue bars). Even though we cannot intuitively assess ±hCA II effects from $(dpH_i/dt)_{Max}$, we know from the corresponding ΔpH_S data in Figure 8*A,B* that the injection of hCA II—by enhancing transmembrane CO_2 gradients—must have increased the CO_2 fluxes.

±hAQP5, ±hCA II, +bCA: Effects on pH_S relaxation

Summary. The layout of Figure 9*A,B* is similar to that of Figure 8*A,B* (i.e., ΔpH_S), except that here in Figure 9*A,B* we examine $(dpH_S/dt)_{Max}$ as we did in Figure 5*A,B*.

Conclusions. For oocytes examined in the presence of bCA:

(a) In the absence of hAQP5, injecting hCA II (gray vs. light-blue bars in Figure 9*A*) produces an increase in $(dpH_S/dt)_{Max}$ during CO_2/HCO_3^- addition; the difference is statistically significant. During CO_2/HCO_3^- removal, the results trend toward a greater magnitude but do not reach statistical significance

[10] See Results > "±hAQP5, +hCA II, +bCA: Effects on ΔpH_S & $(dpH_i/dt)_{Max}$" > *"pH_S"* > *"Interpretation: ΔpH_S (colorful bars) in Figure 8A,B: ±hAQP5, +hCA II, +bCA".*

(Statistics Table 9*B*). These results in Figure 9*A* (–hAQP5, ±hCA II, +bCA) are in contrast to those in Figure 5*A* (–hAQP5, ±hCA II, –bCA), where injected hCA II is without statistically significant effect, and even the trends were mild.

And (b) in oocytes expressing hAQP5, injecting hCA II (black vs. dark blue bars) increases the magnitude of $(dpH_S/dt)_{Max}$ during CO_2/HCO_3^- addition, with a statistically significant difference. This treatment produces a slight upward trend during CO_2/HCO_3^- removal. Note that these increments (due to injecting hCA II) are no greater than for oocytes not expressing hAQP5. Viewed differently, expressing hAQP5 significantly increases the magnitude of $(dpH_S/dt)_{Max}$ in only 1 of 4 cases (CO_2/HCO_3^- removal in the absence of hCA II, gray vs. black bars in Figure 9*B*). These results contrast to those in Figure 5 (– bCA) where—in the presence of hAQP5—increasingly large hCA II injections tended to produce graded increases $(dpH_S/dt)_{Max}$, and for both CO_2/HCO_3^- addition and removal. We note, however, that the hCA II injections in Figure 9 were either 0 or 1 ng, whereas in the Figure 5 (–bCA) study, the hCA II we as high as 100 ng.

(c) Expression of hAQP5 in the absence of hCA II (gray vs. black bars in Figure 9*A,B*) or the presence of hCA II (light- vs. dark-blue bars) has no effect on $(dpH_S/dt)_{Max}$ except during CO_2/HCO_3^- removal in the absence of hCA II (gray vs. black bars, Figure 9*B*). These results contrast with those of Figure 5 (– bCA), where hAQP5 expression increases $(dpH_S/dt)_{Max}$ magnitudes robustly and consistently.

(d) The $(dpH_S/dt)_{Max}$ magnitudes in Figure 9 are ~2- to ~3-fold greater than the analogous ones in Figure 5. The differences are greatest in the absence of hCA II, where the lighter-colored bars in Figure 9 are ~10-fold greater.

Interpretation: $(dpH_S/dt)_{Max}$ in Figure 9A,B; ±hAQP5, ±hCA II, +bCA. Our analysis of these $(dpH_S/dt)_{Max}$ is similar to that for the ΔpH_S data in the previous section.[11]

---

[11] See Results > "±hAQP5, +hCA II, +bCA: Effects on ΔpH_S & $(dpH_i/dt)_{Max}$" > *"pH_S"* > *"Interpretation: ΔpH_S (colorful bars) in Figure 8A,B: ±hAQP5, +hCA II, +bCA".*

±hAQP5, ±hCA II, +bCA: Effects on other oocyte parameters

The four bars in each of the panels of Figure 10 are analogous to the four leftmost bars of the four panels in Figure 6; the difference is that, here in Figure 10, we summarize experiments in which we exposed oocytes to 0.1 mg/ml extracellular bCA.

Initial pH_i Statistical analyses, as in the case of Figure 6*A*, reveal no significant differences among the four mean initial pH_i values in Figure 10*A*. Moreover, Statistics Table 10*E*, which summarizes an analysis of values in Figure 10*A* (+bCA) vs. the gray/black/light-blue/dark-blue bars in Figure 6*A* (–bCA), reveals no significant effect of adding bCA.

ΔpH_i We observe no significant differences among mean ΔpH_i values in Figure 10*B*, as observed among groups in Figure 6*B*. However, Statistics Table 10*F*, which summarizes an analysis of values in Figure 10*B* (+bCA) vs. the gray/black/light-blue/dark-blue bars in Figure 6*B* (–bCA), reveals a small but significant difference due to the addition of bCA. The magnitudes of ΔpH_i values in Figure 6*B* are somewhat smaller, presumably reflecting the slower transmembrane equilibration of CO_2 due to the absence of bCA, particularly at lower levels of injected hCA II.

β_I Continuing the trend from the previous two panels, we observe no significant differences among mean β_I in Figure 10*C*, as described above among analogous conditions in Figure 6*C*. However, Statistics Table 10*G*, which summarizes an analysis of values in Figure 10*C* (+bCA) vs. the gray/black/light-blue/dark-blue bars in Figure 6*C* (–bCA), reveals a small but significant difference—similar to the analysis of the ΔpH_i data above. Because their ΔpH_i magnitudes tend to be smaller, the β_I values in Figure 6*C* (–bCA) are somewhat larger than those in Figure 10*C* (+bCA).

P_f As for the previous three panels, the mean values summarized in Figure 10*D* (+bCA)—now for P_f—are indistinguishable from the comparable values in Figure 6*D* (–bCA). Our statistical analyses in Statistics Table 10*H* reveals no significant effect of bCA on P_f. Thus, we can conclude that extracellular bCA—a mixture of CA I and CA II—does not interfere with the monomeric pores of hAQP5. Moreover, as we did in our analysis of Figure 6*D*, we can conclude, from a comparison of the black and dark-blue bars, that the hCA II does not functionally interfere with the monomeric pores.

Discussion

Historical context

Although previous papers on CO_2 diffusion across membranes have addressed the role of channels or the role of CAs, the present paper is the first to undertake a systematic examination of both channels and CAs, as well as their synergistic interaction to enhance CO_2 fluxes. The underlying principle is Fick's law of diffusion, which we reproduce from Eqn (2):

$$J_{CO_2} = \underbrace{P_{M^*,CO_2}}_{\pm hAQP5} \cdot \underbrace{\left(\underbrace{[CO_2]_{os}}_{\pm bCA} - \underbrace{[CO_2]_{is}}_{\pm hCA\,II} \right)}_{\text{Transmembrane } CO_2 \text{ gradient}} , \quad \textbf{(3)}$$

and embellish to emphasize that the key parameters in the present study increase P_{M^*,CO_2} (i.e., hAQP5) and the transmembrane CO_2 gradient. During CO_2 influx, bCA (when present) in the extracellular fluid maintains a relatively high $[CO_2]_{os}$, whereas hCA II (when present) maintains a relatively low $[CO_2]_{is}$, the result being an enhanced inwardly directed CO_2 gradient. Conversely, during CO_2 efflux, bCA in the extracellular fluid maintains a relatively low $[CO_2]_{os}$ whereas hCA II maintains a relatively high $[CO_2]_{is}$, the result being an enhanced outwardly directed CO_2 gradient.

It is perhaps worth noting that similar principles are at work during O_2 fluxes across the erythrocyte membrane. In that case, according to preliminary results (Moss *et al.*, 2025; Occhipinti *et al.*, 2025; Zhao *et al.*, 2025), it is AQP1, the Rh complex, and as-yet-unidentified channel(s) that make the dominant contribution to P_{M,O_2}. Moreover, it is hemoglobin that maximizes transmembrane O_2 gradients (ignoring hemoglobin diffusion within the cytoplasm) by serving as a sink or source of O_2 near the plasma membrane. In the laboratory experiments on O_2 efflux from RBCs, one can use an extracellular O_2 scavenger like sodium dithionite to consume O_2 near the extracellular face of the membrane, in an action that is analogous to that of bCA in the present experiments on CO_2 efflux.

Working on artificial lipid bilayers, Gutknecht et al. (1977) showed that mobile CA enhances CO_2 fluxes (measured using ^{14}C-labeled CO_2), but only in the presence of sufficient non-CO_2/HCO_3^- buffers (phosphate, HEPES, "Tris"). Their interpretation is that the CA increases the transmembrane CO_2 gradient

by replenishing CO_2 on one side of the membrane and consuming it on the other. This replenishment (or consumption) requires that HCO_3^- diffuse through the unconvected layers on opposite sides of the membrane to serve as either the source or product of the CA reactions. Moreover, the buffers act as either a source of or sink for H^+ in these reactions.

The trio of papers by Musa-Aziz et al. (2014a, 2014b) and Occhipinti et al. (2014) extended this line of reasoning to *Xenopus* oocytes, which they injected with recombinant hCA II (to an apparent concentration ~50% higher than in RBCs) and/or cRNA encoding hCA IV (which contributes to both extracellular-surface and cytosolic CA activity). In addition, they systematically varied $[CO_2]_o$ and $[HEPES]_o$ and performed 3-dimensional reaction-diffusion mathematical modeling to enable a quantitative interpretation of the data. As anticipated from the earlier artificial lipid-bilayer work, they found that each CA alone augmented CO_2 diffusion by increasing transmembrane CO_2 gradients. However, the combination of the two is not simply additive but highly synergistic. The reason is that, with a CA on just one side of the membrane, net CO_2 fluxes are limited by the build-up or depletion of CO_2 on the other—the "choking" (or throttling) effect to which we allude in the Results section of the present paper. They also demonstrated an additional synergism involving an extracellular non-HCO_3^- buffer, (i.e., HEPES), assessed by "trans-side" measurements of pH_i, and examined the impact of increasing $[CO_2]_o$ during CO_2/HCO_3^- application. In their papers, they did not address the issue of CO_2 permeability.

The first studies to address the P_{M,CO_2} term in Eqn (3) were those by Nakhoul et al. (1998) and Cooper & Boron (1998), who showed that AQP1—in addition to being a H_2O channel—is an effective CO_2 channel. (Musa-Aziz et al. (2007) and Geyer et al. (2013) later examined a range of mammalian AQPs and showed that AQP5 has the highest CO_2/H_2O permeability ratio. The only study to broach channel-CA interactions was that by Nakhoul et al. (1998), who studied CO_2-induced pH_i changes in oocytes with the vitelline membrane intact. They found that the stimulatory effect of AQP1 on CO_2 influx into oocytes occurs only with bCA injected into the cytoplasm. In the present paper, the analogous experiment is summarized by the light- vs. dark-blue bars in Figure 3*C*, where hAQP5 expression causes $(dpH_i/dt)_{Max}$

to trend faster. Perhaps a difference, as suggested by others (Vilas *et al.*, 2015), is that CA II binds to AQP1 but not AQP5.

The present paper builds on the work of Musa-Aziz and Occhipinti (Musa-Aziz *et al.*, 2014*a*, 2014*b*; Occhipinti *et al.*, 2014) and generally uses identical approaches, with three important differences:

First, rather than recombinant hCA II, in the present study we use hCA II purified commercially from RBCs.

Second, rather than heterologously expressing hCA IV, we add bCA to the extracellular fluid. The reasons for this switch are fourfold: (1) hCA IV expression in oocytes not only increases cell-surface CA activity, but also cytosolic CA activity. The oocyte membrane confines bCA to the outside of the cell. (2) The co-expression of hCA IV and hAQP5 adds an extra burden of heterologous expression and also introduces potential competition between the injected cRNAs encoding the two proteins ("ribosome steal"). (3) We also chose to add purified CA protein to the bECF because in principle we know the precise increase in CA_o activity, which is difficult to know in the case of protein expression. And (4) we chose bCA because it is a less-expensive combination of bCA I (less active) and bCA II (more active) vs. hCA II; this is an important practical consideration during continuous-flow experiments, which consume considerable volumes of experimental solutions.

Third, rather than working only with oocytes having a background P_{M,CO_2}, we alternated between injections of H_2O and cRNA encoding hAQP5.

pH measurements made "cis" vs. "inter" vs. "trans" to the altered parameter

The papers of (Musa-Aziz *et al.*, 2014*a*, 2014*b*) and Occhipinti et al. (2014) introduced the concept of pH measurements, used as an indirect measure of something else (e.g., CO_2 flux), being made "cis" or "trans" to a compartment with an alteration that directly affects pH (e.g., CA activity, non-HCO_3^- buffering power). Thus, if one wishes to assess the effects on CO_2 flux of injecting (or not injecting) hCA II into the cytosol, the measurement of pH_i—"cis" to the added hCA II—does not provide intuitive insight into the effects of hCA II" on transmembrane CO_2 fluxes. Of course, at the same time as making the pH_i

measurement, one may also be monitoring of pH_S—"trans" to the added hCA II in the same cell. Interpreting the data from such a "trans" perspective does provide intuitive insight into CO_2 fluxes. The same principles apply in the opposite sense if one wishes to assess the effects of adding (or not adding) bCA to the bECF. The measurement of pH_S—"cis" to the added bCA—does not intuitive insight into the effects of bCA on CO_2 fluxes, whereas the measurement of pH_i—"trans"—does.

The reason for the "cis-side" prohibition is that the enzymatic activity of the CA produces or consumes H^+, and thus can produce large pH changes that are independent of—and could conflated with the interpretation of—changes in transmembrane CO_2 fluxes. Thus, intuitive interpretations can be extremely difficult, even though mathematical modeling can unravel alterations in "cis-side" pH from alterations in the flux of CO_2 or other buffer components. Such unraveling was a major component of the studies of Musa-Aziz *et al.* (2014*a*, 2014*b*) and Occhipinti *et al.* (2014), which demonstrated that both cytosolic and extracellular CA increase transmembrane CO_2 gradients and thus increase CO_2 fluxes. Of course, avoiding a prohibited "cis-side" interpretation requires proper experimental design. However, the "cis-side" prohibition is more an issue of data interpretation: when altering any parameter that affects acid-base reaction rates in Figure 1*A*, an intuitive interpretation requires that one examine pH "trans" to the alteration.

Stated simply, "trans-side" pH measurements are valuable for intuitive interpretations because trans-side pH change can occur only as the result of altered CO_2 fluxes across the membrane.

The experiments summarized by Figure 8 are a useful case study. bCA is present continuously in the bECF. Thus, when we inject hCA II, the pH_S measurements—"trans" to the hCA II—do provide intuitive insight into the effect of hCA II on transmembrane CO_2 fluxes because, in this particular comparison, the bCA status is unchanging. Basing one's intuition on pH_i measurements—"cis" to the added hCA II—would be unwise. However, if we compare Figure 8 (+bCA) with Figure 3 (–bCA), an intuitive assessment of bCA effects must come from pH_i measurements—"trans" to the ±bCA condition. Thus, "cis" vs. "trans" is not a matter of data per se, but a matter of perspective during data analysis.

Finally, in Figure 3 and Figure 8 we also assess the effects of expressing the integral membrane protein hAQP5. Both pH_S and pH_i measurements are neither "cis" nor "trans" to the altered expression of hAQP5 and thus the altered P_{M,CO_2}. One might use the term "inter" (Latin, "within", "inside", or "between") to indicate the position of the protein relative to the membrane. In such an "inter" situation, one could use both pH_S and pH_i measurements to assess the data intuitively.

Molecular mechanism of CO_2 permeability

Given the suggestion that AQPs may conduct dissolved gases via the hydrophobic central pore of the tetramer (Wang *et al.*, 2007; Boron, 2010), it is not surprising that molecular dynamics simulations are consistent with the hypothesis that O_2 (Zhang & Chen, 2013) and CO_2 (Alishahi & Kamali, 2019) can diffuse through the central pore of hAQP5. Preliminary data on hAQP5 suggest that (1) mutating amino-acid residues near the outer mouth of the central pore to residues with bulky side chains (e.g., T41F) or (2) creating a divalent-cation binding site (T41H) and then adding Ni^{2+} or Zn^{2+} greatly reduces ΔpH_S, as supported by crystal structures and molecular dynamics (Shinn *et al.*, 2024). In addition, a preliminary report suggests that, with hAQP1, the mercurial pCMBS can block one component of P_{M,CO_2}, the stilbene derivative DIDS can block an equally large component, and the two together than eliminate the CO_2 permeability of hAQP1 (Musa-Aziz *et al.*, 2025). Thus, the emerging picture is that some CO_2 can permeate the four hydrophilic monomeric pores (at least of hAQP1) and that another component—presumably the major component of CO_2—moves through the central pore of hAQP5.

Diagnostic power of $\Delta\Delta\Delta pH_S$ ±hCA II in identifying enhanced CO_2 permeability

In Figure 11, we rearrange CO_2-influx bars from Figure 3*A* so that we can easily compare the effects—on ΔpH_S—of adding a CA, namely hCA II, on the side of the membrane "trans" to the pH_S measurement. The pair of bars on the left of Figure 11*A* shows that, in the absence of hAQP5, injecting 1 ng of hCA II into oocytes has only a minor effect on ΔpH_S. That is, the baseline $\Delta\Delta pH_S$—or $\Delta\Delta pH_{S,Base}$—is small. However, in the presence of a CO_2 channel hAQP5, $\Delta\Delta pH_S$—or $\Delta\Delta pH_{S,hAQP5}$—is substantially greater. The difference between the two $\Delta\Delta pH_S$ values—the $\Delta\Delta\Delta pH_S$ due to the presence of hAQP5 or $\Delta\Delta\Delta pH_{S,hAQP5}$—is statistically significant (Supplemental Table 11*A*).

Figure 11*B* is a rearrangement of two pairs of CO_2-influx bars, but with 100 ng of injected hCA II. The $\Delta\Delta pH_{S,Base}$ is similar to the value in Figure 11*A*. However, here the effect of hAQP5 expression, namely, $\Delta\Delta pH_{S,hAQP5}$ is even greater. Thus, it appears that the greater the level of hCA II, the greater is the effect of hAQP5 expression on $\Delta\Delta pH_S$. Although this set of comparisons is of CO_2 influx, we could reach a similar set of conclusions for CO_2 efflux (i.e., by rearranging bars in Figure 3*B*).

If we did not know the identity of the membrane protein expressed in these experiments, we could deduce that the protein must have a significant CO_2 conductance, assuming that the protein itself lacks significant CA activity. We can imagine that the cytosolic CA, by serving as a sink for CO_2 during influx, sucks CO_2 into the cell. If P_{M,CO_2} is rate limiting, the addition of a CO_2 channel will lead to increased CO_2 influx, a greater decrease in $[CO_2]$ at the extracellular cell surface, and thus a greater ΔpH_S.

Note that in a cell in which it is impractical to inject or express a cytosolic CA, one might use a drug like acetazolamide to block endogenous CA II, and thereby perform an analogous $\Delta\Delta\Delta pH_S$ assay.

Diagnostic power of $\Delta\Delta(dpH_i/dt)_{Max}$ ±bCA in identifying enhanced CO_2 permeability

In Figure 12, we perform the inverse analysis of Figure 11: We rearrange CO_2-influx bars from Figure 3*C* and Figure 8*C* so that we can easily compare the effects—now on $\Delta(dpH_i/dt)_{Max}$—of adding a CA—now bCA—on the side of the membrane "trans" to the pH_i measurement. The pair of bars on the left of Figure 12*A* shows that, in the absence of hAQP5, adding bCA to the bECF produces a modest increase in the magnitude of $(dpH_i/dt)_{Max}$—the $\Delta(dpH_i/dt)_{Max,Base}$. On the other hand, in the presence of the CO_2 channel hAQP5, the magnitude of $(dpH_i/dt)_{Max}$—$\Delta(dpH_i/dt)_{Max,hAQP5}$—is substantially greater. The difference between the two $\Delta(dpH_i/dt)_{Max}$ values—the $\Delta\Delta(dpH_i/dt)_{Max}$ due to the presence of hAQP5 or $\Delta\Delta(dpH_i/dt)_{Max,hAQP5}$—is statistically significant (Supplemental Table 12*A*).

Figure 12*B* shows a similar analysis for CO_2/HCO_3^- removal. Because the $(dpH_i/dt)_{Max}$ values are smaller, the $\Delta(dpH_i/dt)_{Max}$ values also are of smaller magnitude than in Figure 12*B*. In this case, the difference between the two $\Delta(dpH_i/dt)_{Max}$ values is not statistically significant. Thus, this assay may not be practical as shown. A future approach could be to raise $[CO_2]_o$, raise $[HEPES]_o$, inject 100 ng of hCA II,

and raise the bCA level (albeit at the increased cost of the enzyme in a continuously flowing solution). Some combination of these changes would increase the rates of pH_i change, and thereby make it easier to detect $(dpH_i/dt)_{Max}$ differences in both the influx and efflux assays.

Advances and Limitations

Synergisms In the present study, we confirm the strong synergy between extracellular and cytosolic CAs (see Figure 3 and Figure 8). We also identify a strong synergy between a CO_2 channel (i.e., hAQP5) and a cytosolic CA (i.e., hCA II; see pH_S data in Figure 3). Finally, we identify a strong synergy between a CO_2 channel and an extracellular CA (i.e., bCA; see dpH_i/dt data in Figure 8).

"Cis-" vs. "trans-side" effects Our group has previously pointed out the challenges of pH measurements made "cis" to a CA manipulation (Lu *et al.*, 2006). For example, "cis-side" pH_i measurements led to the erroneous conclusion that cytosolic CA II binds to and thereby stimulates the Cl-HCO_3 exchanger AE1, when in fact the added CA II was catalyzing the reaction $HCO_3^- + H^+ \rightarrow CO_2 + H_2O$, and producing a rapid pH_i increase because of catalysis, not transport.

The aforementioned trio of papers (Musa-Aziz *et al.*, 2014*a*, 2014*b*; Occhipinti *et al.*, 2014) systematically deals with the issue of pH measurements made "cis" to a manipulations that impact acid-base chemistry (e.g., modulation of CA activity, alterations in non-HCO_3^- buffering power) and the necessity to focus on "trans" effects. The present paper builds upon and expands these concepts. Note that our modulation of P_{M,CO_2}—an "inter" situation—is neither "cis" nor "trans" to our electrodes and is thus immune from these considerations.

"Inter" effect We introduce this term to describe a maneuver that impacts the membrane separating two solutions (e.g. intra- vs. extracellular). For example, the act of introducing, deleting, mutating, or otherwise changing the activity of an integral membrane protein is "in between" "cis" and "trans". Likewise, altering lipid composition or otherwise altering the chemistry of membrane lipids or their interaction with proteins or other substances would be an "inter" effect.

pH_S relaxation assessed as $(dpH_S/dt)_{Max}$ Although we have previously assessed pH_S relaxation as the time constant of a single-exponential decay, we now introduce a more general tool for describing the initial rate of pH_S decay, especially one that that deviates substantially from an SExp time course. Although we implement this tool using a double-exponential curve fit, in principle we could use any function that, near $t_{Local} = 0$, fits pH_S vs. time with a monotonic decay.

Novel diagnostic paradigms Our approaches for assessing $\Delta\Delta\Delta pH_S$ and $\Delta\Delta(dpH_i/dt)_{Max}$ provide potentially valuable for assessing the CO_2 permeability of candidate membrane proteins.

Limitations A drawback of using bCA rather than hCA IV is that, with bCA added to the bECF, the CA activity in the thin unconvected layer at the oocyte surface is probably less than in a case in which we express hCA IV at the cell surface.

In the present study, recognizing an already large matrix of experimental conditions, we did not explore bCA levels higher than 0.1 mg/ml, levels that may have generated greater $(dpH_i/dt)_{Max}$ signals. In our bCA study, we did not explore hCA II levels greater than 1 ng, levels that presumably would have generated larger ΔpH_S signals.

Unlike the trio of papers noted above, the present study does not include assessments of altered extracellular concentrations of (1) CO_2 (1.5%, 5%, 10% vs. 1.5% in present study) or (2) non-HCO_3^- buffers (1, 5, 25 mM HEPES vs. 5 mM here). Including such analyses in the present study, together with ±hAQP5, would have expanded our experimental matrix to unrealistic levels.

Musa-Aziz et al. (2014b) found that (1) increasing $[CO_2]_o$ markedly increased both ΔpH_S and $(dpH_i/dt)_{Max}$, especially in the presence of hCA IV (their figure 10). The effects of increasing $[HEPES]_o$ were more complex: (2) With 1.5% CO_2, raising $[HEPES]_o$ predictably decreased ΔpH_S (a "cis-side" effect) but did not significantly affect $(dpH_i/dt)_{Max}$ (their figure 13). (3) When they supplemented the hCA IV with extracellular bCA II, still with 1.5% CO_2, the effect of raising $[HEPES]_o$ on $(dpH_i/dt)_{Max}$ became stronger but still not significant (their figure 15). However, (4) when they work with 10% CO_2, the effects of raising $[HEPES]_o$ on $(dpH_i/dt)_{Max}$ were far stronger (their fig 17).

Based on the above observations, we suggest the following for future $(dpH_i/dt)_{Max}$ experiments on oocytes intended to examine the synergy among hAQP5, CA_i, and: In $\Delta\Delta(dpH_i/dt)_{Max}$ protocols, it would be helpful to: (a) raise $[CO_2]_o$ (e.g., to 10%), (b) explore increasing bCA beyond 0.1 mg/ml, and (c) raise $[HEPES]_o$ (e.g., to 25 mM). We also suggest that, in future $\Delta\Delta\Delta pH_S$ protocols, it would be helpful to (a) raise the $[CO_2]_o$ and (b) increase CA_i activity (e.g., employing recombinant hCA II, injecting 100 ng or more of purified hCA II).

References

Alishahi M & Kamali R (2019). A novel molecular dynamics study of CO_2 permeation through aquaporin-5. *Eur Phys J E* **42,** 151.

Blaydon DC, Lind LK, Plagnol V, Linton KJ, Smith FJD, Wilson NJ, McLean WHI, Munro CS, South AP, Leigh IM, O'Toole EA, Lundström A & Kelsell DP (2013). Mutations in AQP5, encoding a water-channel protein, cause autosomal-dominant diffuse nonepidermolytic palmoplantar keratoderma. *Am J Hum Genet* **93,** 330–335.

Boone CD, Pinard M, McKenna R & Silverman D (2014). Catalytic Mechanism of α-Class Carbonic Anhydrases: CO_2 Hydration and Proton Transfer. In *Carbonic Anhydrase: Mechanism, Regulation, Links to Disease, and Industrial Applications*, ed. Frost SC & McKenna R, Subcellular Biochemistry, pp. 31–52. Springer Netherlands, Dordrecht. Available at: https://doi.org/10.1007/978-94-007-7359-2_3.

Boron WF (1977). Intracellular pH transients in giant barnacle muscle fibers. *Am J Physiol* **233,** C61-73.

Boron WF (2010). Sharpey-Schafer lecture: Gas channels. *Exp Physiol* **95,** 1107–1130.

Boron WF & De Weer P (1976). Intracellular pH transients in squid giant axons caused by CO_2, NH_3, and metabolic inhibitors. *J Gen Physiol* **67,** 91–112.

Calvanese L, Pellegrini-Calace M & Oliva R (2013). In silico study of human aquaporin AQP11 and AQP12 channels. *Protein Sci* **22,** 455–466.

Calvetti D, Prezioso J, Occhipinti R, Boron WF & Somersalo E (2020). Computational model of electrode-induced microenvironmental effects on pH measurements near a cell membrane. *SIAM Multiscale Model Simul* **18,** 1053–1075.

Chai RC, Jiang JH, Wong AYK, Jiang F, Gao K, Vatcher G & Yu ACH (2013). AQP5 is differentially regulated in astrocytes during metabolic and traumatic injuries. *Glia* **61,** 1748–1765.

Chandy G, Zampighi GA, Kreman M & Hall JE (1997). Comparison of the water transporting properties of MIP and AQP1. *J Membr Biol* **159,** 29–39.

Chen J, Lecuona E, Briva A, Welch LC & Sznajder JI (2008). Carbonic anhydrase II and alveolar fluid reabsorption during hypercapnia. *Am J Respir Cell Mol Biol* **38,** 32–37.

Cooper GJ & Boron WF (1998). Effect of pCMBS on CO_2 permeability of *Xenopus* oocytes expressing aquaporin 1 or its C189S mutant. *Am J Physiol* **275,** C1481-1486.

Endeward V, Musa-Aziz R, Cooper GJ, Chen L-M, Pelletier MF, Virkki LV, Supuran CT, King LS, Boron WF & Gros G (2006). Evidence that aquaporin 1 is a major pathway for CO_2 transport across the human erythrocyte membrane. *FASEB J* **20,** 1974–1981.

Funaki H, Yamamoto T, Koyama Y, Kondo D, Yaoita E, Kawasaki K, Kobayashi H, Sawaguchi S, Abe H & Kihara I (1998). Localization and expression of AQP5 in cornea, serous salivary glands, and pulmonary epithelial cells. *Am J Physiol* **275,** C1151-1157.

Geyer RR, Musa-Aziz R, Qin X & Boron WF (2013). Relative CO_2/NH_3 selectivities of mammalian aquaporins 0-9. *Am J Physiol Cell Physiol* **304,** C985-994.

Gresz V, Kwon TH, Hurley PT, Varga G, Zelles T, Nielsen S, Case RM & Steward MC (2001). Identification and localization of aquaporin water channels in human salivary glands. *Am J Physiol Gastrointest Liver Physiol* **281,** G247-254.

Gutknecht J, Bisson MA & Tosteson FC (1977). Diffusion of carbon dioxide through lipid bilayer membranes: effects of carbonic anhydrase, bicarbonate, and unstirred layers. *J Gen Physiol* **69,** 779–794.

Heming TA, Geers C, Gros G, Bidani A & Crandall ED (1986). Effects of dextran-bound inhibitors on carbonic anhydrase activity in isolated rat lungs. *J Appl Physiol Bethesda Md 1985* **61,** 1849–1856.

Heymann JB & Engel A (1999). Aquaporins: Phylogeny, structure, and physiology of water channels. *News Physiol Sci Int J Physiol Prod Jointly Int Union Physiol Sci Am Physiol Soc* **14,** 187–193.

Ishibashi K (2009). New members of mammalian aquaporins: AQP10-AQP12. *Handb Exp Pharmacol*251–262.

Ishibashi K, Kuwahara M, Gu Y, Kageyama Y, Tohsaka A, Suzuki F, Marumo F & Sasaki S (1997). Cloning and functional expression of a new water channel abundantly expressed in the testis permeable to water, glycerol, and urea. *J Biol Chem* **272,** 20782–20786.

Ishibashi K, Morishita Y & Tanaka Y (2017). The evolutionary aspects of aquaporin family. In *Aquaporins*, ed. Yang B, Advances in Experimental Medicine and Biology, pp. 35–50. Springer Netherlands, Dordrecht. Available at: https://doi.org/10.1007/978-94-024-1057-0_2.

Ishida N, Hirai SI & Mita S (1997). Immunolocalization of aquaporin homologs in mouse lacrimal glands. *Biochem Biophys Res Commun* **238,** 891–895.

King LS, Kozono D & Agre P (2004). From structure to disease: the evolving tale of aquaporin biology. *Nat Rev Mol Cell Biol* **5,** 687–698.

Krane CM, Fortner CN, Hand AR, McGraw DW, Lorenz JN, Wert SE, Towne JE, Paul RJ, Whitsett JA & Menon AG (2001). Aquaporin 5-deficient mouse lungs are hyperresponsive to cholinergic stimulation. *Proc Natl Acad Sci U S A* **98,** 14114–14119.

Kreda SM, Gynn MC, Fenstermacher DA, Boucher RC & Gabriel SE (2001). Expression and localization of epithelial aquaporins in the adult human lung. *Am J Respir Cell Mol Biol* **24,** 224–234.

Kumari SS, Varadaraj M, Yerramilli VS, Menon AG & Varadaraj K (2012). Spatial expression of aquaporin 5 in mammalian cornea and lens, and regulation of its localization by phosphokinase A. *Mol Vis* **18,** 957–967.

Larsen HS, Aure MH, Peters SB, Larsen M, Messelt EB & Kanli Galtung H (2011). Localization of AQP5 during development of the mouse submandibular salivary gland. *J Mol Histol* **42,** 71–81.

Li C & Wang W (2017). Molecular Biology of Aquaporins. In *Aquaporins*, ed. Yang B, Advances in Experimental Medicine and Biology, pp. 1–34. Springer Netherlands, Dordrecht. Available at: https://doi.org/10.1007/978-94-024-1057-0_1.

Lien YH & Lai LW (1998). Respiratory acidosis in carbonic anhydrase II-deficient mice. *Am J Physiol* **274,** L301-304.

Lu J, Daly CM, Parker MD, Gill HS, Piermarini PM, Pelletier MF & Boron WF (2006). Effect of human carbonic anhydrase II on the activity of the human electrogenic Na/HCO_3 cotransporter NBCe1-A in *Xenopus* oocytes. *J Biol Chem* **281,** 19241–19250.

Ma T, Song Y, Gillespie A, Carlson EJ, Epstein CJ & Verkman AS (1999). Defective secretion of saliva in transgenic mice lacking aquaporin-5 water channels. *J Biol Chem* **274,** 20071–20074.

Matsuzaki T, Hata H, Ozawa H & Takata K (2009). Immunohistochemical localization of the aquaporins AQP1, AQP3, AQP4, and AQP5 in the mouse respiratory system. *Acta Histochem Cytochem* **42,** 159–169.

Matsuzaki T, Tajika Y, Suzuki T, Aoki T, Hagiwara H & Takata K (2003). Immunolocalization of the water channel, aquaporin-5 (AQP5), in the rat digestive system. *Arch Histol Cytol* **66,** 307–315.

Maurel C, Boursiac Y, Luu D-T, Santoni V, Shahzad Z & Verdoucq L (2015). Aquaporins in plants. *Physiol Rev* **95,** 1321–1358.

Michalek K (2016). Aquaglyceroporins in the kidney: present state of knowledge and prospects. *J Physiol Pharmacol Off J Pol Physiol Soc* **67,** 185–193.

Moss FJ & Boron WF (2020). Carbonic anhydrases enhance activity of endogenous Na-H exchangers and not the electrogenic Na/HCO_3 cotransporter NBCe1-A, expressed in *Xenopus* oocytes. *J Physiol* **598,** 5821–5856.

Moss FJ, Mahinthichaichan P, Lodowski DT, Kowatz T, Tajkhorshid E, Engel A, Boron WF & Vahedi-Faridi A (2020). Aquaporin-7: A dynamic aquaglyceroporin with greater water and glycerol permeability than its bacterial homolog GlpF. *Front Physiol*; DOI: 10.3389/fphys.2020.00728.

Moss FJ, Zhao P, Salameh AI, Taki S, Wass AB, Jacobberger JW, Huffman DE, Meyerson HJ, Occhipinti R & Boron WF (2025). Role of channels in the O_2 permeability of murine red blood cells II. Morphological and proteomic studies. *bioRxiv*; DOI: 10.1101/2025.03.05.639962.

Musa-Aziz R, Boron WF & Parker MD (2010). Using fluorometry and ion-sensitive microelectrodes to study the functional expression of heterologously-expressed ion channels and transporters in *Xenopus* oocytes. *Methods San Diego Calif* **51,** 134–145.

Musa-Aziz R, Chen L-M & Boron WF (2007). Differential effects of DIDS on the CO_2 vs NH_3 permeability of AQP1, AmtB, and RhAG. *Proc Int Congr Nephrol Rio Jan Braz.*

Musa-Aziz R, Chen L-M, Pelletier MF & Boron WF (2009). Relative CO_2/NH_3 selectivities of AQP1, AQP4, AQP5, AmtB, and RhAG. *Proc Natl Acad Sci U S A* **106,** 5406–5411.

Musa-Aziz R, Geyer RR, Moss FJ & Boron WF (2025). Mechanism of CO_2 and NH_3 transport through human aquaporin 1: Evidence for parallel CO_2 pathways. *bioRxiv*; DOI: 10.1101/2025.02.28.640247.

Musa-Aziz R, Occhipinti R & Boron WF (2014*a*). Evidence from simultaneous intracellular- and surface-pH transients that carbonic anhydrase II enhances CO_2 fluxes across *Xenopus* oocytes plasma membranes. *Am J Physiol Cell Physiol* **307,** C791-813.

Musa-Aziz R, Occhipinti R & Boron WF (2014*b*). Evidence from simultaneous intracellular- and surface-pH transients that carbonic anhydrase IV enhances CO_2 fluxes across *Xenopus* oocyte plasma membranes. *Am J Physiol Cell Physiol* **307,** C814-840.

Nakhoul NL, Davis BA, Romero MF & Boron WF (1998). Effect of expressing the water channel aquaporin-1 on the CO_2 permeability of *Xenopus* oocytes. *Am J Physiol* **274,** C543-548.

Nejsum LN, Kwon T-H, Jensen UB, Fumagalli O, Frøkiaer J, Krane CM, Menon AG, King LS, Agre PC & Nielsen S (2002). Functional requirement of aquaporin-5 in plasma membranes of sweat glands. *Proc Natl Acad Sci U S A* **99,** 511–516.

Ni Z-X, Cui J-M, Zhang N-Z & Fu B-Q (2017). Structural and evolutionary divergence of aquaporins in parasites (Review). *Mol Med Rep* **15,** 3943–3948.

Nielsen S, King LS, Christensen BM & Agre P (1997). Aquaporins in complex tissues. II. Subcellular distribution in respiratory and glandular tissues of rat. *Am J Physiol-Cell Physiol* **273,** C1549–C1561.

Occhipinti R & Boron WF (2019). Role of carbonic anhydrases and inhibitors in acid-base physiology: Insights from mathematical modeling. *Int J Mol Sci* **20,** 3841.

Occhipinti R, Musa-Aziz R & Boron WF (2014). Evidence from mathematical modeling that carbonic anhydrase II and IV enhance CO_2 fluxes across *Xenopus* oocytes plasma membranes. *Am J Physiol Cell Physiol* **307,** C841-858.

Occhipinti R, Zhao P, Moss FJ & Boron WF (2025). Role of channels in the O_2 permeability of murine red blood cells. III. Mathematical modeling and simulations. *bioRxiv*; DOI: 10.1101/2025.03.05.639964.

Parker MD, Musa-Aziz R, Rojas JD, Choi I, Daly CM & Boron WF (2008). Characterization of human SLC4A10 as an electroneutral Na^+/HCO_3^- cotransporter (NBCn2) with Cl^- self-exchange activity. *J Biol Chem* **283,** 12777–12788.

Parvin MN, Tsumura K, Akamatsu T, Kanamori N & Hosoi K (2002). Expression and localization of AQP5 in the stomach and duodenum of the rat. *Biochim Biophys Acta* **1542,** 116–124.

Procino G, Mastrofrancesco L, Sallustio F, Costantino V, Barbieri C, Pisani F, Schena FP, Svelto M & Valenti G (2011). AQP5 Is expressed In type-B intercalated cells in the collecting duct system of the rat, mouse and human kidney. *Cell Physiol Biochem* **28,** 683–692.

Purkerson JM & Schwartz GJ (2007). The role of carbonic anhydrases in renal physiology. *Kidney Int* **71,** 103–115.

Qin X & Boron WF (2012). A single-amino acid mutation converts human aquaporin 5 to an anion channel. *FASEB J* **26,** 1103.7.

Raina S, Preston GM, Guggino WB & Agre P (1995). Molecular cloning and characterization of an aquaporin cDNA from salivary, lacrimal, and respiratory tissues. *J Biol Chem* **270,** 1908–1912.

Roos A & Boron WF (1981). Intracellular pH. *Physiol Rev* **61,** 296–434.

Shinn E, Kowatz T, Vahedi-Faridi A, Boron WF & Tajkhorshid E (2024). Permeation of CO_2 through the central pore of human AQP5. *Biophys J* **123,** 265a.

Somersalo E, Occhipinti R, Boron WF & Calvetti D (2012). A reaction-diffusion model of CO_2 influx into an oocyte. *J Theor Biol* **309,** 185–203.

Steinfeld S, Cogan E, King LS, Agre P, Kiss R & Delporte C (2001). Abnormal distribution of aquaporin-5 water channel protein in salivary glands from Sjögren's syndrome patients. *Lab Investig J Tech Methods Pathol* **81,** 143–148.

Taki K, Kato H & Yoshida I (1999). Elimination of CO2 in patients with carbonic anhydrase II deficiency, with studies of respiratory function at rest. *Respir Med* **93,** 536–539.

Tsubota K, Hirai S, King LS, Agre P & Ishida N (2001). Defective cellular trafficking of lacrimal gland aquaporin-5 in Sjögren's syndrome. *Lancet Lond Engl* **357,** 688–689.

Vilas G, Krishnan D, Loganathan SK, Malhotra D, Liu L, Beggs MR, Gena P, Calamita G, Jung M, Zimmermann R, Tamma G, Casey JR & Alexander RT (2015). Increased water flux induced by an aquaporin-1/carbonic anhydrase II interaction. *Mol Biol Cell* **26,** 1106–1118.

Wang Y, Cohen J, Boron WF, Schulten K & Tajkhorshid E (2007). Exploring gas permeability of cellular membranes and membrane channels with molecular dynamics. *J Struct Biol* **157,** 534–544.

Wroblewski S (1879). On the nature of the absorption of gases. *Nature* **21,** 190–192.

Yoshimura S, Nakamura H, Horai Y, Nakajima H, Shiraishi H, Hayashi T, Takahashi T & Kawakami A (2016). Abnormal distribution of AQP5 in labial salivary glands is associated with poor saliva secretion in patients with Sjögren's syndrome including neuromyelitis optica complicated patients. *Mod Rheumatol* **26,** 384–390.

Zhang L, Yao D, Zhou F, Zhang Q, Xia Y, Wang Q, Qin A, Zhao J, Li D, Zhou L & Cao Y (2019). The structural basis for glycerol permeation by human AQP7. *bioRxiv* 858332.

Zhang YB & Chen LY (2013). In silico study of Aquaporin V: Effects and affinity of the central pore-occluding lipid. *Biophys Chem* **171,** 24–30.

Zhao P, Moss FJ, Occhipinti R, Geyer RR, Huffman DE, Gros G, Meyerson HJ & Boron W F (2025). Role of channels in the O_2 permeability of murine red blood cells. I. Stopped-flow and hematological studies. *bioRxiv*; DOI: 10.1101/2025.03.05.639948.

Additional information

Competing interests

All authors declare no conflict of interests.

Authors' contributions

D.K.W. contributed to the conception and design of the research, performed the experiments, analyzed data, and interpreted results, wrote the first draft of manuscript, prepared the figures, and edited the manuscript. F.J.M. contributed to the conception and design of the research, interpreted results, performed statistical analyses and edited the figures and manuscript. W.F.B. contributed to the conception and design of the research, interpreted results, and edited the figures and manuscript. All authors approved the final version of the manuscript, all qualify for authorship, and all those who qualify for authorship are listed.

Funding

This work was supported by NIH grants HL160857 and DK128315, and by Office of Naval Research (ONR) grant N00014-11-1-0889, N00014-14-1-0716, and N00014-15-1-2060 and a Multidisciplinary University Research Initiative (MURI) grant N00014-16-1-2535 from the DoD (to W.F.B.). The contributions of W.F.B. and F.J.M. to this work were also supported in part by a Department of Defense, Air Force Research Laboratory 711th Human Performance Wing, Studies and Analysis funding 21-023.

Acknowledgements

We thank Dale E. Huffman for computer support. We acknowledge the assistance of Gerald T. Babcock in his role as laboratory manager. W.F.B. gratefully acknowledges the support of the Myers/Scarpa endowed chair.

Statistics Tables

Statistics Table 3. For clarity within the figure panel, we present tables of *P*-values for one-way ANOVA with Tukey's post-hoc means comparison for the data presented in Figure 3. For all tables, α is 0.05 and significant *P*-values are highlighted by bolding. *A, P*-values for means comparisons of ΔpH_S upon CO_2 addition data. *B, P*-values for means comparisons of ΔpH_S upon CO_2 removal data. *C, P*-values for means comparisons of $(dpH_i/dt)_{Max}$ upon CO_2 addition data. *D, P*-values for means comparisons of $(dpH_i/dt)_{Max}$ upon CO_2 removal data.

3A, ΔpH_S upon CO_2 addition

cRNA		H_2O	hAQP5	H_2O	hAQP5	H_2O	hAQP5	H_2O
	hCA II (ng)	"Tris"	"Tris"	1	1	10	10	100
hAQP5	"Tris"	**0.00150**						
H_2O	1	0.956	**0.0391**					
hAQP5	1	**4.18×10^{-8}**	**0.00247**	**7.19×10^{-8}**				
H_2O	10	0.943	**0.0456**	1.00	**7.72×10^{-8}**			
hAQP5	10	**3.90×10^{-8}**	**7.38×10^{-4}**	**5.43×10^{-8}**	1.00	**5.60×10^{-8}**		
H_2O	100	0.947	**0.0437**	1.00	**7.56×10^{-8}**	1.00	**5.55×10^{-8}**	
hAQP5	100	**2.21×10^{-8}**	**1.34×10^{-7}**	**2.93×10^{-8}**	0.0978	**2.97×10^{-8}**	0.214	**2.95×10^{-8}**

3B, ΔpH_S upon CO_2 removal

cRNA		H_2O	hAQP5	H_2O	hAQP5	H_2O	hAQP5	H_2O
	hCA II (ng)	"Tris"	"Tris"	1	1	10	10	100
hAQP5	"Tris"	**2.03×10^{-4}**						
H_2O	1	0.992	**0.00309**					
hAQP5	1	**4.44×10^{-8}**	**0.0321**	**7.16×10^{-8}**				
H_2O	10	0.995	**0.00249**	1.00	**6.67×10^{-8}**			
hAQP5	10	**4.51×10^{-8}**	**0.0383**	**7.76×10^{-8}**	1.00	**7.15×10^{-8}**		
H_2O	100	0.994	**0.00278**	1.00	**6.91×10^{-8}**	1.00	**7.44×10^{-8}**	
hAQP5	100	**3.17×10^{-8}**	**1.50×10^{-4}**	**3.72×10^{-8}**	0.692	**3.68×10^{-8}**	0.650	**3.70×10^{-8}**

3C, $(dpH_i/dt)_{Max}$ upon CO_2 addition

cRNA		H_2O	hAQP5	H_2O	hAQP5	H_2O	hAQP5	H_2O
	hCA II (ng)	"Tris"	"Tris"	1	1	10	10	100
hAQP5	"Tris"	1.00						
H_2O	1	0.0803	0.0744					
hAQP5	1	**0.00798**	**0.00726**	0.989				
H_2O	10	**3.62×10^{-4}**	**3.25×10^{-4}**	0.624	0.979			
hAQP5	10	**3.76×10^{-5}**	**3.36×10^{-5}**	0.244	0.753	0.998		
H_2O	100	**5.69×10^{-4}**	**5.10×10^{-4}**	0.708	0.991	1.00	0.994	
hAQP5	100	**0.00210**	**0.00189**	0.905	1.00	0.999	0.938	1.00

3D, $(dpH_i/dt)_{Max}$ upon CO_2 removal

cRNA		H_2O	hAQP5	H_2O	hAQP5	H_2O	hAQP5	H_2O
	hCA II (ng)	"Tris"	"Tris"	1	1	10	10	100
hAQP5	"Tris"	1.00						
H_2O	1	0.154	0.141					
hAQP5	1	**0.0330**	**0.0295**	0.998				
H_2O	10	**0.00381**	**0.00335**	0.865	0.995			
hAQP5	10	**4.57×10^{-5}**	**3.97×10^{-4}**	0.479	0.862	0.998		
H_2O	100	**0.00160**	**0.00140**	0.721	0.972	1.00	1.00	
hAQP5	100	**0.0460**	**0.0413**	1.00	1.00	0.988	0.801	0.947

Statistics Table 5. For clarity within the figure panel, we present tables of *P*-values for one-way ANOVA with Tukey's post-hoc means comparison for the data presented in Figure 5. For all tables, α is 0.05 and significant *P*-values are highlighted by bolding. *A, P*-values for means comparisons of $(dpH_S/dt)_{Max}$ upon CO_2 addition. *B, P*-values for means comparisons of $(dpH_S/dt)_{Max}$ upon CO_2 removal. Where the displayed *P*-values is 0.00, this indicates a values less than $<2.22\times10^{-308}$. [12]

5A, $(dpH_S/dt)_{Max}$ upon CO_2 addition

cRNA		H_2O	hAQP5	H_2O	hAQP5	H_2O	hAQP5	H_2O
	hCA II (ng)	"Tris"	"Tris"	1	1	10	10	100
hAQP5	"Tris"	**4.79×10^{-4}**						
H_2O	1	0.998	**0.00518**					
hAQP5	1	**4.73×10^{-8}**	**0.104**	**7.84×10^{-8}**				
H_2O	10	0.975	**0.00655**	1.00	**4.77×10^{-8}**			
hAQP5	10	**3.42×10^{-8}**	**7.41×10^{-4}**	**4.18×10^{-8}**	0.408	**4.03×10^{-8}**		
H_2O	100	0.993	**0.0134**	1.00	**4.89×10^{-7}**	1.00	**4.78×10^{-8}**	
hAQP5	100	**2.85×10^{-8}**	**0.00**	**2.85×10^{-8}**	**4.74×10^{-8}**	**0.00**	**3.95×10^{-4}**	**0.00**

5B, $(dpH_S/dt)_{Max}$ upon CO_2 removal

cRNA		H_2O	hAQP5	H_2O	hAQP5	H_2O	hAQP5	H_2O
	hCA II (ng)	"Tris"	"Tris"	1	1	10	10	100
hAQP5	"Tris"	**0.0151**						
H_2O	1	0.999	0.0862					
hAQP5	1	**7.67×10^{-4}**	0.998	**0.00783**				
H_2O	10	0.995	0.0768	1.00	**0.00516**			
AQP5	10	**0.00116**	0.992	**0.0125**	1.00	**0.00975**		
H_2O	100	0.995	0.165	1.00	**0.00228**	1.00	**0.0303**	
AQP5	100	**3.68×10^{-8}**	**0.0114**	**4.03×10^{-7}**	**0.0280**	**1.21×10^{-7}**	0.144	**2.06×10^{-6}**

[12] 2.22×10^{-308} is the smallest possible value for double type data that a 64-bit system is able to distinguish

Statistics Table 6. For clarity within the figure panel, we present tables of *P*-values for one-way ANOVA with Tukey's post-hoc means comparison for the data presented in Figure 6. For all tables, α is 0.05 and significant *P*-values are highlighted by bolding. *A, P*-values for means comparisons of initial pH_i data. *B, P*-values for means comparisons of ΔpH_i data. *C, P*-values for means comparisons intrinsic buffering power (β_i). *D, P*-values for means comparisons of P_f data.

6A Initial pH_i

cRNA		H_2O	hAQP5	H_2O	hAQP5	H_2O	hAQP5	H_2O
	hCA II (ng)	"Tris"	"Tris"	1	1	10	10	100
hAQP5	"Tris"	0.701						
H_2O	1	0.971	0.997					
hAQP5	1	0.512	1.00	0.978				
H_2O	10	1.00	0.481	0.877	0.309			
hAQP5	10	0.703	1.00	0.998	1.00	0.484		
H_2O	100	1.00	0.569	0.925	0.385	1.00	0.572	
hAQP5	100	0.997	0.972	1.00	0.898	0.970	0.973	0.987

6B ΔpH_i

cRNA		H_2O	hAQP5	H_2O	hAQP5	H_2O	hAQP5	H_2O
	hCA II (ng)	"Tris"	"Tris"	1	1	10	10	100
hAQP5	"Tris"	1.00						
H_2O	1	1.00	1.00					
hAQP5	1	0.679	0.909	0.757				
H_2O	10	0.980	1.00	0.991	0.994			
hAQP5	10	0.0737	0.199	0.0995	0.902	0.460		
H_2O	100	1.00	1.00	1.00	0.748	0.990	0.0963	
hAQP5	100	0.480	0.767	0.563	1.00	0.960	0.976	0.554

6C β_l

cRNA		H_2O	hAQP5	H_2O	hAQP5	H_2O	hAQP5	H_2O
	hCA II (ng)	"Tris"	"Tris"	1	1	10	10	100
hAQP5	"Tris"	0.982						
H_2O	1	0.995	1.00					
hAQP5	1	1.00	0.869	0.934				
H_2O	10	0.876	0.326	0.434	0.984			
hAQP5	10	0.504	0.0905	0.137	0.782	0.998		
H_2O	100	1.00	0.928	0.970	1.00	0.960	0.685	
hAQP5	100	0.720	0.188	0.267	0.926	1.00	1.00	0.867

6D P_f

cRNA		H_2O	hAQP5	H_2O	hAQP5	H_2O	hAQP5	H_2O
	hCA II (ng)	"Tris"	"Tris"	1	1	10	10	100
hAQP5	"Tris"	**6.86×10^{-8}**						
H_2O	1	1.00	**8.93×10^{-7}**					
hAQP5	1	**1.87×10^{-6}**	1.00	**2.79×10^{-7}**				
H_2O	10	1.00	**8.76×10^{-7}**	1.00	**8.85×10^{-7}**			
hAQP5	10	**7.30×10^{-8}**	0.988	**7.23×10^{-8}**	0.996	**7.16×10^{-8}**		
H_2O	100	1.00	**8.96×10^{-7}**	1.00	**6.86×10^{-8}**	1.00	**7.25×10^{-8}**	
hAQP5	100	**7.08×10^{-8}**	1.00	**1.86×10^{-6}**	1.00	**8.93×10^{-7}**	0.999	**1.87×10^{-6}**

Statistics Table 8. For clarity within the figure panel, we present tables of *P*-values for one-way ANOVA with Tukey's post-hoc means comparison for the data presented in Figure 8. For all tables, α is 0.05 and significant *P*-values are highlighted by bolding. *A, P*-values for means comparisons of initial pH_i data. *B, P*-values for means comparisons of ΔpH_i data. *C, P*-values for means comparisons of β_l. *D, P*-values for means comparisons of P_f data.

Panels *E-H* provide descriptive statistics and means comparisons (see Methods, Statistical analysis) for comparisons of data represented by the gray, black light-blue and dark-blue bars in Figure 3 (–bCA) vs. Figure 8 (+bCA). *E*, ΔpH_i during addition of CO_2/HCO_3^-. *F*, ΔpH_i during removal of CO_2/HCO_3^-. *G*, $(dpH_i/dt)_{Max}$ during addition of CO_2/HCO_3^-. *H*, $(dpH_i/dt)_{Max}$ during addition of CO_2/HCO_3^-.

8A ΔpH_i CO_2 addition

cRNA		H_2O	hAQP5	H_2O
	hCA II (ng)	"Tris"	"Tris"	1
hAQP5	"Tris"	1.00		
H_2O	1	**0.00582**	**0.00663**	
hAQP5	1	**6.13×10^{-4}**	**6.99×10^{-4}**	0.757

8B ΔpH_i CO_2 removal

cRNA		H_2O	hAQP5	H_2O
	hCA II (ng)	"Tris"	"Tris"	1
hAQP5	"Tris"	0.996		
H_2O	1	**0.0352**	0.0560	
hAQP5	1	**0.00287**	**0.00478**	0.674

8C $(dpH_i/dt)_{Max}$ CO_2 addition

cRNA		H_2O	hAQP5	H_2O
	hCA II (ng)	"Tris"	"Tris"	1
hAQP5	"Tris"	**0.0331**		
H2O	1	**2.42×10^{-6}**	0.00171	
hAQP5	1	**2.33×10^{-5}**	0.0192	0.707

8D $(dpH_i/dt)_{Max}$ CO_2 removal

cRNA		H_2O	hAQP5	H_2O
	hCA II (ng)	"Tris"	"Tris"	1
hAQP5	"Tris"	0.571		
H2O	1	**1.42×10^{-5}**	**2.49×10^{-4}**	
hAQP5	1	**7.08×10^{-4}**	**0.0135**	0.318

8E, ΔpH_S upon CO_2 addition ±bCA in bECF (Figure 3A vs. Figure 8A)

Descriptive Stats.	**n**	**Mean**	**S.D.**	**S.E.M**				
bECF	32	0.0689	0.0422	0.00746				
bECF + bCA	24	0.286	0.0641	0.0131				
Means comparison		**Mean Diff.**	**S.E.M.**	***Q*-value**	***P*-value**	**α**	**LCL**	**UCL**
bECF vs. bECF + bCA		0.217	0.0142	21.6	**4.53×10^{-8}**	0.0500	0.188	0.245

8F, ΔpH_S upon CO_2 removal ±bCA in bECF (Figure 3B vs. Figure 8B)

Descriptive Stats.	**n**	**Mean**	**S.D.**	**S.E.M**				
bECF	32	-0.0771	0.0487	0.00861				
bECF + bCA	24	-0.386	0.0681	0.0139				
Means comparison		**Mean Diff.**	**S.E.M.**	***Q*-value**	***P*-value**	**α**	**LCL**	**UCL**
bECF vs. bECF + bCA		–0.309	0.0156	28.0	**4.53×10^{-8}**	0.0500	–0.340	–0.278

8G, $(dpH_i/dt)_{Max}$ upon CO_2 addition ±bCA in bECF (Figure 3C vs. Figure 8C)

Descriptive Stats.	**n**	**Mean**	**S.D.**	**S.E.M**				
bECF	32	–0.00315	0.00236	4.18×10^{-4}				
bECF + bCA	24	–0.00528	0.00225	4.60×10^{-4}				
Means comparison		**Mean Diff.**	**S.E.M.**	***Q*-value**	***P*-value**	**α**	**LCL**	**UCL**
bECF vs. bECF + bCA		–0.00213	6.25×10^{-4}	4.83	**0.00122**	0.0500	–0.00339	-8.81×10^{-4}

8H, $(dpH_i/dt)_{Max}$ upon CO_2 removal ±bCA in bECF (Figure 3D vs. Figure 8D)

Descriptive Stats.	**n**	**Mean**	**S.D.**	**S.E.M**				
bECF	32	0.00183	0.00125	2.22×10^{-4}				
bECF + bCA	24	0.00323	0.00161	3.29×10^{-4}				
Means comparison		**Mean Diff.**	**S.E.M.**	***Q*-value**	***P*-value**	**α**	**LCL**	**UCL**
bECF vs. bECF + bCA		0.00140	3.83×10^{-4}	5.17	$\mathbf{5.82\times10^{-7}}$	0.0500	6.32×10^{-4}	0.00217

Statistics Table 9. For clarity within the figure panel, we present tables of *P*-values for one-way ANOVA with Tukey's post-hoc means comparison for the data presented in Figure 9. For all tables, α is 0.05 and significant *P*-values are highlighted by bolding. *A, P*-values for means comparisons of $(dpH_S/dt)_{Max}$ on CO_2 addition. *B, P*-values for means comparisons of $(dpH_S/dt)_{Max}$ on CO_2 removal. *C, P*-values for means comparisons of β_i. *D, P*-values for means comparisons of P_f data.

9A $(dpH_S/dt)_{Max}$ on CO_2 addition

cRNA		H_2O	hAQP5	H_2O
	hCA II (ng)	"Tris"	"Tris"	1
hAQP5	"Tris"	0.960		
H_2O	1	**3.38×10^{-4}**	**0.00103**	
hAQP5	1	**0.00221**	**0.00674**	0.842

9B $(dpH_S/dt)_{Max}$ on CO_2 removal

cRNA		H_2O	hAQP5	H_2O
	hCA II (ng)	"Tris"	"Tris"	1
hAQP5	"Tris"	**0.0288**		
H_2O	1	0.625	0.281	
hAQP5	1	0.0604	0.984	0.461

Statistics Table 10. For clarity within the figure panel, we present tables of *P*-values for one-way ANOVA with Tukey's post-hoc means comparison for the data presented in Figure 10. For all tables, α is 0.05 and significant *P*-values are highlighted by bolding. *A, P*-values for means comparisons of initial pH_i data. *B, P*-values for means comparisons of ΔpH_i data. *C, P*-values for means comparisons of β_l. *D, P*-values for means comparisons of P_f data.

Panels *E-H* provide descriptive statistics and means comparisons (see Methods, Statistical analysis) for comparisons of data represented by the gray, black light-blue and dark-blue bars in Figure 6 (–bCA) vs. Figure 10 (+bCA). *E*, Initial pH_i. *F*, ΔpH_i amplitude on addition of CO_2/HCO_3^-. *G*, β_l. *H*, P_f.

10A initial pH_i

cRNA		H_2O	hAQP5	H_2O
	hCA II (ng)	"Tris"	"Tris"	1
hAQP5	"Tris"	0.752		
H_2O	1	1.00	0.727	
hAQP5	1	0.939	0.974	0.925

10B ΔpH_i data

cRNA		H_2O	hAQP5	H_2O
	hCA II (ng)	"Tris"	"Tris"	1
hAQP5	"Tris"	0.798		
H_2O	1	1.00	0.779	
hAQP5	1	0.486	0.949	0.465

10C Buffering power (β_i)

cRNA		H_2O	hAQP5	H_2O
	hCA II (ng)	"Tris"	"Tris"	1
hAQP5	"Tris"	0.994		
H_2O	1	1.00	0.994	
hAQP5	1	0.652	0.799	0.659

10D P_f data

cRNA		H_2O	hAQP5	H_2O
	hCA II (ng)	"Tris"	"Tris"	1
hAQP5	"Tris"	**2.10×10^{-12}**		
H_2O	1	0.999	**2.10×10^{-12}**	
hAQP5	1	**2.10×10^{-12}**	0.999	**2.10×10^{-12}**

10E, initial pH_i values ±bCA in bECF (Figure 6A vs. Figure 10A)

Descriptive Stats.	**n**	**Mean**	**S.D.**	**S.E.M**				
bECF	32	7.30	0.0551	0.00975				
bECF + bCA	24	7.31	0.0603	0.0123				
Means comparison		**Mean Diff.**	**S.E.M.**	***Q*-value**	***P*-value**	**α**	**LCL**	**UCL**
bECF vs. bECF + bCA		0.00669	0.0155	0.610	0.668	0.0500	–0.0244	0.0378

10F, ΔpH_i upon CO_2 addition ±bCA in bECF (Figure 6B vs. Figure 10B)

Descriptive Stats.	**n**	**Mean**	**S.D.**	**S.E.M**				
bECF	32	–0.258	0.0258	0.00456				
bECF + bCA	24	–0.285	0.0308	0.00628				
Means comparison		**Mean Diff.**	**S.E.M.**	***Q*-value**	***P*-value**	**α**	**LCL**	**UCL**
bECF vs. bECF + bCA		–0.0270	0.00756	5.04	**7.74×10^{-4}**	0.0500	0.0118	0.0421

10G, β_i values for oocytes ±bCA in bECF (Figure 6C vs. Figure 10C)

Descriptive Stats.	**n**	**Mean**	**S.D.**	**S.E.M**				
bECF	32	13.6	1.93	0.341				
bECF + bCA	24	11.6	1.73	0.353				
Means comparison		**Mean Diff.**	**S.E.M.**	***Q*-value**	***P*-value**	**α**	**LCL**	**UCL**
bECF vs. bECF + bCA		–2.03	0.498	5.75	**1.55×10^{-4}**	0.0500	–3.02	–1.03

10H, P_f ±bCA in bECF (Figure 6D vs. Figure 10D)

Descriptive Stats.	**n**	**Mean**	**S.D.**	**S.E.M**				
bECF	32	0.00196	0.00184	3.25×10^{-4}				
bECF + bCA	30	0.00204	0.00192	3.50×10^{-4}				
Means comparison		**Mean Diff.**	**S.E.M.**	***Q*-value**	***P*-value**	**α**	**LCL**	**UCL**
bECF vs. bECF + bCA		8.03×10^{-5}	4.77×10^{-4}	0.238	0.867	0.0500	-8.74×10^{-4}	0.00103

Supplemental Statistics Tables

Supplemental Table 3*A*. Statistics Summary for Figure 3*A*, i) Descriptive Statistics for data presented in Figure 3*A*, ΔpHs upon CO_2 addition. ii) Overall one-way ANOVA results for data presented in Figure 3*A*. DF is degrees of freedom. iii) Tukey's means comparison analysis for all data presented in Figure 3*A*. Threshold for significance α=0.05. Standard error of the mean = 0.0116. Mean difference for each comparison (Mean Diff.), lower confidence limit (LCL), upper confidence limit (UCL).

i. Descriptive Statistics

	n	Mean	Standard Deviation	SE of Mean
H_2O + Tris	8	0.0285	0.00895	0.00316
hAQP5 + Tris	8	0.0787	0.0181	0.00641
H_2O + 1 ng hCA II	8	0.0411	0.0115	0.00406
hAQP5 + 1 ng hCA II	8	0.127	0.0246	0.00869
H_2O + 10 ng hCA II	8	0.0418	0.00938	0.00332
hAQP5 + 10 ng hCA II	8	0.131	0.0262	0.00925
H_2O + 100 ng hCA II	8	0.0416	0.00948	0.00335
hAQP5 + 100 ng hCA II	8	0.160	0.0478	0.0169

ii. Overall ANOVA Table

Variation	DF	Sum of Squares	Mean Square	*F*-value	*P*-value
Between Groups	7	0.147	0.0210	39.2	2.44×10^{-19}
Within Groups	56	0.0301	5.37×10^{-4}		
Total	63	0.177			

iii. Tukey Test

Condition A	Condition B	Mean Diff.	*Q*-value	*P*-value	Sig.	LCL	UCL
hAQP5 + Tris	H_2O + Tris	0.0502	6.13	0.00150	✓	0.0137	0.0867
H_2O + 1 ng hCA II	H_2O + Tris	0.0126	1.54	0.956	–	–0.0238	0.0491
H_2O + 1 ng hCA II	hAQP5 + Tris	–0.0376	4.59	0.0391	✓	–0.0741	–0.00110
hAQP5 + 1 ng hCA II	H_2O + Tris	0.0986	12.0	4.18×10^{-8}	✓	0.0622	0.135
hAQP5 + 1 ng hCA II	hAQP5 + Tris	0.0484	5.91	0.00247	✓	0.0120	0.0849
hAQP5 + 1 ng hCA II	H_2O + 1ng hCA II	0.0860	10.5	7.19×10^{-8}	✓	0.0495	0.122
H_2O + 10 ng hCA II	H_2O + Tris	0.0133	1.63	0.943	–	–0.0232	0.0498
H_2O + 10 ng hCA II	hAQP5 + Tris	–0.0369	4.50	0.0456	✓	–0.0734	-4.10×10^{-4}
H_2O + 10 ng hCA II	H_2O + 1ng hCA II	6.88×10^{-4}	0.0839	1.00	–	–0.0358	0.0372
H_2O + 10 ng hCA II	hAQP5 + 1ng hCA II	–0.0853	10.4	7.72×10^{-8}	✓	–0.122	–0.0488
hAQP5 + 10 ng hCA II	H_2O + Tris	0.103	12.6	3.90×10^{-8}	✓	0.0664	0.139

hAQP5 + 10 ng hCA II	hAQP5 + Tris	0.0527	6.43	7.38×10^{-4}	✓	0.0162	0.0892
hAQP5 + 10 ng hCA II	H_2O + 1 ng hCA II	0.0902	11.0	5.43×10^{-8}	✓	0.0538	0.127
hAQP5 + 10 ng hCA II	hAQP5 + 1 ng hCA II	0.00424	0.518	1.00	–	–0.0322	0.0407
hAQP5 + 10 ng hCA II	H_2O + 10 ng hCA II	0.0896	10.9	5.60×10^{-8}	✓	0.0531	0.126
H_2O + 100 ng hCA II	H_2O + Tris	0.0131	1.60	0.947	–	–0.0234	0.0496
H_2O + 100 ng hCA II	hAQP5 + Tris	–0.0371	4.53	0.0437	✓	–0.0736	-6.01×10^{-4}
H_2O + 100 ng hCA II	H_2O + 1 ng hCA II	4.96×10^{-4}	0.0606	1.00	–	–0.0360	0.0370
H_2O + 100 ng hCA II	hAQP5 + 1 ng hCA II	–0.0855	10.4	7.56×10^{-8}	✓	–0.122	–0.0490
H_2O + 100 ng hCA II	H_2O + 10 ng hCA II	-1.91×10^{-4}	0.0233	1.00	–	–0.0367	0.0363
H_2O + 100 ng hCA II	hAQP5 + 10 ng hCA II	–0.0898	11.0	5.55×10^{-8}	✓	–0.126	–0.0533
hAQP5 +100 ng hCA II	H_2O + Tris	0.132	16.1	2.21×10^{-8}	✓	0.0955	0.168
hAQP5 +100 ng hCA II	hAQP5 + Tris	0.0817	9.98	1.34×10^{-7}	✓	0.0453	0.118
hAQP5 +100 ng hCA II	H_2O + 1 ng hCA II	0.119	14.6	2.93×10^{-8}	✓	0.0828	0.156
hAQP5 +100 ng hCA II	hAQP5 + 1 ng hCA II	0.0333	4.06	0.0978	–	–0.00318	0.0698
hAQP5 +100 ng hCA II	H_2O + 10 ng hCA II	0.119	14.5	2.97×10^{-8}	✓	0.0821	0.155
hAQP5 +100 ng hCA II	hAQP5 + 10 ng hCA II	0.0291	3.55	0.214	–	–0.00742	0.0655
hAQP5 +100 ng hCA II	H_2O + 100 ng hCA II	0.119	14.5	2.95×10^{-8}	✓	0.0823	0.155

Supplemental Table 3*B*. Statistics Summary for Figure 3*B*, i) Descriptive Statistics for data presented in Figure 3*B*, ΔpHs upon CO_2 removal. ii) Overall one-way ANOVA results for data presented in Figure 3*B*. DF is degrees of freedom. iii) Tukey's means comparison analysis for all data presented in Figure 3*B*. Threshold for significance α=0.05. Standard error of the mean = 0.0132. Mean difference for each comparison (Mean Diff.), lower confidence limit (LCL), upper confidence limit (UCL).

i. Descriptive Statistics

	n	Mean	Standard Deviation	SE of Mean
H_2O + Tris	8	–0.03093	0.00994	0.00352
hAQP5 + Tris	8	–0.09598	0.02688	0.0095
H_2O + 1 ng hCA II	8	–0.04167	0.01131	0.004
hAQP5 + 1 ng hCA II	8	–0.13982	0.02817	0.00996
H_2O + 10 ng hCA II	8	–0.04078	0.01032	0.00365
hAQP5 + 10 ng hCA II	8	–0.13894	0.03249	0.01149
H_2O + 100 ng hCA II	8	–0.04123	0.0107	0.00378
hAQP5 + 100 ng hCA II	8	–0.16218	0.05069	0.01792

ii. Overall ANOVA

Variation	DF	Sum of Squares	Mean Square	*F*-value	*P*-value
Between Groups	7	0.165	0.0236	33.8	6.93×10^{-18}
Within Groups	56	0.0391	6.99×10^{-4}		
Total	63	0.204			

iii. Tukey Test

Condition A	Condition B	Mean Diff.	*Q*-value	*P*-value	Sig.	LCL	UCL
hAQP5 + Tris	H_2O + Tris	–0.0650	6.96	2.03×10^{-4}	✓	–0.107	–0.0234
H_2O + 1 ng hCA II	H_2O + Tris	–0.0107	1.15	0.992	–	–0.0524	0.0309
H_2O + 1 ng hCA II	hAQP5 + Tris	0.0543	5.81	0.00309	✓	0.0127	0.0959
hAQP5 + 1 ng hCA II	H_2O + Tris	–0.109	11.7	4.44×10^{-8}	✓	–0.150	–0.0673
hAQP5 + 1 ng hCA II	hAQP5 + Tris	–0.0438	4.69	0.0321	✓	–0.0854	–0.00223
hAQP5 + 1 ng hCA II	H_2O + 1 ng hCA II	–0.0981	10.5	7.16×10^{-8}	✓	–0.140	–0.0565
H_2O + 10 ng hCA II	H_2O + Tris	–0.00985	1.05	0.995	–	–0.0515	0.0318
H_2O + 10 ng hCA II	hAQP5 + Tris	0.0552	5.91	0.00249	✓	0.0136	0.0968
H_2O + 10 ng hCA II	H_2O + 1 ng hCA II	8.96×10^{-4}	0.0959	1.00	–	–0.0407	0.0425
H_2O + 10 ng hCA II	hAQP5 + 1 ng hCA II	0.0990	10.6	6.67×10^{-8}	✓	0.0574	0.141
hAQP5 + 10 ng hCA II	H_2O + Tris	–0.108	11.6	4.51×10^{-8}	✓	–0.150	–0.0664
hAQP5 + 10 ng hCA II	hAQP5 + Tris	–0.0430	4.60	0.0383	✓	–0.0846	–0.00136

hAQP5 + 10 ng hCA II	H_2O + 1 ng hCA II	–0.0973	10.4	7.76×10^{-8}	✓	–0.139	–0.0557
hAQP5 + 10 ng hCA II	hAQP5 + 1 ng hCA II	8.74×10^{-4}	0.0935	1.00	–	–0.0407	0.0425
hAQP5 + 10 ng hCA II	H_2O + 10 ng hCA II	–0.0982	10.5	7.15×10^{-8}	✓	–0.140	–0.0566
H_2O + 100 ng hCA II	H_2O + Tris	–0.0103	1.10	0.994	–	–0.0519	0.0313
H_2O + 100 ng hCA II	hAQP5 + Tris	0.0547	5.86	0.00278	✓	0.0131	0.0964
H_2O + 100 ng hCA II	H_2O + 1 ng hCA II	4.40×10^{-4}	0.0471	1.00	–	–0.0412	0.0420
H_2O + 100 ng hCA II	hAQP5 + 1 ng hCA II	0.0986	10.5	6.91×10^{-8}	✓	0.0570	0.140
H_2O + 100 ng hCA II	H_2O + 10 ng hCA II	-4.56×10^{-4}	0.0488	1.00	–	–0.0421	0.0412
H_2O + 100 ng hCA II	hAQP5 + 10ng hCA II	0.0977	10.5	7.44×10^{-8}	✓	0.0561	0.139
hAQP5 +100 ng hCAII	H_2O + Tris	–0.131	14.0	3.17×10^{-8}	✓	–0.173	–0.0896
hAQP5 +100 ng hCA II	hAQP5 + Tris	–0.0662	7.08	1.50×10^{-4}	✓	–0.108	–0.0246
hAQP5 +100 ng hCA II	H_2O + 1 ng hCA II	–0.121	12.9	3.72×10^{-8}	✓	–0.162	–0.0789
hAQP5 +100 ng hCAII	hAQP5 + 1 ng hCA II	–0.0224	2.39	0.692	–	–0.0640	0.0192
hAQP5 +100 ng hCA II	H_2O + 10 ng hCA II	–0.121	13.0	3.68×10^{-8}	✓	–0.163	–0.0798
hAQP5 +100 ng hCA II	hAQP5 + 10 ng hCA II	–0.0232	2.49	0.650	–	–0.0648	0.0184
hAQP5 +100 ng hCA II	H_2O + 100 ng hCA II	–0.121	12.9	3.70×10^{-8}	✓	–0.163	–0.0793

Supplemental Table 3C. Statistics Summary for Figure 3*C*, i) Descriptive Statistics for data presented in Figure 3*C*, $(dpH_i/dt)_{Max}$ upon CO_2 addition. ii) Overall one-way ANOVA results for data presented in Figure 3*C*. DF is degrees of freedom. iii) Tukey's means comparison analysis for all data presented in Figure 3*C*. Threshold for significance α=0.05. Standard error of the mean = 0.0112. Mean difference for each comparison (Mean Diff.), lower confidence limit (LCL), upper confidence limit (UCL).

i. Descriptive Statistics

	n	Mean	Standard Deviation	SE of Mean
H_2O + Tris	8	–0.00126	2.08×10^{-4}	7.35×10^{-5}
hAQP5 + Tris	8	–0.00122	1.57×10^{-4}	5.55×10^{-5}
H_2O + 1 ng hCA II	8	–0.00458	0.00214	7.57×10^{-4}
hAQP5 + 1 ng hCA II	8	–0.00553	0.00171	6.06×10^{-4}
H_2O + 10 ng hCA II	8	–0.00660	0.00293	0.00104
hAQP5 + 10 ng hCA II	8	–0.00732	0.00236	8.36×10^{-4}
H_2O + 100 ng hCA II	8	–0.00645	0.0029	0.00102
hAQP5 + 100 ng hCA II	8	–0.00601	0.00318	0.00113

ii. Overall ANOVA

Variation	DF	Sum of Squares	Mean Square	*F*-value	*P*-value
Between Groups	7	3.17×10^{-4}	4.53×10^{-5}	8.98	2.25×10^{-7}
Within Groups	56	2.82×10^{-4}	5.04×10^{-6}		
Total	63	5.99×10^{-4}			

iii. Tukey Test

Condition A	Condition B	Mean Diff.	*Q*-value	*P*-value	Sig.	LCL	UCL
hAQP5 + Tris	H_2O + Tris	3.53×10^{-5}	0.0445	1.00	–	–0.00350	0.00357
H_2O + 1 ng hCA II	H_2O + Tris	–0.00332	4.18	0.0803	–	–0.00685	2.14×10^{-4}
H_2O + 1 ng hCA II	hAQP5 + Tris	–0.00335	4.23	0.0744	–	–0.00689	1.79×10^{-4}
hAQP5 + 1 ng hCA II	H_2O + Tris	–0.00427	5.38	0.00798	✓	–0.00780	-7.35×10^{-4}
hAQP5 + 1 ng hCA II	hAQP5 + Tris	–0.00430	5.42	0.00726	✓	–0.00784	-7.71×10^{-4}
hAQP5 + 1 ng hCA II	H_2O + 1 ng hCA II	-9.50×10^{-4}	1.20	0.989	–	–0.00448	0.00258
H_2O + 10 ng hCA II	H_2O + Tris	–0.00534	6.73	3.62×10^{-4}	✓	–0.00887	–0.00180
H_2O + 10 ng hCA II	hAQP5 + Tris	–0.00537	6.77	3.25×10^{-4}	✓	–0.00891	–0.00184
H_2O + 10 ng hCA II	H_2O + 1 ng hCA II	–0.00202	2.54	0.624	–	–0.00555	0.00152
H_2O + 10 ng hCA II	hAQP5 + 1 ng hCA II	–0.00107	1.35	0.979	–	–0.00460	0.00247
hAQP5 + 10 ng hCA II	H_2O + Tris	–0.00606	7.63	3.76×10^{-5}	✓	–0.00959	–0.00252
hAQP5 + 10 ng hCA II	hAQP5 + Tris	–0.00609	7.68	3.36×10^{-5}	✓	–0.00963	–0.00256

hAQP5 + 10 ng hCA II	H_2O + 1 ng hCA II	–0.00274	3.45	0.244	–	–0.00627	7.97×10^{-4}
hAQP5 + 10 ng hCA II	hAQP5 + 1 ng hCA II	–0.00179	2.25	0.753	–	–0.00532	0.00175
hAQP5 + 10 ng hCA II	H_2O + 10 ng hCA II	-7.19×10^{-4}	0.906	0.998	–	–0.00425	0.00281
H_2O + 100 ng hCA II	H_2O + Tris	–0.00519	6.54	5.69×10^{-4}	✓	–0.00872	–0.00166
H_2O + 100 ng hCA II	hAQP5 + Tris	–0.00522	6.58	5.11×10^{-4}	✓	–0.00876	–0.00169
H_2O + 100 ng hCA II	H_2O + 1ng hCA II	–0.00187	2.36	0.708	–	–0.00540	0.00166
H_2O + 100 ng hCA II	hAQP5 + 1ng hCA II	-9.20×10^{-4}	1.16	0.991	–	–0.00445	0.00261
H_2O + 100 ng hCA II	H_2O + 10ng hCA II	1.48×10^{-4}	0.187	1.00	–	–0.00339	0.00368
H_2O + 100 ng hCA II	hAQP5 + 10ng hCA II	8.67×10^{-4}	1.09	0.994	–	–0.00267	0.00440
hAQP5 +10 0ng hCA II	H_2O + Tris	–0.00475	5.98	0.00210	✓	–0.00828	–0.00121
hAQP5 +100 ng hCA II	hAQP5 + Tris	–0.00478	6.03	0.00189	✓	–0.00832	–0.00125
hAQP5 +100 ng hCA II	H_2O + 1ng hCA II	–0.00143	1.80	0.905	–	–0.00496	0.00210
hAQP5 +100 ng hCA II	hAQP5 + 1ng hCA II	-4.79×10^{-4}	0.604	1.00	–	–0.00401	0.00305
hAQP5 +100 ng hCA II	H_2O + 10ng hCA II	5.89×10^{-4}	0.743	0.999	–	–0.00294	0.00412
hAQP5 +100 ng hCA II	hAQP5 + 10ng hCA II	0.00131	1.65	0.938	–	–0.00223	0.00484
hAQP5 +100 ng hCA II	H_2O + 100ng hCA II	4.41×10^{-4}	0.556	1.00	–	–0.00309	0.00397

Supplemental Table 3*D*. Statistics Summary for Figure 3*D*, i) Descriptive Statistics for data presented in Figure 3*D*, $(dpH_i/dt)_{Max}$ upon CO_2 removal. ii) Overall one-way ANOVA results for data presented in Figure 3*D*. DF is degrees of freedom. iii) Tukey's means comparison analysis for all data presented in Figure 3*D*. Threshold for significance α=0.05. Standard error of the mean = 6.27×10^{-4}. Mean difference for each comparison (Mean Diff.), lower confidence limit (LCL), upper confidence limit (UCL).

i. Descriptive Statistics

	n	Mean	Standard Deviation	SE of Mean
H_2O + Tris	8	8.35×10^{-4}	1.34×10^{-4}	4.74×10^{-5}
hAQP5 + Tris	8	8.07×10^{-4}	6.85×10^{-5}	2.42×10^{-5}
H_2O + 1 ng hCA II	8	0.00263	0.00119	4.19×10^{-4}
hAQP5 + 1 ng hCA II	8	0.00306	8.73×10^{-4}	3.08×10^{-4}
H_2O + 10 ng hCA II	8	0.00355	0.00121	4.29×10^{-4}
hAQP5 + 10 ng hCA II	8	0.00399	0.00139	4.92×10^{-4}
H_2O + 100 ng hCA II	8	0.00373	0.00266	9.39×10^{-4}
hAQP5 + 100 ng hCA II	8	0.00297	0.00134	4.74×10^{-4}

ii. Overall ANOVA

Variation	DF	Sum of Squares	Mean Square	*F*-value	*P*-value
Between Groups	7	8.57×10^{-5}	1.22×10^{-5}	6.78	7.89×10^{-6}
Within Groups	56	1.01×10^{-4}	1.81×10^{-6}		
Total	63	1.87×10^{-4}			

iii. Tukey Test

Condition A	Condition B	Mean Diff.	*Q*-value	*P*-value	Sig.	LCL	UCL
hAQP5 + Tris	H_2O + Tris	-2.75×10^{-5}	0.0579	1.00	–	–0.00214	0.00209
H_2O + 1 ng hCA II	H_2O + Tris	0.00179	3.77	0.154	–	-3.22×10^{-4}	0.00391
H_2O + 1 ng hCA II	hAQP5 + Tris	0.00182	3.83	0.141	–	-2.95×10^{-4}	0.00394
hAQP5 + 1 ng hCA II	H_2O + Tris	0.00222	4.68	0.0329	✓	1.07×10^{-4}	0.00434
hAQP5 + 1 ng hCA II	hAQP5 + Tris	0.00225	4.74	0.0295	✓	1.34×10^{-4}	0.00437
hAQP5 + 1 ng hCA II	H_2O + 1 ng hCA II	4.29×10^{-4}	0.903	0.998	–	–0.00169	0.00255
H_2O + 10 ng hCA II	H_2O + Tris	0.00272	5.72	0.00381	✓	6.02×10^{-4}	0.00483
H_2O + 10 ng hCA II	hAQP5 + Tris	0.00275	5.78	0.00335	✓	6.29×10^{-4}	0.00486
H_2O + 10 ng hCA II	H_2O + 1ng hCA II	9.24×10^{-4}	1.94	0.865	–	–0.00119	0.00304
H_2O + 10 ng hCA II	hAQP5 + 1ng hCA II	4.95×10^{-4}	1.04	0.995	–	–0.00162	0.00261
hAQP5 + 10 ng hCA II	H_2O + Tris	0.00315	6.63	4.57×10^{-4}	✓	0.00103	0.00527
hAQP5 + 10 ng hCA II	hAQP5 + Tris	0.00318	6.69	3.97×10^{-4}	✓	0.00106	0.00529

hAQP5 + 10 ng hCA II	H_2O + 1 ng hCA II	0.00136	2.85	0.479	–	-7.59×10^{-4}	0.00347
hAQP5 + 10 ng hCA II	hAQP5 + 1 ng hCA II	9.28×10^{-4}	1.95	0.862	–	–0.00119	0.00304
hAQP5 + 10 ng hCA II	H_2O + 10 ng hCA II	4.33×10^{-4}	0.911	0.998	–	–0.00168	0.00255
H_2O + 100ng hCA II	H_2O + Tris	0.00290	6.10	0.00160	✓	7.84×10^{-4}	0.00502
H_2O + 100ng hCA II	hAQP5 + Tris	0.00293	6.16	0.00140	✓	8.11×10^{-4}	0.00504
H_2O + 100ng hCA II	H_2O + 1 ng hCA II	0.00111	2.33	0.721	–	–0.00101	0.00322
H_2O + 100ng hCA II	hAQP5 + 1 ng hCA II	6.77×10^{-4}	1.42	0.972	–	–0.00144	0.00279
H_2O + 100ng hCA II	H_2O + 10 ng hCA II	1.82×10^{-4}	0.383	1.00	–	–0.00193	0.00230
H_2O + 100ng hCA II	hAQP5 + 10 ng hCA II	-2.51×10^{-4}	0.528	1.00	–	–0.00237	0.00187
hAQP5 +100ng hCA II	H_2O + Tris	0.00214	4.50	0.0460	✓	2.19×10^{-5}	0.00425
hAQP5 +100ng hCA II	hAQP5 + Tris	0.00217	4.56	0.0413	✓	4.94×10^{-5}	0.00428
hAQP5 +100ng hCA II	H_2O + 1 ng hCA II	3.44×10^{-4}	0.724	1.00	–	–0.00177	0.00246
hAQP5 +100ng hCA II	hAQP5 + 1 ng hCA II	-8.49×10^{-5}	0.179	1.00	–	–0.00220	0.00203
hAQP5 +100ng hCA II	H_2O + 10 ng hCA II	-5.80×10^{-4}	1.22	0.988	–	–0.00270	0.00154
hAQP5 +100ng hCA II	hAQP5 + 10 ng hCA II	–0.00101	2.13	0.801	–	–0.00313	0.00110
hAQP5 +100ng hCA II	H_2O + 100 ng hCA II	-7.62×10^{-4}	1.60	0.947	–	–0.00288	0.00135

Supplemental Table 5*A*. Statistics Summary for Figure 5*A*, i) Descriptive Statistics for data presented in Figure 5*A*, $(dpH_S/dt)_{Max}$ upon CO_2 addition. ii) Overall one-way ANOVA results for data presented in Figure 5*A*. DF is degrees of freedom. iii) Tukey's means comparison analysis for all data presented in Figure 5*A*. Threshold for significance α=0.05. Standard error of the mean (SEM). Mean difference for each comparison (Mean Diff.), lower confidence limit (LCL), upper confidence limit (UCL). Where the displayed *P*-values is 0.00, this indicates a values less than $<2.22\times10^{-308}$. [13]

i. Descriptive Statistics

	n	Mean	Standard Deviation	SE of Mean
H_2O + Tris	8	-6.14×10^{-4}	1.81×10^{-4}	6.39×10^{-5}
hAQP5 + Tris	10	–0.00171	2.19×10^{-4}	6.92×10^{-5}
H_2O + 1 ng h CAII	8	-7.81×10^{-4}	3.15×10^{-4}	1.11×10^{-4}
hAQP5 + 1 ng h CAII	15	–0.00230	4.30×10^{-4}	1.11×10^{-4}
H_2O + 10 ng h CAII	10	-8.51×10^{-4}	1.48×10^{-4}	4.66×10^{-5}
hAQP5 + 10 ng h CAII	9	–0.00275	6.86×10^{-4}	2.29×10^{-4}
H_2O + 100 ng h CAII	7	-8.21×10^{-4}	2.07×10^{-4}	7.84×10^{-5}
hAQP5 + 100 ng h CAII	12	–0.00379	9.53×10^{-4}	2.75×10^{-4}

ii. Overall ANOVA

Variation	DF	Sum of Squares	Mean Square	*F*-value	*P*-value
Between Groups	7	9.44×10^{-5}	1.35×10^{-5}	52.7	1.27×10^{-25}
Within Groups	71	1.82×10^{-5}	2.56×10^{-7}		
Total	78	1.13×10^{-4}			

iii. Tukey Test

Condition A	Condition B	Mean Diff.	SEM	*Q*-value	*P*-value	Sig.	LCL	UCL
hAQP5 + Tris	H_2O + Tris	−0.00110	2.40×10^{-4}	6.49	4.79×10^{-4}	✓	–0.00214	0.00209
H_2O + 1 ng hCA II	H_2O + Tris	-1.67×10^{-4}	2.53×10^{-4}	0.933	0.998	–	-3.22×10^{-4}	0.00391
H_2O + 1 ng hCA II	hAQP5 + Tris	9.34×10^{-4}	2.40×10^{-4}	5.50	0.00518	✓	-2.95×10^{-4}	0.00394
hAQP5 + 1 ng hCA II	H_2O + Tris	−0.00168	2.21×10^{-4}	10.8	4.73×10^{-8}	✓	1.07×10^{-4}	0.00434
hAQP5 + 1 ng hCA II	hAQP5 + Tris	-5.84×10^{-4}	2.06×10^{-4}	4.00	0.104		1.34×10^{-4}	0.00437
hAQP5 + 1 ng hCA II	H_2O + 1ng hCA II	−0.00152	2.21×10^{-4}	9.69	7.84×10^{-8}	✓	–0.00169	0.00255

[13] 2.22×10^{-308} is the smallest possible value for double type data that a 64-bit system is able to distinguish

H_2O + 10 ng hCA II	H_2O + Tris	-2.37×10^{-4}	2.40×10^{-4}	1.40	0.975		6.02×10^{-4}	0.00483
H_2O + 10 ng hCA II	hAQP5 + Tris	8.64×10^{-4}	2.26×10^{-4}	5.40	0.00655	✓	6.29×10^{-4}	0.00486
H_2O + 10 ng hCA II	H_2O + 1 ng hCA II	-7.00×10^{-5}	2.40×10^{-4}	0.413	1.000	–	–0.00119	0.00304
H_2O + 10 ng hCA II	hAQP5 + 1 ng hCA II	0.00145	2.06×10^{-4}	9.92	4.77×10^{-8}	✓	–0.00162	0.00261
hAQP5 + 10 ng hCA II	H_2O + Tris	−0.00214	2.46×10^{-4}	12.3	3.42×10^{-8}	✓	0.00103	0.00527
hAQP5 + 10 ng hCA II	hAQP5 + Tris	−0.00104	2.32×10^{-4}	6.32	7.41×10^{-4}	✓	0.00106	0.00529
hAQP5 + 10 ng hCA II	H_2O + 1 ng hCA II	−0.00197	2.46×10^{-4}	11.3	4.18×10^{-8}	✓	-7.59×10^{-4}	0.00347
hAQP5 + 10 ng hCA II	hAQP5 + 1 ng hCA II	-4.54×10^{-4}	2.13×10^{-4}	3.01	0.408	–	–0.00119	0.00304
hAQP5 + 10 ng hCA II	H_2O + 10ng hCA II	−0.00190	2.32×10^{-4}	11.6	4.03×10^{-8}	✓	–0.00168	0.00255
H_2O + 100 ng hCA II	H_2O + Tris	-2.07×10^{-4}	2.62×10^{-4}	1.12	0.993		7.84×10^{-4}	0.00502
H_2O + 100ng hCA II	hAQP5 + Tris	8.94×10^{-4}	2.49×10^{-4}	5.07	0.0134	✓	8.11×10^{-4}	0.00504
H_2O + 100 ng hCA II	H_2O + 1 ng hCA II	-3.97×10^{-5}	2.62×10^{-4}	0.215	1.000	–	–0.00101	0.00322
H_2O + 100 ng hCA II	hAQP5 + 1ng hCA II	0.00148	2.32×10^{-4}	9.03	4.89×10^{-7}	✓	–0.00144	0.00279
H_2O + 100ng hCA II	H_2O + 10ng hCA II	3.03×10^{-5}	2.49×10^{-4}	0.172	1.000	–	–0.00193	0.00230
H_2O + 100 ng hCA II	hAQP5 + 10 ng hCA II	0.00193	2.55×10^{-4}	10.7	4.78×10^{-8}	✓	–0.00237	0.00187
hAQP5 +100 ng hCA II	H_2O + Tris	−0.00317	2.31×10^{-4}	19.4	0.00	✓	2.19×10^{-5}	0.00425
hAQP5 +100 ng hCA II	hAQP5 + Tris	−0.00207	2.17×10^{-4}	13.5	2.85×10^{-8}	✓	4.94×10^{-5}	0.00428
hAQP5 +100 ng hCA II	H_2O + 1 ng hCA II	−0.00301	2.31×10^{-4}	18.4	0.00	✓	–0.00177	0.00246
hAQP5 +100 ng hCA II	hAQP5 + 1 ng hCA II	−0.00149	1.96×10^{-4}	10.7	4.74×10^{-8}	✓	–0.00220	0.00203
hAQP5 +100 ng hCA II	H_2O + 10 ng hCA II	−0.00294	2.17×10^{-4}	19.2	0.00	✓	–0.00270	0.00154
hAQP5 +100 ng hCA II	hAQP5 + 10 ng hCA II	−0.00104	2.23×10^{-4}	6.56	3.95×10^{-4}	✓	–0.00313	0.00110
hAQP5 +100 ng hCA II	H_2O + 100 ng hCA II	−0.00297	2.41×10^{-4}	17.4	0.00	✓	–0.00288	0.00135

Supplemental Table 5*B*. Statistics Summary for Figure 5*B*, i) Descriptive Statistics for data presented in Figure 5*B*, $(dpH_S/dt)_{Max}$ upon CO_2 removal. ii) Overall one-way ANOVA results for data presented in Figure 5*A*. DF is degrees of freedom. iii) Tukey's means comparison analysis for all data presented in Figure 5*B*. Threshold for significance α=0.05. Standard error of the mean (SEM). Mean difference for each comparison (Mean Diff.), lower confidence limit (LCL), upper confidence limit (UCL). Where the displayed *P*-values is 0.00, this indicates a values less than $<2.22\times10^{-308}$. [14]

i. Descriptive Statistics

	n	Mean	Standard Deviation	SE of Mean
H_2O + Tris	8	4.13×10^{-4}	2.42×10^{-4}	8.55×10^{-5}
hAQP5 + Tris	10	0.00136	8.19×10^{-4}	2.59×10^{-4}
H_2O + 1 ng hCA II	8	5.84×10^{-4}	3.49×10^{-4}	1.23×10^{-4}
hAQP5 + 1 ng hCA II	15	0.00151	6.52×10^{-4}	1.68×10^{-4}
H_2O + 10 ng hCA II	10	6.17×10^{-4}	1.45×10^{-4}	4.60×10^{-5}
hAQP5 + 10 ng hCA II	9	0.00157	6.00×10^{-4}	2.00×10^{-4}
H_2O + 100 ng hCA II	7	6.33×10^{-4}	1.66×10^{-4}	6.28×10^{-5}
hAQP5 + 100 ng hCA II	12	0.00224	7.43×10^{-4}	2.14×10^{-4}

ii. Overall ANOVA

Variation	DF	Sum of Squares	Mean Square	*F*-value	*P*-value
Between Groups	7	2.96×10^{-5}	4.23×10^{-6}	13.3	7.77×10^{-11}
Within Groups	71	2.26×10^{-5}	3.18×10^{-7}		
Total	78	5.22×10^{-5}			

iii. Tukey Test

Condition A	Condition B	Mean Diff.	SEM	*Q*-value	*P*-value	Sig.	LCL	UCL
hAQP5 + Tris	H_2O + Tris	9.49×10^{-4}	2.67×10^{-4}	5.02	0.0151	✓	1.14×10^{-4}	0.00178
H_2O + 1 ng hCA II	H_2O + Tris	1.71×10^{-4}	2.82×10^{-4}	0.859	0.999	–	-7.09×10^{-4}	0.00105
H_2O + 1 ng hCA II	hAQP5 + Tris	-7.78×10^{-4}	2.67×10^{-4}	4.11	0.0862		–0.00161	5.76×10^{-5}
hAQP5 + 1 ng hCA II	H_2O + Tris	0.00110	2.47×10^{-4}	6.30	7.67×10^{-4}	✓	3.29×10^{-4}	0.00187
hAQP5 + 1 ng hCA II	hAQP5 + Tris	1.51×10^{-4}	2.30×10^{-4}	0.928	0.998	–	-5.68×10^{-4}	8.70×10^{-4}
hAQP5 + 1 ng hCA II	H_2O + 1ng hCA II	9.29×10^{-4}	2.47×10^{-4}	5.32	0.00783	✓	1.58×10^{-4}	0.00170

[14] 2.22×10^{-308} is the smallest possible value for double type data that a 64-bit system is able to distinguish

H_2O + 10 ng hCA II	H_2O + Tris	2.04×10^{-4}	2.67×10^{-4}	1.08	0.995	–	-6.31×10^{-4}	0.00104
H_2O + 10 ng hCA II	hAQP5 + Tris	-7.45×10^{-4}	2.52×10^{-4}	4.18	0.0768	–	–0.00153	4.23×10^{-5}
H_2O + 10 ng hCA II	H_2O + 1 ng hCA II	3.25×10^{-5}	2.67×10^{-4}	0.172	1.000	–	-8.03×10^{-4}	8.68×10^{-4}
H_2O + 10 ng hCA II	hAQP5 + 1 ng hCA II	-8.96×10^{-4}	2.30×10^{-4}	5.51	0.00516	✓	–0.00161	-1.77×10^{-4}
hAQP5 + 10 ng hCA II	H_2O + Tris	0.00116	2.74×10^{-4}	5.99	0.00166	✓	3.04×10^{-4}	0.00202
hAQP5 + 10 ng hCA II	hAQP5 + Tris	2.11×10^{-4}	2.59×10^{-4}	1.15	0.992	–	-5.98×10^{-4}	0.00102
hAQP5 + 10 ng hCA II	H_2O + 1 ng hCA II	9.89×10^{-4}	2.74×10^{-4}	5.11	0.0125	✓	1.33×10^{-4}	0.00184
hAQP5 + 10 ng hCA II	hAQP5 + 1 ng hCA II	6.02×10^{-5}	2.38×10^{-4}	0.358	1.000	–	-6.82×10^{-4}	8.03×10^{-4}
hAQP5 + 10 ng hCA II	H_2O + 10ng hCA II	9.56×10^{-4}	2.59×10^{-4}	5.22	0.00975	✓	1.47×10^{-4}	0.00177
H_2O + 100 ng hCA II	H_2O + Tris	2.20×10^{-4}	2.92×10^{-4}	1.07	0.995	–	-6.91×10^{-4}	0.00113
H_2O + 100ng hCA II	hAQP5 + Tris	-7.28×10^{-4}	2.78×10^{-4}	3.71	0.165	–	–0.00160	1.39×10^{-4}
H_2O + 100 ng hCA II	H_2O + 1 ng hCA II	4.91×10^{-5}	2.92×10^{-4}	0.238	1.000	–	-8.62×10^{-4}	9.60×10^{-4}
H_2O + 100 ng hCA II	hAQP5 + 1ng hCA II	-8.79×10^{-4}	2.58×10^{-4}	4.82	0.0228	✓	–0.00169	–7.36E-5
H_2O + 100ng hCA II	H_2O + 10ng hCA II	1.66×10^{-5}	2.78×10^{-4}	0.0847	1.00	–	-8.51×10^{-4}	8.84×10^{-5}
H_2O + 100 ng hCA II	hAQP5 + 10 ng hCA II	-9.40×10^{-4}	2.84×10^{-4}	4.68	0.0303	✓	–0.00183	-5.25×10^{-5}
hAQP5 +100 ng hCA II	H_2O + Tris	0.00183	2.57×10^{-4}	10.0	3.68×10^{-8}	✓	0.00102	0.00263
hAQP5 +100 ng hCA II	hAQP5 + Tris	8.79×10^{-4}	2.41×10^{-4}	5.15	0.0114	✓	1.25×10^{-4}	0.00163
hAQP5 +100 ng hCA II	H_2O + 1 ng hCA II	0.00166	2.57×10^{-4}	9.11	4.03×10^{-7}	✓	8.53×10^{-4}	0.00246
hAQP5 +100 ng hCA II	hAQP5 + 1 ng hCA II	7.28×10^{-4}	2.18×10^{-4}	4.72	0.0280	✓	4.63×10^{-5}	0.00141
hAQP5 +100 ng hCA II	H_2O + 10 ng hCA II	0.00162	2.41×10^{-4}	9.52	1.21×10^{-7}	✓	8.70×10^{-4}	0.00238
hAQP5 +100 ng hCA II	hAQP5 + 10 ng hCA II	6.68×10^{-4}	2.49×10^{-4}	3.80	0.144	–	-1.08×10^{-4}	0.00144
hAQP5 +100 ng hCA II	H_2O + 100 ng hCA II	0.00161	2.68×10^{-4}	8.48	2.16×10^{-6}	–	7.70×10^{-4}	0.00244

Supplemental Table 6*A*. Statistics Summary for Figure 6*A*, i) Descriptive Statistics for data presented in Figure 6A, Initial pH_i. ii) Overall one-way ANOVA results for data presented in Figure 6*A*. DF is degrees of freedom. iii) Tukey's means comparison analysis for all data presented in Figure 6*A*. Threshold for significance α=0.05. Standard error of the mean = 0.0262. Mean difference for each comparison (Mean Diff.), lower confidence limit (LCL), upper confidence limit (UCL).

i. Descriptive Statistics

	n	Mean	Standard Deviation	SE of Mean
H_2O + Tris	8	7.27	0.0486	0.0172
hAQP5 + Tris	8	7.31	0.0512	0.0181
H_2O + 1 ng hCA II	8	7.30	0.0614	0.0217
hAQP5 + 1 ng hCA II	8	7.32	0.0512	0.0181
H_2O + 10 ng hCA II	8	7.26	0.0452	0.0160
hAQP5 + 10 ng hCA II	8	7.31	0.0352	0.0124
H_2O + 100 ng hCA II	8	7.26	0.0614	0.0217
hAQP5 + 100 ng hCA II	8	7.29	0.0593	0.0210

ii. Overall ANOVA Table

Variation	DF	Sum of Squares	Mean Square	*F*-value	*P*-value
Between Groups	7	0.0324	0.00462	1.68	0.131
Within Groups	56	0.154	0.00274		
Total	63	0.186			

iii. Tukey Test

Condition A	Condition B	Mean Diff.	*Q*-value	*P*-value	Sig.	LCL	UCL
hAQP5 + Tris	H_2O + Tris	0.0440	2.37	0.701	–	–0.0385	0.126
H_2O + 1 ng hCA II	H_2O + Tris	0.0264	1.43	0.971	–	–0.0561	0.109
H_2O + 1 ng hCA II	hAQP5 + Tris	–0.0176	0.948	0.997	–	–0.100	0.0649
hAQP5 + 1 ng hCA II	H_2O + Tris	0.0515	2.78	0.512	–	–0.0309	0.134
hAQP5 + 1 ng hCA II	hAQP5 + Tris	0.00759	0.410	1.000	–	–0.0749	0.0900
hAQP5 + 1 ng hCA II	H_2O + 1 ng hCA II	0.0252	1.36	0.978	–	–0.0573	0.108
H_2O + 10 ng hCA II	H_2O + Tris	–0.00884	0.477	1.000	–	–0.0913	0.0736
H_2O + 10 ng hCA II	hAQP5 + Tris	–0.0528	2.85	0.481	–	–0.135	0.0297
H_2O + 10 ng hCA II	H_2O + 1 ng hCA II	–0.0352	1.90	0.877	–	–0.118	0.0472
H_2O + 10 ng hCA II	hAQP5 + 1 ng hCA II	–0.0604	3.26	0.309	–	–0.143	0.0221
hAQP5 + 10 ng hCA II	H_2O + Tris	0.0439	2.37	0.703	–	–0.0386	0.126
hAQP5 + 10 ng hCA II	hAQP5 + Tris	-1.08×10^{-4}	0.00586	1.00	–	–0.0826	0.0824

hAQP5 + 10 ng hCA II	H_2O + 1 ng hCA II	0.0175	0.943	0.998	–	–0.0650	0.0999
hAQP5 + 10 ng hCA II	hAQP5 + 1 ng hCA II	–0.00770	0.416	1.000	–	–0.0902	0.0748
hAQP5 + 10 ng hCA II	H_2O + 10ng hCA II	0.0527	2.84	0.484	–	–0.0298	0.135
H_2O + 100 ng hCA II	H_2O + Tris	–0.00531	0.287	1.000	–	–0.0878	0.0772
H_2O + 100ng hCA II	hAQP5 + Tris	–0.0493	2.66	0.569	–	–0.132	0.0332
H_2O + 100 ng hCA II	H_2O + 1 ng hCA II	–0.0317	1.71	0.925	–	–0.114	0.0508
H_2O + 100 ng hCA II	hAQP5 + 1 ng hCA II	–0.0569	3.07	0.385	–	–0.139	0.0256
H_2O + 100ng hCA II	H_2O + 10 ng hCA II	0.00353	0.191	1.000	–	–0.0789	0.0860
H_2O + 100 ng hCA II	hAQP5 + 10 ng hCA II	–0.0492	2.65	0.572	–	–0.132	0.0333
hAQP5 +100 ng hCA II	H_2O + Tris	0.0177	0.957	0.997	–	–0.0647	0.100
hAQP5 +100 ng hCA II	hAQP5 + Tris	–0.0262	1.42	0.972	–	–0.109	0.0562
hAQP5 +100 ng hCA II	H_2O + 1 ng hCA II	–0.00866	0.468	1.000	–	–0.0911	0.0738
hAQP5 +100 ng hCA II	hAQP5 + 1 ng hCA II	–0.0338	1.83	0.898	–	–0.116	0.0486
hAQP5 +100 ng hCA II	H_2O + 10 ng hCA II	0.0266	1.43	0.970	–	–0.0559	0.109
hAQP5 +100 ng hCA II	hAQP5 + 10 ng hCA II	–0.0261	1.41	0.973	–	–0.109	0.0563
hAQP5 +100 ng hCA II	H_2O + 100 ng hCA II	0.0230	1.24	0.987	–	–0.0594	0.105

Supplemental Table 6*B*. Statistics Summary for Figure 6*B*, i) Descriptive Statistics for data presented in Figure 6B, ΔpH_i. ii) Overall one-way ANOVA results for data presented in Figure 6*B*. DF is degrees of freedom. iii) Tukey's means comparison analysis for all data presented in Figure 6*B*. Threshold for significance α=0.05. Standard error of the mean = 0.0137. Mean difference for each comparison (Mean Diff.), lower confidence limit (LCL), upper confidence limit (UCL).

i. Descriptive Statistics

	n	Mean	Standard Deviation	SE of Mean
H_2O + Tris	8	0.251	0.0220	0.00778
hAQP5 + Tris	8	0.257	0.0253	0.00894
H_2O + 1 ng hCA II	8	0.252	0.0296	0.0105
hAQP5 + 1 ng hCA II	8	0.274	0.0234	0.00828
H_2O + 10 ng hCA II	8	0.264	0.0209	0.00740
hAQP5 + 10 ng hCA II	8	0.292	0.0238	0.00841
H_2O + 100 ng hCA II	8	0.252	0.0254	0.00898
hAQP5 + 100 ng hCAII	8	0.278	0.0422	0.0149

ii. Overall ANOVA Table

Variation	DF	Sum of Squares	Mean Square	*F*-value	*P*-value
Between Groups	7	0.0125	0.00178	2.39	0.0329
Within Groups	56	0.0419	7.47×10^{-4}		
Total	63	0.0543			

iii. Tukey Test

Condition A	Condition B	Mean Diff.	*Q*-value	*P*-value	Sig.	LCL	UCL
hAQP5 + Tris	H_2O + Tris	0.00615	0.636	1.000	–	–0.0369	0.0492
H_2O + 1 ng hCA II	H_2O + Tris	0.00173	0.179	1.000	–	–0.0413	0.0448
H_2O + 1 ng hCA II	hAQP5 + Tris	–0.00442	0.457	1.000	–	–0.0475	0.0386
hAQP5 + 1 ng hCA II	H_2O + Tris	0.0234	2.42	0.679	–	–0.0196	0.0664
hAQP5 + 1 ng hCA II	hAQP5 + Tris	0.0173	1.79	0.909	–	–0.0258	0.0603
hAQP5 + 1 ng hCA II	H_2O + 1 ng hCA II	0.0217	2.24	0.757	–	–0.0214	0.0647
H_2O + 10 ng hCA II	H_2O + Tris	0.0129	1.34	0.980	–	–0.0301	0.0560
H_2O + 10 ng hCA II	hAQP5 + Tris	0.00677	0.700	1.000	–	–0.0363	0.0498
H_2O + 10 ng hCA II	H_2O + 1 ng hCA II	0.0112	1.16	0.991	–	–0.0319	0.0542
H_2O + 10 ng hCA II	hAQP5 + 1 ng hCA II	–0.0105	1.09	0.994	–	–0.0535	0.0325
hAQP5 + 10 ng hCA II	H_2O + Tris	0.0409	4.23	0.0737	–	–0.00212	0.0840
hAQP5 + 10 ng hCA II	hAQP5 + Tris	0.0348	3.60	0.199	–	–0.00828	0.0778

hAQP5 + 10 ng hCA II	H_2O + 1 ng hCA II	0.0392	4.05	0.0995	–	–0.00386	0.0822
hAQP5 + 10 ng hCA II	hAQP5 + 1 ng hCA II	0.0175	1.81	0.902	–	–0.0255	0.0605
hAQP5 + 10 ng hCA II	H_2O + 10ng hCA II	0.0280	2.90	0.460	–	–0.0150	0.0710
H_2O + 100 ng hCA II	H_2O + Tris	0.00154	0.160	1.000	–	–0.0415	0.0446
H_2O + 100ng hCA II	hAQP5 + Tris	–0.00461	0.477	1.000	–	–0.0476	0.0384
H_2O + 100 ng hCA II	H_2O + 1 ng hCA II	-1.90×10^{-4}	0.0197	1.00	–	–0.0432	0.0428
H_2O + 100 ng hCA II	hAQP5 + 1ng hCA II	–0.0219	2.26	0.748	–	–0.0649	0.0212
H_2O + 100ng hCA II	H_2O + 10ng hCA II	–0.0114	1.18	0.990	–	–0.0544	0.0317
H_2O + 100 ng hCA II	hAQP5 + 10 ng hCA II	–0.0394	4.07	0.0963	–	–0.0824	0.00367
hAQP5 +100 ng hCA II	H_2O + Tris	0.0276	2.85	0.480	–	–0.0155	0.0706
hAQP5 +100 ng hCA II	hAQP5 + Tris	0.0214	2.22	0.767	–	–0.0216	0.0645
hAQP5 +100 ng hCA II	H_2O + 1 ng hCA II	0.0258	2.67	0.563	–	–0.0172	0.0689
hAQP5 +100 ng hCA II	hAQP5 + 1 ng hCA II	0.00417	0.431	1.000	–	–0.0389	0.0472
hAQP5 +100 ng hCA II	H_2O + 10 ng hCA II	0.0147	1.52	0.960	–	–0.0284	0.0577
hAQP5 +100 ng hCA II	hAQP5 + 10 ng hCA II	–0.0133	1.38	0.976	–	–0.0564	0.0297
hAQP5 +100 ng hCA II	H_2O + 100 ng hCA II	0.0260	2.69	0.554	–	–0.0170	0.0691

Supplemental Table 6*C*. Statistics Summary for Figure 6*C*, i) Descriptive Statistics for data presented in Figure 6*C*, β_i. ii) Overall one-way ANOVA results for data presented in Figure 6*C*. DF is degrees of freedom. iii) Tukey's means comparison analysis for all data presented in Figure 6*C*. Threshold for significance α=0.05. Standard error of the mean = 0.942. Mean difference for each comparison (Mean Diff.), lower confidence limit (LCL), upper confidence limit (UCL).

i. Descriptive Statistics

	n	Mean	Standard Deviation	SE of Mean
H_2O + Tris	8	13.4	2.20	0.779
hAQP5 + Tris	8	14.2	2.14	0.758
H_2O + 1 ng hCA II	8	14.1	2.07	0.731
hAQP5 + 1 ng hCA II	8	12.9	1.21	0.427
H_2O + 10 ng hCA II	8	12.1	2.03	0.718
hAQP5 + 10 ng hCA II	8	11.5	1.23	0.435
H_2O + 100 ng hCA II	8	13.1	2.26	0.799
hAQP5 + 100 ng hCA II	8	11.8	1.57	0.556

ii. Overall ANOVA Table

Variation	DF	Sum of Squares	Mean Square	*F*-value	*P*-value
Between Groups	7	57.6	8.22	2.32	0.0379
Within Groups	56	199	3.55		
Total	63	256			

iii. Tukey Test

Condition A	Condition B	Mean Diff.	*Q*-value	*P*-value	Sig.	LCL	UCL
hAQP5 + Tris	H_2O + Tris	0.873	1.31	0.982	–	–2.09	3.84
H_2O + 1 ng hCA II	H_2O + Tris	0.699	1.05	0.995	–	–2.27	3.67
H_2O + 1 ng hCA II	hAQP5 + Tris	–0.173	0.260	1.000	–	–3.14	2.79
hAQP5 + 1 ng hCA II	H_2O + Tris	–0.414	0.621	1.000	–	–3.38	2.55
hAQP5 + 1 ng hCA II	hAQP5 + Tris	–1.29	1.93	0.869	–	–4.25	1.68
hAQP5 + 1 ng hCA II	H_2O + 1 ng hCA II	–1.11	1.67	0.934	–	–4.08	1.85
H_2O + 10 ng hCA II	H_2O + Tris	–1.27	1.91	0.876	–	–4.24	1.70
H_2O + 10 ng hCA II	hAQP5 + Tris	–2.14	3.22	0.326	–	–5.11	0.824
H_2O + 10 ng hCA II	H_2O + 1 ng hCA II	–1.97	2.96	0.434	–	–4.93	0.997
H_2O + 10 ng hCA II	hAQP5 + 1 ng hCA II	–0.856	1.28	0.984	–	–3.82	2.11
hAQP5 + 10 ng hCA II	H_2O + Tris	–1.87	2.80	0.504	–	–4.83	1.10
hAQP5 + 10 ng hCA II	hAQP5 + Tris	–2.74	4.11	0.0905	–	–5.70	0.227
hAQP5 + 10 ng hCA II	H_2O + 1 ng hCA II	–2.57	3.85	0.137	–	–5.53	0.401

hAQP5 + 10 ng hCA II	hAQP5 + 1 ng hCA II	–1.45	2.18	0.782	–	–4.42	1.51
hAQP5 + 10 ng hCA II	H_2O + 10ng hCA II	–0.597	0.895	0.998	–	–3.56	2.37
H_2O + 100 ng hCA II	H_2O + Tris	–0.261	0.392	1.000	–	–3.23	2.71
H_2O + 100ng hCA II	hAQP5 + Tris	–1.13	1.70	0.928	–	–4.10	1.83
H_2O + 100 ng hCA II	H_2O + 1 ng hCA II	–0.960	1.44	0.970	–	–3.93	2.01
H_2O + 100 ng hCA II	hAQP5 + 1ng hCA II	0.153	0.229	1.000	–	–2.81	3.12
H_2O + 100ng hCA II	H_2O + 10ng hCA II	1.01	1.51	0.960	–	–1.96	3.97
H_2O + 100 ng hCA II	hAQP5 + 10 ng hCA II	1.60	2.41	0.685	–	–1.36	4.57
hAQP5 +100 ng hCA II	H_2O + Tris	–1.55	2.33	0.720	–	–4.52	1.41
hAQP5 +100 ng hCA II	hAQP5 + Tris	–2.42	3.64	0.188	–	–5.39	0.542
hAQP5 +100 ng hCA II	H_2O + 1 ng hCA II	–2.25	3.38	0.267	–	–5.22	0.715
hAQP5 +100 ng hCA II	hAQP5 + 1 ng hCA II	–1.14	1.71	0.926	–	–4.10	1.83
hAQP5 +100 ng hCA II	H_2O + 10 ng hCA II	–0.282	0.424	1.000	–	–3.25	2.68
hAQP5 +100 ng hCA II	hAQP5 + 10 ng hCA II	0.314	0.472	1.000	–	–2.65	3.28
hAQP5 +100 ng hCA II	H_2O + 100 ng hCA II	–1.29	1.94	0.867	–	–4.26	1.68

Supplemental Table 6*D*. Statistics Summary for Figure 6*D*, i) Descriptive Statistics for data presented in Figure 6*D*, P_f. ii) Overall one-way ANOVA results for data presented in Figure 6*D*. DF is degrees of freedom. iii) Tukey's means comparison analysis for all data presented in Figure 6*D*. Threshold for significance α=0.05. Standard error of the mean = 1.68×10^{-4}. Mean difference for each comparison (Mean Diff.), lower confidence limit (LCL), upper confidence limit (UCL).

i. Descriptive Statistics

	n	Mean	Standard Deviation	SE of Mean
H_2O + Tris	8	1.60×10^{-4}	9.95×10^{-5}	3.52×10^{-5}
hAQP5 + Tris	8	0.00373	4.41×10^{-4}	1.56×10^{-4}
H_2O + 1 ng hCA II	8	1.90×10^{-4}	1.10×10^{-4}	3.90×10^{-5}
hAQP5 + 1 ng hCA II	8	0.00376	4.48×10^{-4}	1.58×10^{-4}
H_2O + 10 ng hCA II	8	2.35×10^{-4}	2.01×10^{-4}	7.11×10^{-5}
hAQP5 + 10 ng hCA II	8	0.00388	5.32×10^{-4}	1.88×10^{-4}
H_2O + 100 ng hCA II	8	1.82×10^{-4}	1.50×10^{-4}	5.31×10^{-5}
hAQP5 + 100 ng hCA II	8	0.00378	3.80×10^{-4}	1.34×10^{-4}

ii. Overall ANOVA Table

Variation	DF	Sum of Squares	Mean Square	*F*-value	*P*-value
Between Groups	7	2.07×10^{-4}	2.96×10^{-5}	261	2.53×10^{-4}
Within Groups	56	6.35×10^{-6}	1.13×10^{-7}		
Total	63	2.13×10^{-4}			

iii. Tukey Test

Condition A	Condition B	Mean Diff.	*Q*-value	*P*-value	Sig.	LCL	UCL
hAQP5 + Tris	H_2O + Tris	0.00357	30.0	6.86×10^{-8}	✓	0.00304	0.00410
H_2O + 1 ng hCA II	H_2O + Tris	3.02×10^{-5}	0.254	1.00	–	-5.00×10^{-4}	5.60×10^{-4}
H_2O + 1 ng hCA II	hAQP5 + Tris	–0.00354	29.8	8.93×10^{-7}	✓	–0.00407	–0.00301
hAQP5 + 1 ng hCA II	H_2O + Tris	0.00360	30.2	1.87×10^{-6}	✓	0.00307	0.00413
hAQP5 + 1 ng hCA II	hAQP5 + Tris	2.33×10^{-5}	0.196	1.00	–	-5.07×10^{-4}	5.53×10^{-4}
hAQP5 + 1 ng hCA II	H_2O + 1ng hCA II	0.00357	30.0	2.79×10^{-7}	✓	0.00304	0.00410
H_2O + 10 ng hCA II	H_2O + Tris	7.45×10^{-5}	0.626	1.00	–	-4.56×10^{-4}	6.05×10^{-4}
H_2O + 10 ng hCA II	hAQP5 + Tris	–0.00350	29.4	8.76×10^{-7}	✓	–0.00403	–0.00297
H_2O + 10 ng hCA II	H_2O + 1 ng hCA II	4.43×10^{-5}	0.372	1.00	–	-4.86×10^{-4}	5.74×10^{-4}
H_2O + 10 ng hCA II	hAQP5 + 1 ng hCA II	–0.00352	29.6	8.85×10^{-7}	✓	–0.00405	–0.00299
hAQP5 + 10 ng hCA II	H_2O + Tris	0.00372	31.2	7.30×10^{-8}	✓	0.00319	0.00425
hAQP5 + 10 ng hCA II	hAQP5 + Tris	1.46×10^{-4}	1.23	0.988	–	-3.84×10^{-4}	6.77×10^{-4}
hAQP5 + 10 ng hCA II	H_2O + 1 ng hCA II	0.00369	31.0	7.23×10^{-8}	✓	0.00316	0.00422

hAQP5 + 10 ng hCA II	hAQP5 + 1 ng hCA II	1.23×10^{-4}	1.03	0.996	–	$^{-4}.07\times10^{-4}$	6.53×10^{-4}
hAQP5 + 10 ng hCA II	H_2O + 10ng hCA II	0.00364	30.6	7.16×10^{-8}	✓	0.00311	0.00418
H_2O + 100 ng hCA II	H_2O + Tris	2.18×10^{-5}	0.183	1.000	–	-5.08×10^{-4}	5.52×10^{-4}
H_2O + 100ng hCA II	hAQP5 + Tris	–0.00355	29.8	8.96×10^{-7}	✓	–0.00408	–0.00302
H_2O + 100 ng hCA II	H_2O + 1 ng hCA II	-8.37×10^{-6}	0.0703	1.00	–	-5.38×10^{-4}	5.22×10^{-4}
H_2O + 100 ng hCA II	hAQP5 + 1 ng hCA II	–0.00357	30.0	6.86×10^{-8}	✓	–0.00410	–0.00304
H_2O + 100ng hCA II	H_2O + 10 ng hCA II	-5.27×10^{-5}	0.442	1.00	–	-5.83×10^{-4}	4.77×10^{-4}
H_2O + 100 ng hCA II	hAQP5 + 10 ng hCA II	–0.00370	31.1	7.25×10^{-8}	✓	–0.00423	–0.00317
hAQP5 +100 ng hCA II	H_2O + Tris	0.00362	30.4	7.08×10^{-8}	✓	0.00309	0.00415
hAQP5 +100 ng hCA II	hAQP5 + Tris	4.36×10^{-5}	0.366	1.00	–	-4.87×10^{-4}	5.74×10^{-4}
hAQP5 +100 ng hCA II	H_2O + 1 ng hCA II	0.00359	30.1	1.86×10^{-6}	✓	0.00306	0.00412
hAQP5 +100 ng hCA II	hAQP5 + 1 ng hCA II	2.03×10^{-5}	0.170	1.00	–	-5.10×10^{-4}	5.50×10^{-4}
hAQP5 +100 ng hCA II	H_2O + 10 ng hCA II	0.00354	29.7	8.93×10^{-7}	✓	0.00301	0.00407
hAQP5 +100 ng hCA II	hAQP5 + 10 ng hCA II	-1.03×10^{-4}	0.864	0.999	–	-6.33×10^{-4}	4.27×10^{-4}
hAQP5 +100 ng hCA II	H_2O + 100 ng hCA II	0.00359	30.2	1.87×10^{-6}	✓	0.00306	0.00412

Supplemental Table 8*A*. Statistics Summary for Figure 8*A*, i) Descriptive Statistics for data presented in Figure 8*A*, ΔpHS upon CO2 addition. ii) Overall one-way ANOVA results for data presented in **Figure 8*A***. DF is degrees of freedom. iii) Tukey's means comparison analysis for all data presented in **Figure 8*A***. Threshold for significance α=0.05. Standard error of the mean = 0.0235. Mean difference for each comparison (Mean Diff.), lower confidence limit (LCL), upper confidence limit (UCL).

i. *Descriptive Statistics*

	n	Mean	Standard Deviation	SE of Mean
H_2O + Tris	6	0.235	0.235	0.0112
hAQP5 + Tris	6	0.236	0.236	0.00784
H_2O + 1ng hCA II	6	0.324	0.324	0.0196
hAQP5 + 1ng hCA II	6	0.347	0.347	0.0230

ii. Overall ANOVA Table

Variation	DF	Sum of Squares	Mean Square	*F*-value	*P*-value
Between Groups	3	0.0614	0.0205	12.4	8.35×10^{-5}
Within Groups	20	0.0330	0.00165		
Total	23	0.0944			

iii. Tukey Test

Condition A	Condition B	Mean Diff.	*Q*-value	*P*-value	Sig.	LCL	UCL
hAQP5 + Tris	H_2O + Tris	0.00134	0.0810	1.000	–	–0.0643	0.0670
H_2O + 1 ng hCA II	H_2O + Tris	0.0889	5.36	0.00582	✓	0.0232	0.155
H_2O + 1 ng hCA II	hAQP5 + Tris	0.0875	5.28	0.00663	✓	0.0219	0.153
hAQP5 + 1 ng hCA II	H_2O + Tris	0.112	6.76	6.13×10^{-4}	✓	0.0464	0.178
hAQP5 + 1 ng hCA II	hAQP5 + Tris	0.111	6.68	6.99×10^{-4}	✓	0.0451	0.176
hAQP5 + 1 ng hCA II	H_2O + 1 ng hCA II	0.0232	1.40	0.757	–	–0.0425	0.0888

Supplemental Table 8*B*. Statistics Summary for Figure 8*B*, i) Descriptive Statistics for data presented in Figure 8*B*, ΔpHs upon CO_2 removal. ii) Overall one-way ANOVA results for data presented in Figure 8*B*. DF is degrees of freedom. iii) Tukey's means comparison analysis for all data presented in Figure 8*B*. Threshold for significance α=0.05. Standard error of the mean = 0.0282. Mean difference for each comparison (Mean Diff.), lower confidence limit (LCL), upper confidence limit (UCL).

i. Descriptive Statistics

	n	Mean	Standard Deviation	SE of Mean
H_2O + Tris	6	–0.335	0.0523	0.0213
hAQP5 + Tris	6	–0.341	0.0314	0.0128
H_2O + 1 ng hCA II	6	–0.418	0.0546	0.0223
hAQP5 + 1 ng hCA II	6	–0.450	0.0531	0.0217

ii. Overall ANOVA Table

Variation	DF	Sum of Squares	Mean Square	*F*-value	*P*-value
Between Groups	3	0.0590	0.0197	8.26	9.03×10^{-4}
Within Groups	20	0.0476	0.00238		
Total	23	0.107			

iii. Tukey Test

Condition A	Condition B	Mean Diff.	*Q*-value	*P*-value	Sig.	LCL	UCL
hAQP5 + Tris	H_2O + Tris	–0.00633	0.318	0.996	–	–0.0852	0.0725
H_2O + 1 ng hCA II	H_2O + Tris	–0.0836	4.20	0.0352	✓	–0.162	–0.00478
H_2O + 1 ng hCA II	hAQP5 + Tris	–0.0773	3.88	0.0560	–	–0.156	0.00156
hAQP5 + 1 ng hCA II	H_2O + Tris	–0.116	5.80	0.00287	✓	–0.194	–0.0367
hAQP5 + 1 ng hCA II	hAQP5 + Tris	–0.109	5.48	0.00478	✓	–0.188	–0.0304
hAQP5 + 1 ng hCA II	H_2O + 1 ng hCA II	–0.0319	1.60	0.674	–	–0.111	0.0469

Supplemental Table 8*C*. Statistics Summary for Figure 8*C*, i) Descriptive Statistics for data presented in Figure 8*C*, $(dpH_i/dt)_{Max}$ upon CO_2 addition. ii) Overall one-way ANOVA results for data presented in Figure 8*C*. DF is degrees of freedom. iii) Tukey's means comparison analysis for all data presented in Figure 8*C*. Threshold for significance α=0.05. Standard error of the mean = 6.72×10^{-4}. Mean difference for each comparison (Mean Diff.), lower confidence limit (LCL), upper confidence limit (UCL).

i. Descriptive Statistics

	n	Mean	Standard Deviation	SE of Mean
H_2O + Tris	6	–0.00250	7.09×10^{-4}	2.89×10^{-4}
hAQP5 + Tris	6	–0.00451	0.00110	4.48×10^{-4}
H_2O + 1 ng hCA II	6	–0.00742	9.98×10^{-4}	4.08×10^{-4}
hAQP5 + 1 ng hCA II	6	–0.00670	0.00165	6.73×10^{-4}

ii. Overall ANOVA Table

Variation	DF	Sum of Squares	Mean Square	*F*-value	*P*-value
Between Groups	3	8.95×10^{-5}	2.98×10^{-5}	22.0	1.50×10^{-6}
Within Groups	20	2.71×10^{-5}	1.35×10^{-6}		
Total	23	1.17×10^{-4}			

iii. Tukey Test

Condition A	Condition B	Mean Diff.	*Q*-value	*P*-value	Sig.	LCL	UCL
hAQP5 + Tris	H_2O + Tris	–0.00201	4.24	0.0331	✓	–0.00389	-1.33×10^{-4}
H_2O + 1 ng hCA II	H_2O + Tris	–0.00492	10.4	2.42×10^{-6}	✓	–0.00680	–0.00304
H_2O + 1 ng hCA II	hAQP5 + Tris	–0.00291	6.12	0.00171	✓	–0.00479	–0.00103
hAQP5 + 1 ng hCA II	H_2O + Tris	–0.00420	8.84	2.33×10^{-5}	✓	–0.00608	–0.00232
hAQP5 + 1 ng hCA II	hAQP5 + Tris	–0.00218	4.60	0.0192	✓	–0.00407	-3.05×10^{-4}
hAQP5 + 1 ng hCA II	H_2O + 1 ng hCA II	7.23×10^{-4}	1.52	0.707	–	–0.00116	0.00260

Supplemental Table 8*D*. Statistics Summary for Figure 8*D*, i) Descriptive Statistics for data presented in Figure 8*D*, $(dpH_i/dt)_{Max}$ upon CO_2 removal. ii) Overall one-way ANOVA results for data presented in Figure 8*D*. DF is degrees of freedom. iii) Tukey's means comparison analysis for all data presented in Figure 8*D*. Threshold for significance α=0.05. Standard error of the mean = 5.20×10^{-4}. Mean difference for each comparison (Mean Diff.), lower confidence limit (LCL), upper confidence limit (UCL).

i. Descriptive Statistics

	n	Mean	Standard Deviation	SE of Mean
H_2O + Tris	6	0.00161	6.45×10^{-4}	2.63×10^{-4}
hAQP5 + Tris	6	0.00229	5.65×10^{-4}	2.31×10^{-4}
H_2O + 1ng hCA II	6	0.00498	9.28×10^{-4}	3.79×10^{-4}
hAQP5 + 1ng hCA II	6	0.00406	0.00129	5.25×10^{-4}

ii. Overall ANOVA Table

Variation	DF	Sum of Squares	Mean Square	*F*-value	*P*-value
Between Groups	3	4.36×10^{-5}	1.45×10^{-5}	17.9	6.92×10^{-7}
Within Groups	20	1.62×10^{-5}	8.12×10^{-7}		
Total	23	5.99×10^{-5}			

iii. Tukey Test

Condition A	Condition B	Mean Diff.	*Q*-value	*P*-value	Sig.	LCL	UCL
hAQP5 + Tris	H_2O + Tris	6.78×10^{-4}	1.84	0.571	–	-7.78×10^{-4}	0.00213
H_2O + 1 ng hCA II	H_2O + Tris	0.00337	9.16	1.42×10^{-5}	✓	0.00192	0.00483
H_2O + 1 ng hCA II	hAQP5 + Tris	0.00269	7.32	2.49×10^{-4}	✓	0.00124	0.00415
hAQP5 + 1 ng hCA II	H_2O + Tris	0.00245	6.67	7.08×10^{-4}	✓	9.97×10^{-4}	0.00391
hAQP5 + 1 ng hCA II	hAQP5 + Tris	0.00178	4.82	0.0135	✓	3.19×10^{-4}	0.00323
hAQP5 + 1 ng hCA II	H_2O + 1 ng hCA II	-9.18×10^{-4}	2.50	0.318	–	–0.00237	5.38×10^{-4}

Supplemental Table 9A. Statistics Summary for Figure 9*A*, i) Descriptive Statistics for data presented in **Figure 9*A***, $(dpH_S/dt)_{Max}$ upon CO_2 addition. ii) Overall one-way ANOVA results for data presented in **Figure 9*A***. DF is degrees of freedom. iii) Tukey's means comparison analysis for all data presented in **Figure 9*A***. Threshold for significance α=0.05. Standard error of the mean = 8.10 ×10–4. Mean difference for each comparison (Mean Diff.), lower confidence limit (LCL), upper confidence limit (UCL).

i. *Descriptive Statistics*

	n	Mean	Standard Deviation	SE of Mean
H_2O + Tris	6	–0.00502	0.00137	5.58×10^{-4}
hAQP5 + Tris	6	–0.00541	0.00185	7.53×10^{-4}
H_2O + 1 ng hCA II	6	–0.00910	9.11×10^{-4}	3.72×10^{-4}
hAQP5 + 1 ng hCA II	6	–0.00843	0.00133	5.43×10^{-4}

ii. Overall ANOVA Table

Variation	DF	Sum of Squares	Mean Square	*F*-value	*P*-value
Between Groups	3	7.74×10^{-5}	2.58×10^{-5}	13.1	5.83×10^{-5}
Within Groups	20	3.94×10^{-5}	1.97×10^{-5}		
Total	23	1.17×10^{-5}			

iii. Tukey Test

Condition A	Condition B	Mean Diff.	*Q*-value	*P*-value	Sig.	LCL	UCL
hAQP5 + Tris	H_2O + Tris	-3.98×10^{-4}	0.695	0.960	–	–0.00267	0.00187
H_2O + 1 ng hCA II	H_2O + Tris	–0.00408	7.13	3.38×10^{-4}	✓	–0.00635	–0.00182
H_2O + 1 ng hCA II	hAQP5 + Tris	–0.00369	6.43	0.00103	✓	–0.00595	–0.00142
hAQP5 + 1 ng hCA II	H_2O + Tris	–0.00342	5.96	0.00221	✓	–0.00568	–0.00115
hAQP5 + 1 ng hCA II	hAQP5 + Tris	–0.00302	5.27	0.00674	✓	–0.00528	-7.50×10^{-4}
hAQP5 + 1 ng hCA II	H_2O + 1 ng hCA II	6.68×10^{-4}	1.17	0.842	–	–0.00160	0.00294

Supplemental Table 9*B*. Statistics Summary for Figure 9*B*, i) Descriptive Statistics for data presented in **Figure 9*B***, $(dpH_S/dt)_{Max}$ upon CO_2 removal. ii) Overall one-way ANOVA results for data presented in **Figure 9*B***. DF is degrees of freedom. iii) Tukey's means comparison analysis for all data presented in **Figure 9*B***. Threshold for significance α=0.05. Standard error of the mean = 7.71 $\times 10^{-4}$. Mean difference for each comparison (Mean Diff.), lower confidence limit (LCL), upper confidence limit (UCL).

i. *Descriptive Statistics*

	n	Mean	Standard Deviation	SE of Mean
H_2O + Tris	6	0.00271	9.14×10^{-4}	3.73×10^{-4}
hAQP5 + Tris	6	0.00507	0.00180	7.34×10^{-4}
H_2O + 1 ng hCA II	6	0.00364	0.00127	5.18×10^{-4}
hAQP5 + 1 ng hCA II	6	0.00479	0.00120	4.91×10^{-4}

ii. *Overall ANOVA Table*

Variation	DF	Sum of Squares	Mean Square	*F*-value	*P*-value
Between Groups	3	2.13×10^{-5}	7.12×10^{-6}	3.99	0.0222
Within Groups	20	3.56×10^{-5}	1.78×10^{-6}		
Total	23	5.70×10^{-5}			

iii. *Tukey Test*

Condition A	Condition B	Mean Diff.	*Q*-value	*P*-value	Sig.	LCL	UCL
hAQP5 + Tris	H_2O + Tris	0.00236	4.33	0.0288	✓	2.04×10^{-4}	0.00452
H_2O + 1 ng hCA II	H_2O + Tris	9.36×10^{-4}	1.72	0.625	–	–0.00122	0.00309
H_2O + 1 ng hCA II	hAQP5 + Tris	–0.00143	2.62	0.281	–	–0.00358	7.32×10^{-4}
hAQP5 + 1 ng hCA II	H_2O + Tris	0.00209	3.83	0.0604	–	-7.19×10^{-5}	0.00424
hAQP5 + 1 ng hCA II	hAQP5 + Tris	-2.76×10^{-4}	0.506	0.984	–	–0.00243	0.00188
hAQP5 + 1 ng hCA II	H_2O + 1 ng hCA II	0.00115	2.11	0.461	–	–0.00101	0.00331

Supplemental Table 10*A*. Statistics Summary for Figure 10*A*, i) Descriptive Statistics for data presented in Figure 10*A*, initial pH_i values. ii) Overall one-way ANOVA results for data presented in Figure 10*A*. DF is degrees of freedom. iii) Tukey's means comparison analysis for all data presented in Figure 10*A*. Threshold for significance α=0.05. Standard error of the mean = 0.0353. Mean difference for each comparison (Mean Diff.), lower confidence limit (LCL), upper confidence limit (UCL).

i. Descriptive Statistics

	n	Mean	Standard Deviation	SE of Mean
H_2O + Tris	6	7.29	0.0530	0.0216
hAQP5 + Tris	6	7.32	0.0741	0.0303
H_2O + 1 ng hCA II	6	7.28	0.0685	0.0280
hAQP5 + 1 ng hCA II	6	7.31	0.0441	0.0180

ii. Overall ANOVA Table

Variation	DF	Sum of Squares	Mean Square	*F*-value	*P*-value
Between Groups	3	0.00556	0.00185	0.497	0.689
Within Groups	20	0.0747	0.00373		
Total	23	0.0802			

iii. Tukey Test

Condition A	Condition B	Mean Diff.	*Q*-value	*P*-value	Sig.	LCL	UCL
hAQP5 + Tris	H_2O + Tris	0.0352	1.41	0.752	–	–0.0635	0.134
H_2O + 1 ng hCA II	H_2O + Tris	–0.00157	0.0629	1.000	–	–0.100	0.0972
H_2O + 1 ng hCA II	hAQP5 + Tris	–0.0368	1.47	0.727	–	–0.136	0.0620
hAQP5 + 1 ng hCA II	H_2O + Tris	0.0203	0.813	0.939	–	–0.0785	0.119
hAQP5 + 1 ng hCA II	hAQP5 + Tris	–0.0149	0.599	0.974	–	–0.114	0.0838
hAQP5 + 1 ng hCA II	H_2O + 1 ng hCA II	0.0218	0.876	0.925	–	–0.0769	0.121

Supplemental Table 10*B*. Statistics Summary for Figure 10*B*, i) Descriptive Statistics for data presented in Figure 10*B*, ΔpH_i values. ii) Overall one-way ANOVA results for data presented in Figure 10*B*. DF is degrees of freedom. iii) Tukey's means comparison analysis for all data presented in Figure 10*B*. Threshold for significance α=0.05. Standard error of the mean = 0.0177. Mean difference for each comparison (Mean Diff.), lower confidence limit (LCL), upper confidence limit (UCL).

i. Descriptive Statistics

	n	Mean	Standard Deviation	SE of Mean
H_2O + Tris	6	–0.275	0.0274	0.0112
hAQP5 + Tris	6	–0.291	0.0117	0.00477
H_2O + 1 ng hCA II	6	–0.275	0.0374	0.0153
hAQP5 + 1 ng hCA II	6	–0.301	0.0383	0.0157

ii. Overall ANOVA Table

Variation	DF	Sum of Squares	Mean Square	*F*-value	*P*-value
Between Groups	3	0.00297	9.90×10^{-4}	1.05	0.391
Within Groups	20	0.0188	9.40×10^{-4}		
Total	23	0.0218			

iii. Tukey Test

Condition A	Condition B	Mean Diff.	*Q*-value	*P*-value	Sig.	LCL	UCL
hAQP5 + Tris	H_2O + Tris	–0.0161	1.29	0.798	–	–0.0334	0.0657
H_2O + 1 ng hCA II	H_2O + Tris	6.38×10^{-4}	0.0510	1.000	–	–0.0502	0.0489
H_2O + 1 ng hCA II	hAQP5 + Tris	0.0168	1.34	0.779	–	–0.0663	0.0327
hAQP5 + 1 ng hCA II	H_2O + Tris	–0.0256	2.05	0.486	–	–0.0239	0.0752
hAQP5 + 1 ng hCA II	hAQP5 + Tris	–0.00948	0.758	0.949	–	–0.0401	0.0590
hAQP5 + 1 ng hCA II	H_2O + 1ng hCA II	–0.0263	2.10	0.465	–	–0.0233	0.0758

Supplemental Table 10*C*. Statistics Summary for Figure 10*C*, i) Descriptive Statistics for data presented in Figure 10*C*, intrinsic buffering power (β_i). ii) Overall one-way ANOVA results for data presented in Figure 10*C*. DF is degrees of freedom. iii) Tukey's means comparison analysis for all data presented in Figure 10*C*. Threshold for significance α=0.05. Standard error of the mean = 1.02. Mean difference for each comparison (Mean Diff.), lower confidence limit (LCL), upper confidence limit (UCL).

i. Descriptive Statistics

	n	Mean	Standard Deviation	SE of Mean
H_2O + Tris	6	12.0	2.10	0.855
hAQP5 + Tris	6	11.7	1.63	0.664
H_2O + 1 ng hCA II	6	12.0	1.87	0.762
hAQP5 + 1 ng hCA II	6	10.8	1.43	0.586

ii. Overall ANOVA Table

Variation	DF	Sum of Squares	Mean Square	*F*-value	*P*-value
Between Groups	3	5.77	1.92	0.612	0.615
Within Groups	20	62.9	3.14		
Total	23	68.6			

iii. Tukey Test

Condition A	Condition B	Mean Diff.	*Q*-value	*P*-value	Sig.	LCL	UCL
hAQP5 + Tris	H_2O + Tris	–0.265	0.366	0.994	–	–3.13	2.60
H_2O + 1 ng hCA II	H_2O + Tris	–0.0111	0.0154	1.000	–	–2.88	2.85
H_2O + 1 ng hCA II	hAQP5 + Tris	0.253	0.350	0.994	–	–2.61	3.12
hAQP5 + 1 ng hCA II	H_2O + Tris	–1.20	1.65	0.652	–	–4.06	1.67
hAQP5 + 1 ng hCA II	hAQP5 + Tris	–0.932	1.29	0.799	–	–3.80	1.93
hAQP5 + 1 ng hCA II	H_2O + 1 ng hCA II	–1.19	1.64	0.659	–	–4.05	1.68

Supplemental Table 10*D*. Statistics Summary for Figure 10*D*, i) Descriptive Statistics for data presented in Figure 10*D*, P_f. ii) Overall one-way ANOVA results for data presented in Figure 10*D*. DF is degrees of freedom. iii) Tukey's means comparison analysis for all data presented in Figure 10*D*. Threshold for significance α=0.05. Standard error of the mean for Tukey's Test (SEM). Mean difference for each comparison (Mean Diff.), lower confidence limit (LCL), upper confidence limit (UCL).

i. Descriptive Statistics

	n	Mean	Standard Deviation	SE of Mean
H_2O + Tris	8	1.91×10^{-4}	2.19×10^{-4}	7.74×10^{-5}
hAQP5 + Tris	7	1.67×10^{-4}	1.18×10^{-4}	4.47×10^{-5}
H_2O + 1 ng hCA II	7	0.00389	3.34×10^{-4}	1.26×10^{-4}
hAQP5 + 1 ng hCA II	8	0.00391	4.82×10^{-4}	1.70×10^{-4}

ii. Overall ANOVA Table

Variation	DF	Sum of Squares	Mean Square	*F*-value	*P*-value
Between Groups	3	1.04×10^{-4}	3.46×10^{-5}	331	7.92×10^{-21}
Within Groups	26	2.72×10^{-6}	1.04×10^{-7}		
Total	29	1.07×10^{-4}			

iii. Tukey Test

Condition A	Condition B	Mean Diff.	SEM	*Q*-value	*P*-value	Sig.	LCL	UCL
H_2O + 1 ng hCA II	H_2O + Tris	-2.44×10^{-5}	1.67×10^{-4}	0.206	0.999	–	-4.83×10^{-4}	4.34×10^{-4}
hAQP5 + Tris	H_2O + Tris	0.00370	1.67×10^{-4}	31.3	2.10×10^{-12}	✓	0.00324	0.00416
H_2O + 1 ng hCA II	hAQP5 + Tris	0.00372	1.73×10^{-4}	30.5	2.10×10^{-12}	✓	0.00325	0.00420
hAQP5 + 1 ng hCA II	H_2O + Tris	0.00372	1.62×10^{-4}	32.6	2.10×10^{-12}	✓	0.00328	0.00416
hAQP5 + 1 ng hCA II	H_2O + 1 ng hCA II	0.00375	1.67×10^{-4}	31.7	2.10×10^{-12}	✓	0.00329	0.00420
hAQP5 + 1 ng hCA II	hAQP5 + Tris	2.32×10^{-5}	1.67×10^{-4}	0.196	0.999	–	-4.36×10^{-4}	4.82×10^{-4}

Supplemental Table 11*A*. Statistics Summary for Figure 11*A*, i) Descriptive Statistics for data presented in Figure 11*A*, which are the ΔpH_S upon CO_2 addition data rearranged from Figure 3*A* to juxtapose two hAQP5 absent bars and two heterologously expressed hAQP5 bars. ii) Overall one-way ANOVA results for only data bars presented in Figure 11*A* extracted from Figure 3*A*. DF is degrees of freedom. iii) Tukey's means comparison analysis for all data presented in Figure 11*A*. iv) Descriptive Statistics for data presented in Figure 11*A*, to analyze $\Delta\Delta_{Base}$ vs. $\Delta\Delta_{AQP5}$ when adding 1 ng hCA II, on the "trans" side of the membrane to the pH_S measurement. v) One-way ANOVA results for $\Delta\Delta_{Base}$ vs. $\Delta\Delta_{AQP5}$ data presented in Figure 11*A*. vi) Tukey's means comparison analysis for $\Delta\Delta_{Base}$ vs. $\Delta\Delta_{AQP5}$ data presented in Figure 11*A*. Threshold for significance α=0.05. Standard error of the mean for Tukey's Test (SEM). Mean difference for each comparison (Mean Diff.), lower confidence limit (LCL), upper confidence limit (UCL).

i. Descriptive Statistics for ΔpH_S on CO_2 addition

	n	Mean	Standard Deviation	SE of Mean
H_2O + Tris	8	0.0285	0.00895	0.00316
hAQP5 + Tris	8	0.0787	0.0181	0.00641
H_2O + 1 ng hCA II	8	0.0411	0.0115	0.00406
hAQP5 + 1 ng hCA II	8	0.127	0.0246	0.00869

ii. Overall ANOVA Table for ΔpH_S on CO_2 addition

Variation	DF	Sum of Squares	Mean Square	*F*-value	*P*-value
Between Groups	3	0.0471	0.0157	54.8	7.63×10^{-12}
Within Groups	28	0.00802	2.86×10^{-4}		
Total	31	0.0552			

iii. Tukey Test for ΔpH_S on CO_2 addition

Condition A	Condition B	Mean Diff.	SEM	*Q*-value	*P*-value	Sig.	LCL	UCL
hAQP5 + Tris	H_2O + Tris	0.0502	0.00846	8.39	1.25×10^{-5}	✓	0.0271	0.0733
H_2O + 1 ng hCA II	H_2O + Tris	0.0126	0.00846	2.11	0.455	–	–0.0105	0.0357
H_2O + 1 ng hCA II	hAQP5 + Tris	–0.0376	0.00846	6.28	7.00×10^{-4}	✓	–0.0607	–0.0145
hAQP5 + 1 ng hCA II	H_2O + Tris	0.0986	0.00846	16.5	0.00	✓	0.0755	0.122
hAQP5 + 1 ng hCA II	hAQP5 + Tris	0.0484	0.00846	8.09	2.20×10^{-5}	✓	0.0253	0.0715
hAQP5 + 1 ng hCA II	H_2O + 1 ng hCA II	0.0860	0.00846	14.4	6.50×10^{-7}	✓	0.0629	0.109

iv. Descriptive Statistics for ΔΔpHs on CO_2 addition

	n	Mean	Standard Deviation	SE of Mean
$\Delta\Delta_{Base}$	8	0.0126	0.0115	0.00406
$\Delta\Delta_{hAQP5}$	8	0.0484	0.0246	0.00869

v. Overall ANOVA Table for ΔΔpHs on CO_2 addition

Variation	DF	Sum of Squares	Mean Square	*F*-value	*P*-value
Between Groups	1	0.00513	0.00513	13.9	0.00223
Within Groups	14	0.00516	3.68×10^{-4}		
Total	15	0.0103			

vi. Tukey Test for ΔΔpHs on CO_2 addition

Condition A	Condition B	Mean Diff.	SEM	*Q*-value	*P*-value	Sig.	LCL	UCL
$\Delta\Delta_{Base}$	$\Delta\Delta_{AQP5}$	0.0358	0.00960	5.28	0.00224	✓	0.0152	0.0564

Supplemental Table 11*B*. Statistics Summary for Figure 11*B*, i) Descriptive Statistics for data presented in Figure 11*B*, which are the ΔpH_S upon CO_2 removal data rearranged from Figure 3*B* to juxtapose two hhAQP5 absent bars and two heterologously expressed hAQP5 bars. ii) Overall one-way ANOVA results for only data bars presented in Figure 11*B* extracted from Figure 3*B*. DF is degrees of freedom. iii) Tukey's means comparison analysis for all data presented in Figure 11*B*. iv) Descriptive Statistics for data presented in Figure 11*B*, to analyze $\Delta\Delta_{Base}$ vs. $\Delta\Delta_{AQP5}$ when adding 1 ng hCA II, on the "trans" side of the membrane to the pH_S measurement. v) One-way ANOVA results for $\Delta\Delta_{Base}$ vs. $\Delta\Delta_{AQP5}$ data presented in Figure 11*B*. vi) Tukey's means comparison analysis for $\Delta\Delta_{Base}$ vs. $\Delta\Delta_{AQP5}$ data presented in Figure 11*B*. Threshold for significance α=0.05. Standard error of the mean for Tukey's Test (SEM). Mean difference for each comparison (Mean Diff.), lower confidence limit (LCL), upper confidence limit (UCL).

i. Descriptive Statistics for ΔpH_S on CO_2 addition

	n	Mean	Standard Deviation	SE of Mean
H_2O + Tris	8	0.0285	0.00895	0.00316
hAQP5 + Tris	8	0.0787	0.0181	0.00641
H_2O + 100 ng hCA II	8	0.0416	0.00948	0.00335
hAQP5 + 100 ng hCA II	8	0.160	0.0478	0.0169

ii. Overall ANOVA Table for ΔpH_S on CO_2 addition

Variation	DF	Sum of Squares	Mean Square	*F*-value	*P*-value
Between Groups	3	0.0845	0.0282	40.4	2.61×10^{-10}
Within Groups	28	0.0195	6.97×10^{-4}		
Total	31	0.104			

iii. Tukey Test for ΔpH_S on CO_2 addition

Condition A	Condition B	Mean Diff.	SEM	*Q*-value	*P*-value	Sig.	LCL	UCL
hAQP5 + Tris	H_2O + Tris	0.0502	0.0132	5.38	0.00374	✓	0.0142	0.0862
H_2O + 100 ng hCA II	H_2O + Tris	0.0131	0.0132	1.41	0.754	–	-0.0229	0.0492
H_2O + 100 ng hCA II	hAQP5 + Tris	–0.0371	0.0132	3.97	0.0419	✓	-0.0731	–0.00104
hAQP5 + 100 ng hCA II	H_2O + Tris	0.132	0.0132	14.1	2.23×10^{-7}	✓	0.0959	0.168
hAQP5 + 100 ng hCAII	hAQP5 + Tris	0.0817	0.0132	8.76	6.27×10^{-6}	✓	0.0457	0.118
hAQP5 + 100 ng hCA II	H_2O + 100 ng hCA II	0.119	0.0132	12.7	0.00	✓	0.0828	0.155

iv. Descriptive Statistics for ΔΔpHs on CO_2 addition

	n	Mean	Standard Deviation	SE of Mean
$\Delta\Delta_{Base}$	8	0.0131	0.00948	0.00335
$\Delta\Delta_{hAQP5}$	8	0.0817	0.0478	0.0169

v. Overall ANOVA Table

Variation	DF	Sum of Squares	Mean Square	*F*-value	*P*-value
Between Groups	1	0.0188	0.0188	15.8	0.00137
Within Groups	14	0.0166	0.00119		
Total	15	0.0355			

vi. Tukey Test

Condition A	Condition B	Mean Diff.	SEM	*Q*-value	*P*-value	Sig.	LCL	UCL
$\Delta\Delta_{Base}$	$\Delta\Delta_{AQP5}$	0.0686	0.0172	5.63	0.00137	✓	0.0316	0.106

Supplemental Table 12A. Statistics Summary for Figure 12*A*, i) Descriptive Statistics for data presented in Figure 12*A*, for comparison of select $-(dpH_i/dt)_{Max}$ bars extracted from Figure 3*C* and Figure 8*C* to analyze $-(dpH_i/dt)_{Max}$ upon CO_2 addition in the absence or presence of bCA in bECF, on the "trans" side of the membrane to the pH_i measurement. ii) Overall one-way ANOVA results for $-(dpH_i/dt)_{Max}$ data presented in Figure 12*A*. DF is degrees of freedom. iii) Tukey's means comparison analysis for $-(dpH_i/dt)_{Max}$ the subset of data presented in Figure 12*A*. iv) Descriptive Statistics for data presented in Figure 12*A*, to analyze Δ_{Base} vs. Δ_{AQP5}. v) One-way ANOVA results for Δ_{Base} vs. Δ_{AQP5} data presented in Figure 12*A*. vi) Tukey's means comparison analysis for $\Delta\Delta_{Base}$ vs. $\Delta\Delta_{AQP5}$ data presented in Figure 12*A*. Threshold for significance α=0.05. Standard error of the mean for Tukey's Test (SEM). Mean difference for each comparison (Mean Diff.), lower confidence limit (LCL), upper confidence limit (UCL).

i. Descriptive Statistics for $-(dpH_i/dt)_{Max}$ on CO_2 addition

	n	Mean	Standard Deviation	SE of Mean
H_2O + Tris	8	–0.00126	2.08×10^{-4}	7.35×10^{-5}
H_2O + Tris + bCA_{bECF}	6	–0.00250	7.09×10^{-4}	2.89×10^{-4}
hAQP5 + Tris	8	–0.00122	1.57×10^{-4}	5.55×10^{-5}
hAQP5 + Tris+ bCA_{bECF}	6	–0.00451	0.00110	4.48×10^{-4}

ii. Overall ANOVA Table for $-(dpH_i/dt)_{Max}$ on CO_2 addition

Variation	DF	Sum of Squares	Mean Square	*F*-value	*P*-value
Between Groups	3	4.73×10^{-5}	1.58×10^{-5}	42.0	1.04×10^{-9}
Within Groups	24	9.00×10^{-6}	3.75×10^{-7}		
Total	27	5.63×10^{-5}			

iii. Tukey Test for $-(dpH_i/dt)_{Max}$ on CO_2 addition

Condition A	Condition B	Mean Diff.	SEM	*Q*-value	*P*-value	Sig.	LCL	UCL
H_2O + Tris + bCA_{bECF}	H_2O + Tris	–0.00124	3.31×10^{-4}	5.30	0.00513	✓	–0.00215	-3.27×10^{-4}
hAQP5 + Tris	H_2O + Tris	3.53×10^{-5}	3.06×10^{-4}	0.163	0.999	–	-8.09×10^{-4}	8.80×10^{-4}
hAQP5 + Tris	H_2O + Tris + bCA_{bECF}	0.00127	3.31×10^{-4}	5.45	0.00396	✓	3.62×10^{-4}	0.00219
hAQP5 + Tris+ bCA_{bECF}	H_2O + Tris	–0.00325	3.31×10^{-4}	13.9	4.43×10^{-7}	✓	–0.00417	–0.00234
hAQP5 + Tris+ bCA_{bECF}	H_2O + Tris + bCA_{bECF}	–0.00201	3.54×10^{-4}	8.05	4.07×10^{-5}	✓	–0.00299	–0.00104
hAQP5 + Tris+ bCA_{bECF}	hAQP5 + Tris	–0.00329	3.31×10^{-4}	14.1	4.47×10^{-7}	✓	–0.00420	–0.00238

iv. Descriptive Statistics for Δ_{hhAQP5} vs Δ_{Base} for $-(dpH_i/dt)_{Max}$ on CO_2 addition

	n	Mean	Standard Deviation	SE of Mean
Δ_{Base}	6	–0.00124	7.09×10^{-4}	2.89×10^{-4}
Δ_{AQP5}	6	–0.00329	0.00110	4.48×10^{-4}

v. Overall ANOVA Table

Variation	DF	Sum of Squares	Mean Square	*F*-value	*P*-value
Between Groups	1	1.26×10^{-5}	1.26×10^{-5}	14.8	0.00325
Within Groups	10	8.53×10^{-6}	8.53×10^{-7}		
Total	11	2.11×10^{-5}			

vi. Tukey Test

Condition A	Condition B	Mean Diff.	SEM	*Q*-value	*P*-value	Sig.	LCL	UCL
Δ_{Base}	Δ_{AQP5}	–0.00205	5.33×10^{-4}	5.43	0.00325	✓	–0.00324	-8.61×10^{-4}

Supplemental Table 12B. Statistics Summary for Figure 12*B*, i) Descriptive Statistics for data presented in Figure 12*B*, for comparison of select –(dpH$_i$/dt)$_{Max}$ bars extracted from Figure 3*D* and Figure 8*D* to analyze +(dpH$_i$/dt)$_{Max}$ upon CO_2 removal in the absence or presence of bCA in bECF, on the "trans" side of the membrane to the pH$_i$ measurement. ii) Overall one-way ANOVA results for +(dpH$_i$/dt)$_{Max}$ data presented in Figure 12*B*. DF is degrees of freedom. iii) Tukey's means comparison analysis for +(dpH$_i$/dt)$_{Max}$ data presented in Figure 12*B*. iv) Descriptive Statistics for data presented in Figure 12*B*, to analyze Δ_{Base} vs. Δ_{AQP5}. v) One-way ANOVA results for Δ_{Base} vs. Δ_{AQP5} data presented in Figure 12*B*. vi) Tukey's means comparison analysis for $\Delta\Delta_{Base}$ vs. $\Delta\Delta_{AQP5}$ data presented in Figure 12*B*. Threshold for significance α=0.05. Standard error of the mean for Tukey's Test (SEM). Mean difference for each comparison (Mean Diff.), lower confidence limit (LCL), upper confidence limit (UCL).

i. Descriptive Statistics for +(dpH$_i$/dt)$_{Max}$ on CO_2 removal

	n	Mean	Standard Deviation	SE of Mean
H_2O + Tris	8	8.35×10^{-4}	1.34×10^{-4}	4.74×10^{-5}
H_2O + Tris + bCA$_{bECF}$	6	0.00161	6.45×10^{-4}	2.63×10^{-4}
hAQP5 + Tris	8	8.07×10^{-4}	6.85×10^{-5}	2.42×10^{-5}
hAQP5 + Tris+ bCA$_{bECF}$	6	0.00229	5.65×10^{-4}	2.31×10^{-4}

ii. Overall ANOVA Table for +(dpH$_i$/dt)$_{Max}$ on CO_2 removal

Variation	DF	Sum of Squares	Mean Square	*F*-value	*P*-value
Between Groups	3	1.01×10^{-5}	3.35×10^{-6}	21.0	6.82×10^{-7}
Within Groups	24	3.84×10^{-6}	1.60×10^{-7}		
Total	27	1.39×10^{-5}			

iii. Tukey Test for +(dpH$_i$/dt)$_{Max}$ on CO_2 removal

Condition A	Condition B	Mean Diff.	SEM	*Q*-value	*P*-value	Sig.	LCL	UCL
H_2O + Tris + bCA$_{bECF}$	H_2O + Tris	7.72×10^{-4}	2.16×10^{-4}	5.06	0.00778	✓	1.76×10^{-4}	0.00137
hAQP5 + Tris	H_2O + Tris	-2.75×10^{-5}	2.00×10^{-4}	0.195	0.999	–	-5.79×10^{-4}	5.24×10^{-4}
hAQP5 + Tris	H_2O + Tris + bCA$_{bECF}$	-7.99×10^{-4}	2.16×10^{-4}	5.24	0.00572	✓	-0.00140	-2.04×10^{-4}
hAQP5 + Tris+ bCA$_{bECF}$	H_2O + Tris	0.00145	2.16×10^{-4}	9.50	3.43×10^{-6}	✓	8.55×10^{-4}	0.00205
hAQP5 + Tris+ bCA$_{bECF}$	H_2O + Tris + bCA$_{bECF}$	6.78×10^{-4}	2.31×10^{-4}	4.16	0.0338	✓	4.15×10^{-5}	0.00131
hAQP5 + Tris+ bCA$_{bECF}$	hAQP5 + Tris	0.00148	2.16×10^{-4}	9.68	2.54×10^{-6}	✓	8.82×10^{-4}	0.00207

iv. Descriptive Statistics for Δ_{AQP5} vs Δ_{Base} for $-(dpH_i/dt)_{Max}$ on CO_2 removal

	n	Mean	Standard Deviation	SE of Mean
Δ_{Base}	6	7.72×10^{-4}	6.45×10^{-4}	2.63×10^{-4}
Δ_{AQP5}	6	0.00148	5.65×10^{-4}	2.31×10^{-4}

v. Overall ANOVA Table

Variation	DF	Sum of Squares	Mean Square	*F*-value	*P*-value
Between Groups	1	1.49×10^{-6}	1.49×10^{-6}	4.06	0.0715
Within Groups	10	3.68×10^{-6}	3.68×10^{-7}		
Total	11	5.17×10^{-6}			

vi. Tukey Test

Condition A	Condition B	Mean Diff.	SEM	*Q*-value	*P*-value	Sig.	LCL	UCL
Δ_{Base}	Δ_{AQP5}	7.06×10^{-4}	3.50×10^{-4}	2.85	0.0715	✓	-7.43×10^{-5}	0.00149

Figure Legends

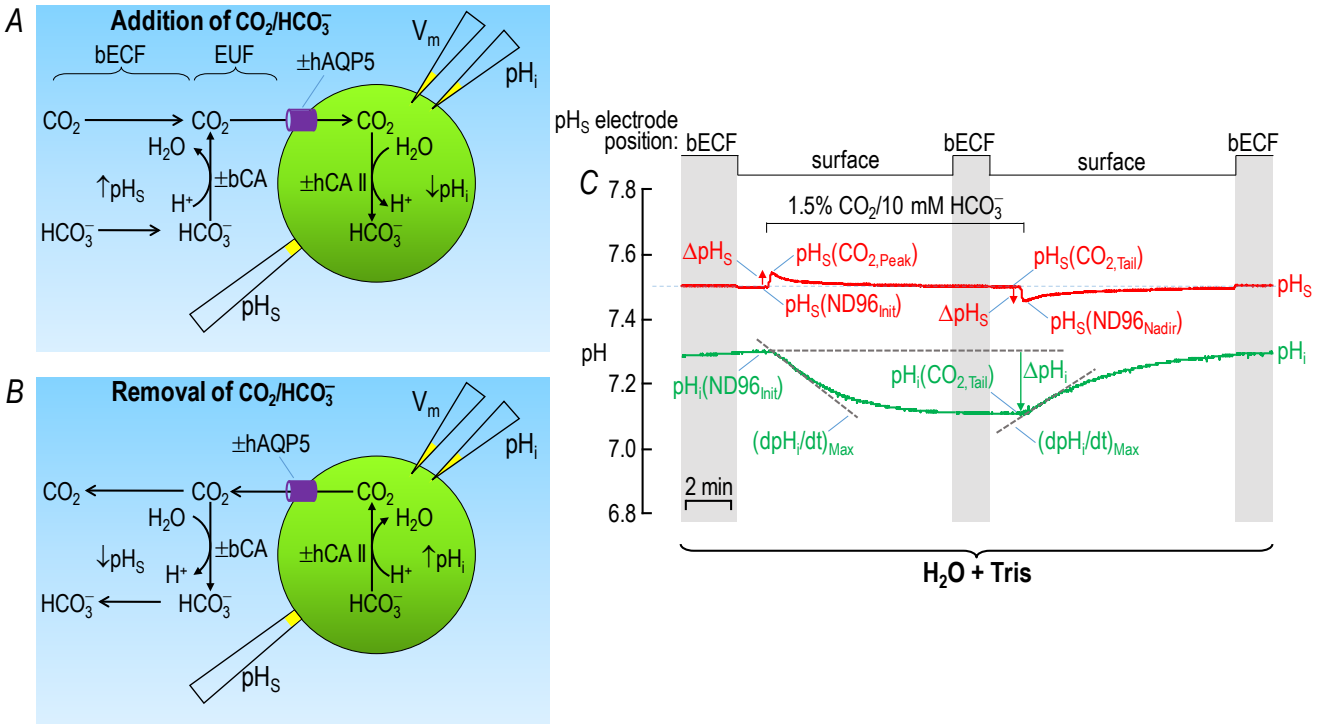

Figure 1 Design of experiments. *A,* model cell showing CO_2 influx. The green circle represents a *Xenopus laevis* oocyte. Arrows with sharper arrowheads indicate the direction of diffusion. Arrows with blunter arrowheads indicate the direction of a chemical reaction. Upward and downward arrows associated with pH_S and pH_i indicate the direction of a pH change. The purple cylinder represents a human (h) AQP5 tetramer heterologously expressed in the membrane. We impale a *Xenopus laevis* oocyte with both a pH_i and V_m electrode, and used a blunt, polished electrode to monitor pH_S.

±, presence or absence; bECF, bulk extracellular fluid; bCA, extracellular bovine carbonic anhydrase (a mixture of CA I and CA II); EUF, extracellular unconvected fluid; hCA II, intracellular purified carbonic anhydrase II protein from human erythrocytes.

B, Model cell showing CO_2 efflux. All events occur in a direction opposite to that in *A*.

C, Representative experiment. We dissected the oocyte on Day 0, injected it with H_2O (as a control for cRNA encoding hAQP5) on Day 1, and then with "Tris" (as a control for hCA II protein)

on Day 4. The stair-step line at the top of the panel indicates the position of the tip of the pH_S electrode. The vertical shaded bars indicate the time during which the pH_S-electrode tip is in the bECF for recalibration at pH_o = 7.50; at other times, the pH_S-electrode tip dimples the cell surface. The flowing solution is ND96 except for the period labeled "1.5 CO_2/10 mM HCO_3^-." The red record represents the time course of pH_S, and the green record, the time course of pH_i. We provide detailed definitions of the red and green labels in Methods.[15]

[15] See Methods">"Calculation of ΔpH_S", "Methods">"Determination of "maximal" dpH_i/dt", "Methods">"Calculation of intrinsic intracellular buffering power"

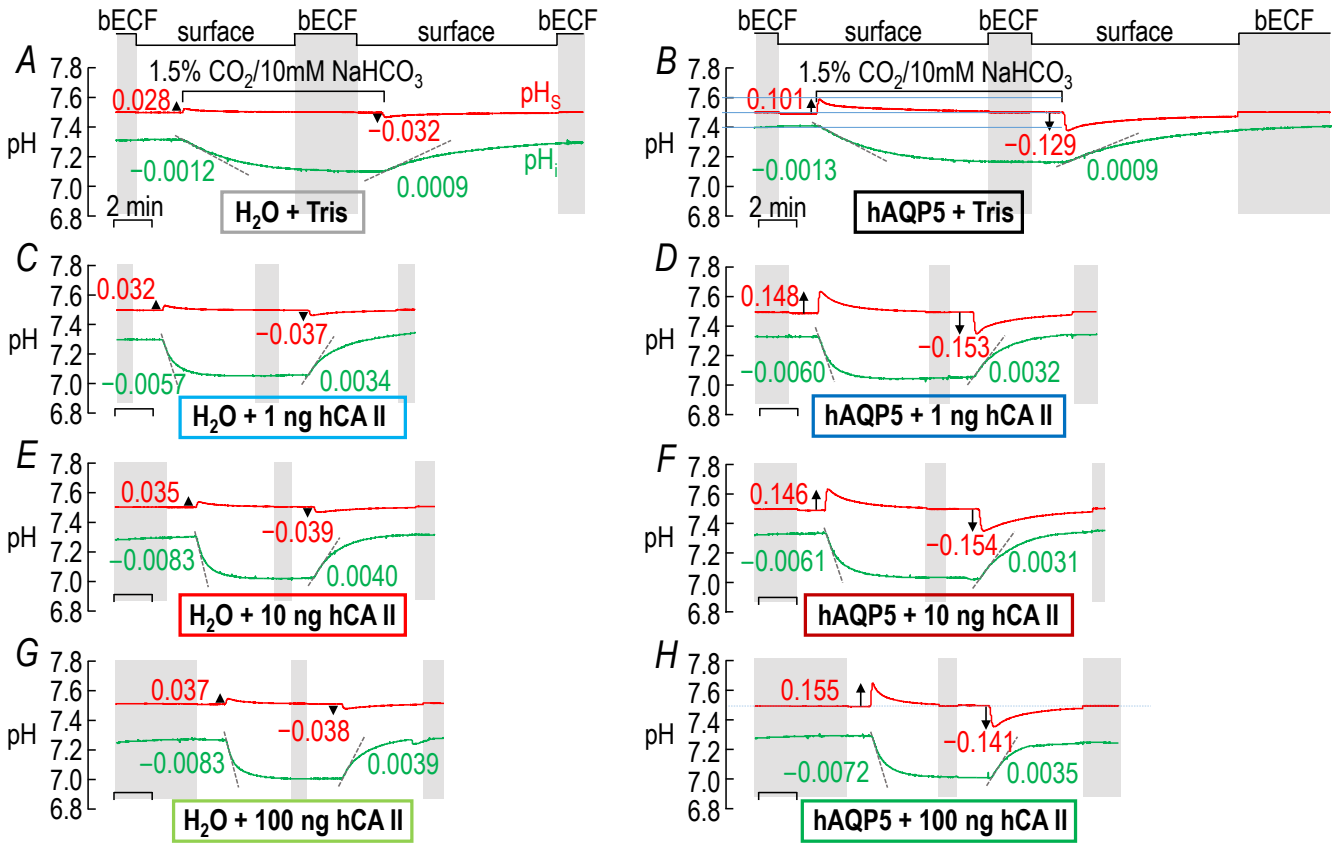

Figure 2 Representative pH_S and pH_i recordings: ±hAQP5, Δcytosolic hCA II, all in the absence of extracellular bCA (i.e., –bCA).

A, "H_2O + Tris". We injected this oocyte with H_2O (as a control for cRNA encoding hAQP5) on Day 1, and then with "Tris" (as a control for hCA II) on Day 4.

B, "hAQP5 + Tris". This oocyte, we injected on Day 1 with cRNA encoding hAQP5, and then on Day 4 with "Tris".

C, "H_2O + 1 ng hCA II". Similar to panel *A* except that on Day 4, we injected the oocyte with hCA II enzyme dissolved in "Tris".

D, "hAQP5 +1 ng hCA II". Similar to panel *B* except that on Day 4, we injected the oocyte with hCA II enzyme dissolved in "Tris".

E, "H_2O + 10 ng hCA II".

F, “hAQP5 + 10 ng hCA II”.

G, “H_2O + 100 ng hCA II”.

H, “hAQP5 + 100 ng hCA II”.

The “Δ” in the title and elsewhere in the paper implies that we choose among several levels of injected hCA II. The numbers in red are ΔpH_s and in green are $(dpH_i/dt)_{Max}$ for the oocyte presented here. The stair-step line at the top of *A* and *B* indicates the position of the pH_S electrode. The vertical shaded bars indicate times during which the pH_S electrode is in the bulk extracellular fluid (bECF) for recalibration; at other times, the pH_S electrode dimples the cell surface for actual pH_S measurements. The colors of the rectangles that surround the panel labels (e.g., “H_2O + Tris”) correspond to the colors of the bars in Figure 3 and later figures.

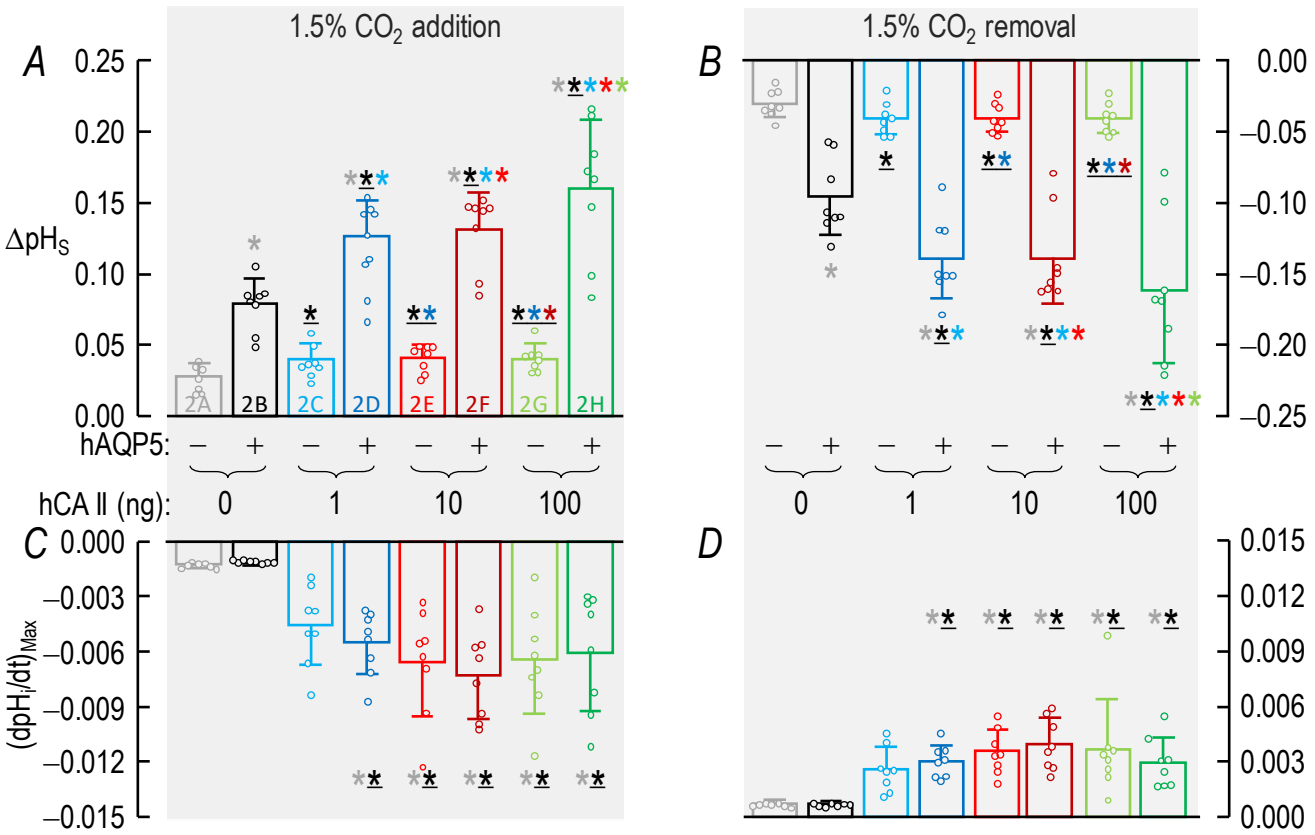

Figure 3 Summary of ΔpH_S and $(dpH_i/dt)_{Max}$ data from experiments like those in Figure 2: ±hAQP5, Δcytosolic hCA II, all in the absence of extracellular bCA (i.e., –bCA).

A, Summary of ΔpH_S upon addition of 1.5% CO_2/10 mM HCO_3^-. We computed individual ΔpH_S values as outlined in "Methods" > "Electrophysiological measurements" > "Calculation of ΔpH_S".

B, Summary of ΔpH_S upon removal of 1.5% CO_2/10 mM HCO_3^-.

C, Summary of $(dpH_i/dt)_{Max}$ upon addition of 1.5% CO_2/10 mM HCO_3^-. We computed individual ΔpH_S values as outlined in "Methods" > "Electrophysiological measurements" > "Calculation of "maximal" dpH_S/dt".

D, Summary of $(dpH_i/dt)_{Max}$ upon removal of 1.5% CO_2/10 mM HCO_3^-.

The "Δ" in the title and elsewhere in the paper implies that we choose among several levels of injected hCA II. Data are presented as mean ± SD. "–" and lighter-colored bars indicate that we injected oocytes with H_2O; "+" and darker-colored bars, with cRNA encoding hAQP5 on Day

1. “0”, “1”, “10” and “100” indicate the amount of hCA II (ng) injected into oocytes on Day 4. Gray/black and light-/dark-blue, red, and green pairs of bars indicate 8 groups of oocytes. These colors correspond to the colors of the rectangles that surround panel labels (e.g., “H_2O + Tris”) in Figure 2. A star associated with a bar indicates a statistically significant difference when comparing the bar to another bar with the same color as the star. The star/bar combinations are meant to be read right to left; we indicate statistical significance between two bars only once, associating the star with the bar further to the right. Thus, the mean value represented by the dark-green bar in panel *A* differs significantly from the means of the following bars: light gray, black (underscored to indicate darker than gray), light blue, light red, and light green. Conversely, the gray bar, which has no stars, differs significantly from the means of all bars with a gray star. The absence of a star indicates a lack of statistical significance. See Statistics Table 3 for *P*-values.

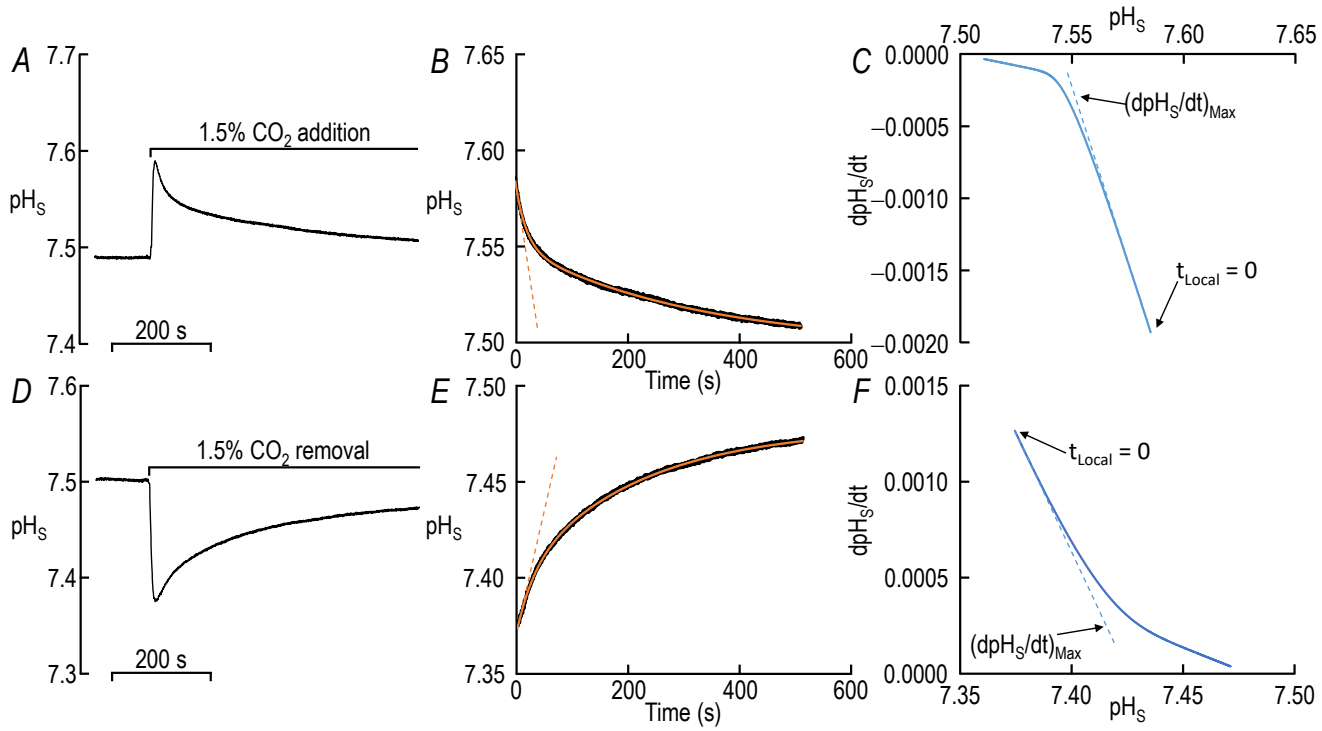

Figure 4 Analysis of $(dpH_S/dt)_{Max}$, the magnitude of maximal rate of relaxation of pH_S.

A, Time course of surface pH (pH_S) during addition of 1.5% CO_2/10 mM HCO_3^-. This is a reproduction—with a magnified y-axis—of the red record (during CO_2 addition) in Figure 2*B*.

B, Detail of panel *A*, showing only the pH_S relaxation, beginning from the time (t_{Local} = 0 s) of fastest pH_S descent. The jittery black record is the actual pH_S recording; the smooth orange curve is the result of a double-exponential (DExp) curve fit. The dashed red line has a dpH_S/dt-vs.-time slope that is the derivative of the fitted DExp function at t_{Local} = 0 s.

C, Dependence of dpH_S/dt on pH_S during addition of CO_2/HCO_3^- application. We obtained dpH_S/dt by computing the derivative of the DExp best-fit function at the time that corresponds to the indicated pH_S. Note that real time runs from right to left. The dashed blue line has a dpH_S/dt-vs.-pH_S slope that corresponds to the value at t_{Local} = 0 s. A perfect single-exponential fit of pH_S vs. time would have produced a straight line in this dpH_S/dt-vs.-pH_S plot. Thus, the break in the blue curve near pH_S = 7.54 is the demarcation between the dominance of a rapid/initial process and a slower/later process.

D, Time course of pH_S during removal of 1.5% CO_2/10 mM HCO_3^-. This is a reproduction—with a magnified y-axis—of the red record (during CO_2 removal) in Figure 2*B*.

E, Detail of panel *D*, processed as in panel *B*.

F, Dependence of dpH_S/dt on pH_S during CO_2/HCO_3^- removal, processed as in panel *C*. Note that real time runs from left to right.

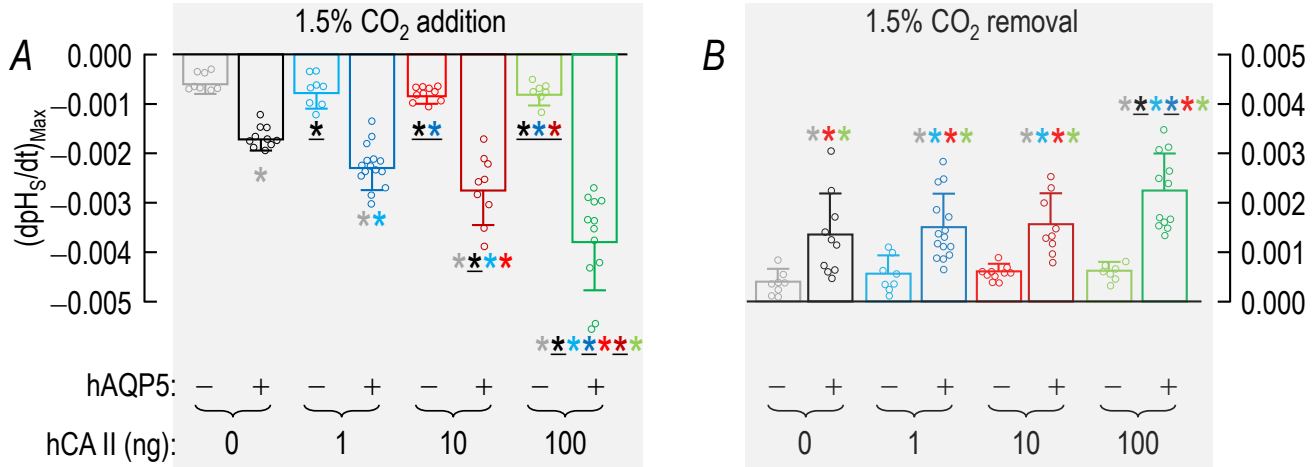

Figure 5 Summary of $(dpH_S/dt)_{Max}$ data from experiments like those in Figure 2: ±hAQP5, Δcytosolic hCA II, all in the absence of extracellular bCA (i.e., –bCA).

A, Summary of $(dpH_S/dt)_{Max}$ upon addition of 1.5% CO_2/10 mM HCO_3^-. We computed individual $(dpH_S/dt)_{Max}$ values as described in Figure 4.

B, Summary of $(dpH_S/dt)_{Max}$ upon removal of 1.5% CO_2/10 mM HCO_3^-.

The "Δ" in the title and elsewhere in the paper implies that we choose among several levels of injected hCA II. Data are presented as mean ± SD. "–" and lighter-colored bars indicate that we injected oocytes with H_2O; "+" and darker-colored bars, with cRNA encoding hAQP5 on Day 1. "0", "1", "10" and "100" indicate the amount of hCA II (ng) injected into oocytes on Day 4. Gray/black and light-/dark-blue, red, and green pairs of bars indicate 8 groups of oocytes. These colors correspond to the colors of the rectangles that surround panel labels (e.g., "H_2O + Tris") in Figure 2. A star associated with a bar indicates a statistically significant difference when comparing the bar to another bar with the same color as the star. The star/bar combinations are meant to be read right to left; we indicate statistical significance between two bars only once, associating the star with the bar further to the right. Thus, the mean value represented by the dark green bar in panel *A* differs significantly from the means of the following bars: light gray, black (underscored to indicate darker than gray), light blue, dark blue, light red, dark red, and light green. Conversely, the gray bar, which has no stars, differs significantly from the means of

all bars with a gray star. The absence of a star indicates a lack of statistical significance. See Statistics Table 5 for *P*-values.

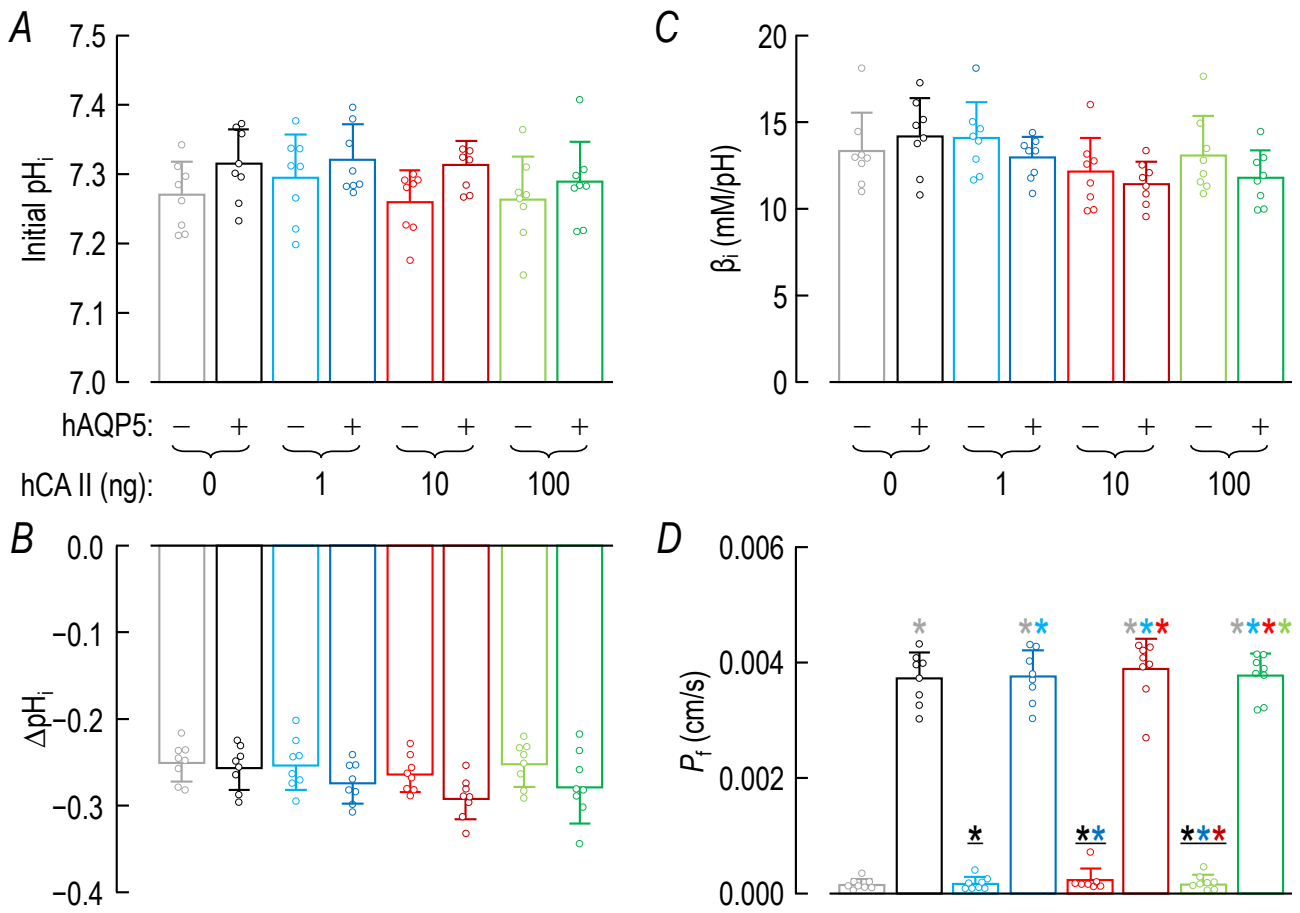

Figure 6 Summary of other oocyte parameters from experiments like those in Figure 2: ±hAQP5, Δcytosolic hCA II, all in the absence of extracellular bCA (i.e., –bCA).

A, Summary of initial pH_i values. We computed individual initial pH_i, ΔpH_i (see panel *B*), and β_i (see panel *C*) values as outlined in "Methods" > "Electrophysiological measurements" > "Calculation of intrinsic intracellular buffering power".

B, Summary of ΔpH_i elicited by addition of 1.5% CO_2/10 mM HCO_3^-.

C, Summary of intrinsic buffering power (β_i).

D, Summary of P_f. We computed individual initial pH_i, ΔpH_i (see panel *B*), and β_i (see panel *C*) values as outlined in "Methods" > "Electrophysiological measurements" > "Measurement of P_f".

The "Δ" in the title and elsewhere in the paper implies that we choose among several levels of injected hCA II. Data are presented as mean ± SD. "–" and lighter-colored bars indicate that we injected oocytes injected with H_2O; "+" and darker-colored bars, with cRNA encoding hAQP5 on Day 1. "0", "1", "10" and "100" indicate the amount of hCA II (ng) injected into oocytes on Day 4. Gray/black and light-/dark-blue, red, and green pairs of bars indicate 8 groups of oocytes. These colors correspond to the colors of the rectangles that surround panel labels (e.g., "H_2O + Tris") in Figure 2. A star associated with a bar indicates a statistically significant difference when comparing the bar to another bar with the same color as the star. The star/bar combinations are meant to be read right to left; we indicate statistical significance between two bars only once, associating the star with the bar further to the right. Thus, the mean value represented by the dark green bar in panel *D* differs significantly from the means of the following bars: light gray, light blue, light red, and light green. Conversely, the gray bar, which has no stars, differs significantly from the means of all bars with a gray star. The absence of a star indicates a lack of statistical significance. See Statistics Table 6 for *P*-values.

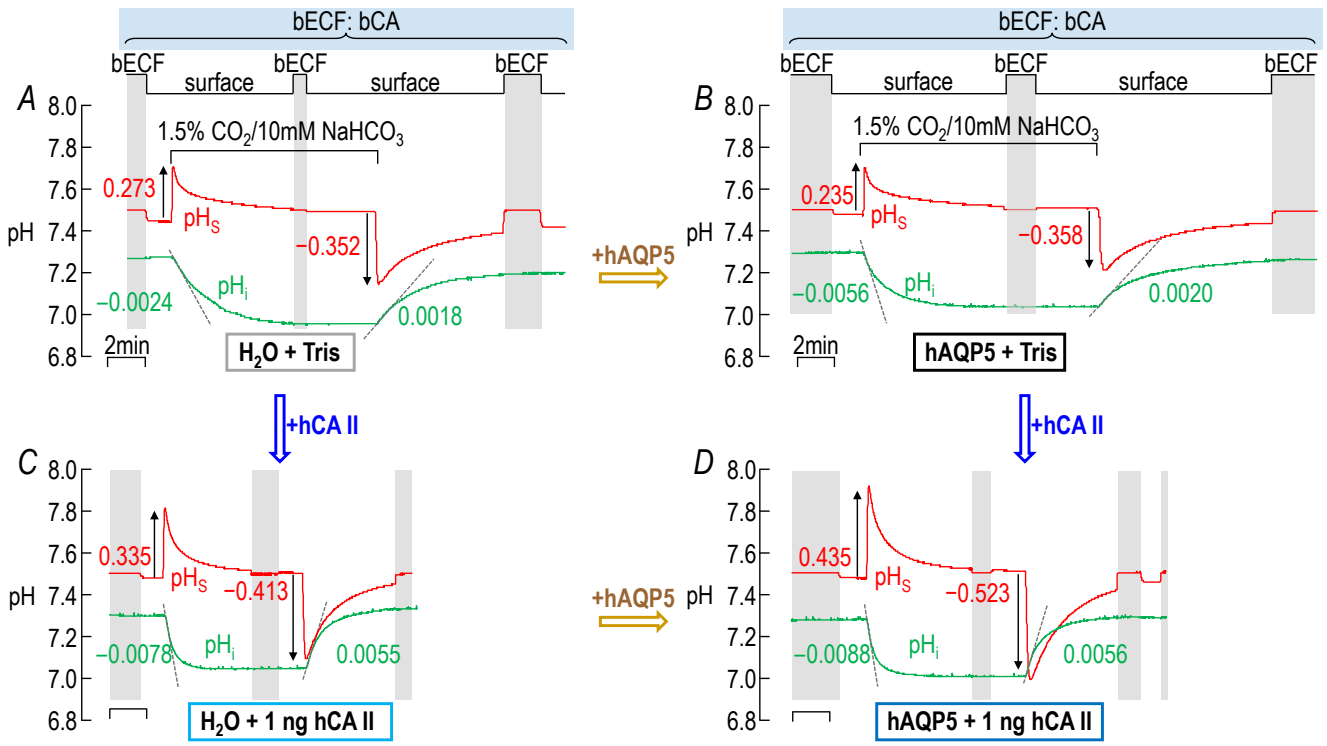

Figure 7 Representative pH_S and pH_i recordings: ±hAQP5, ±cytosolic hCA II, all in the presence of extracellular bCA (i.e., +bCA).

A, "H_2O + Tris". We injected this oocyte with H_2O (as a control for cRNA encoding hAQP5) on Day 1, and then with "Tris" (as a control for bCA II) on Day 4.

B, "hAQP5 + Tris". This oocyte, we injected on Day 1 with cRNA encoding hAQP5, and then on Day 4 with "Tris".

C, H_2O + 1 ng hCA II". Similar to panel *A* except that on Day 4, we injected the oocyte with hCA II enzyme dissolved in "Tris".

D, "hAQP5 + 1 ng hCA II". Similar to panel *B* except that on Day 4, we injected the oocyte with hCA II enzyme dissolved in "Tris".

The numbers in red are ΔpH_s and in green are $(dpH_i/dt)_{Max}$ for the oocytes presented here. The stair-step line at the top of *A* and *B* indicates the position of the pH_S electrode. The vertical shaded bars indicate times during which the pH_S electrode is in the bulk extracellular fluid (bECF)

for recalibration; at other times, the pHs electrode dimples the cell surface for actual pHs measurements. The colors of the rectangles that surround the panel labels (e.g., "H_2O + Tris") correspond to the colors of the bars in Figure 8 and later figures. ECF: bCA indicates that we obtained all measurements while exposing oocytes to solutions containing 0.1 mg/ml of bCA.

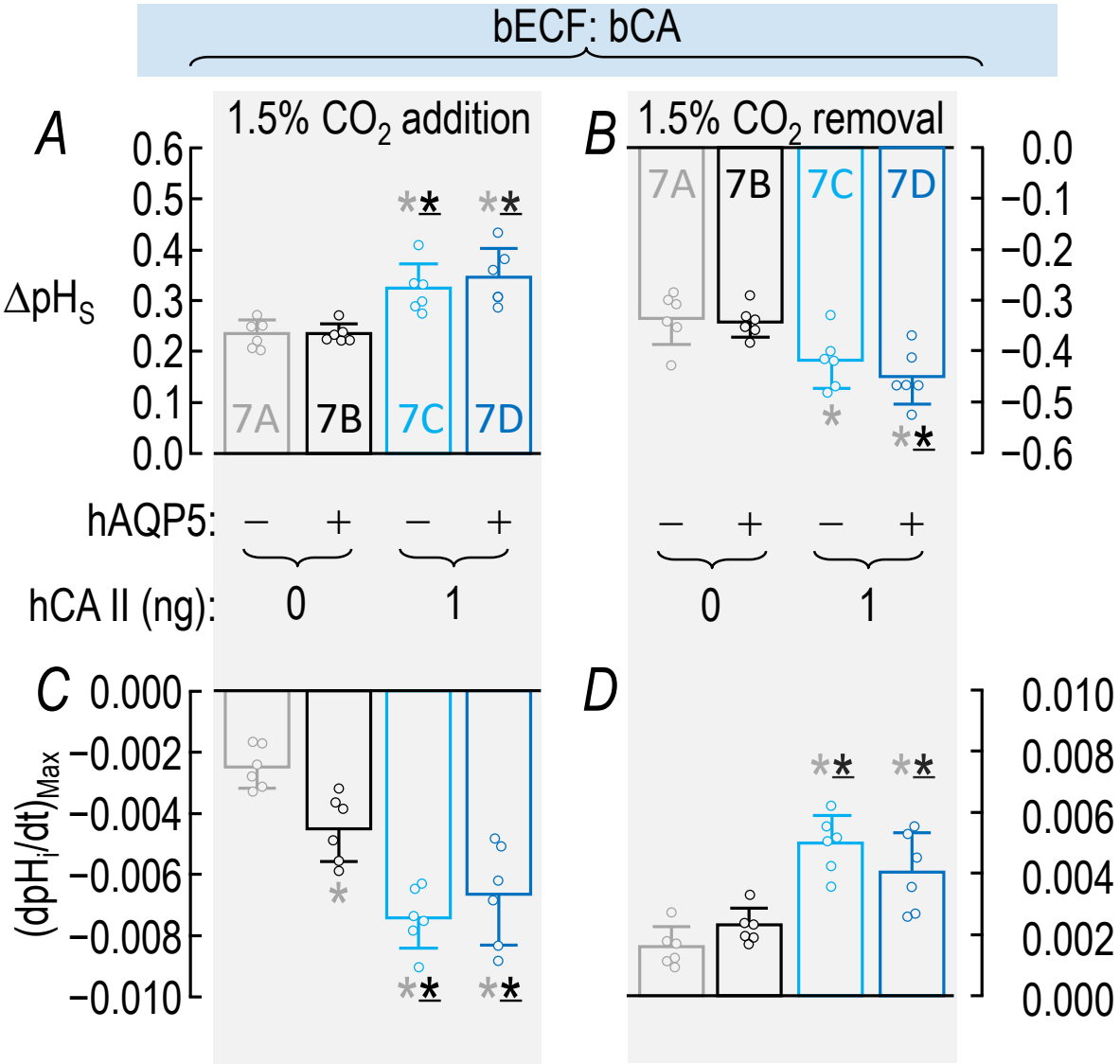

Figure 8 Summary of ΔpHs and (dpHi/dt)Max data from experiments like those in Figure 7: ±hAQP5, ± cytosolic hCA II, all in the presence of extracellular bCA (i.e., +bCA). This figure is analogous to Figure 3, which summarized ΔpHs and (dpHi/dt)Max data obtained from oocytes in the absence of bCA.

A, Summary of ΔpHs upon addition of 1.5% CO_2/10 mM HCO_3^-. We computed individual ΔpHs values as outlined in "Methods" > "Electrophysiological measurements" > "Calculation of ΔpHs".

B, Summary of ΔpHs upon removal of 1.5% CO_2/10 mM HCO_3^-.

C, Summary of $(dpH_i/dt)_{Max}$ upon addition of 1.5% CO_2/10 mM HCO_3^-. We computed individual ΔpH_S values as outlined in "Methods" > "Electrophysiological measurements" > "Calculation of "maximal" dpH_S/dt".

D, Summary of $(dpH_i/dt)_{Max}$ upon removal of 1.5% CO_2/10 mM HCO_3^-.

Data are presented as mean ± SD. "–" and lighter-colored bars indicate that we injected oocytes injected with H_2O; "+" and darker-colored bars, with cRNA encoding hAQP5 on Day 1. "0" and "1", indicate the amount of hCA II (ng) injected into oocytes on Day 4 Gray/black and light-/dark-blue pairs of bars indicate 4 groups of oocytes. These colors correspond to the colors of the rectangles that surround panel labels (e.g., "H_2O + Tris") in Figure 7. A star associated with a bar indicates a statistically significant difference when comparing the bar to another bar with the same color as the star. The star/bar combinations are meant to be read right to left; we indicate statistical significance between two bars only once, associating the star with the bar further to the right. Thus, the mean value represented by the dark-blue bar in panel *A* differs significantly from the means of the light-gray and black (underscored to indicate darker than gray) bars. Conversely, the gray bar, which has no stars, differs significantly from the means of the two bars with a gray star. The absence of a star indicates a lack of statistical significance. See Statistics Table 8 for *P*-values.

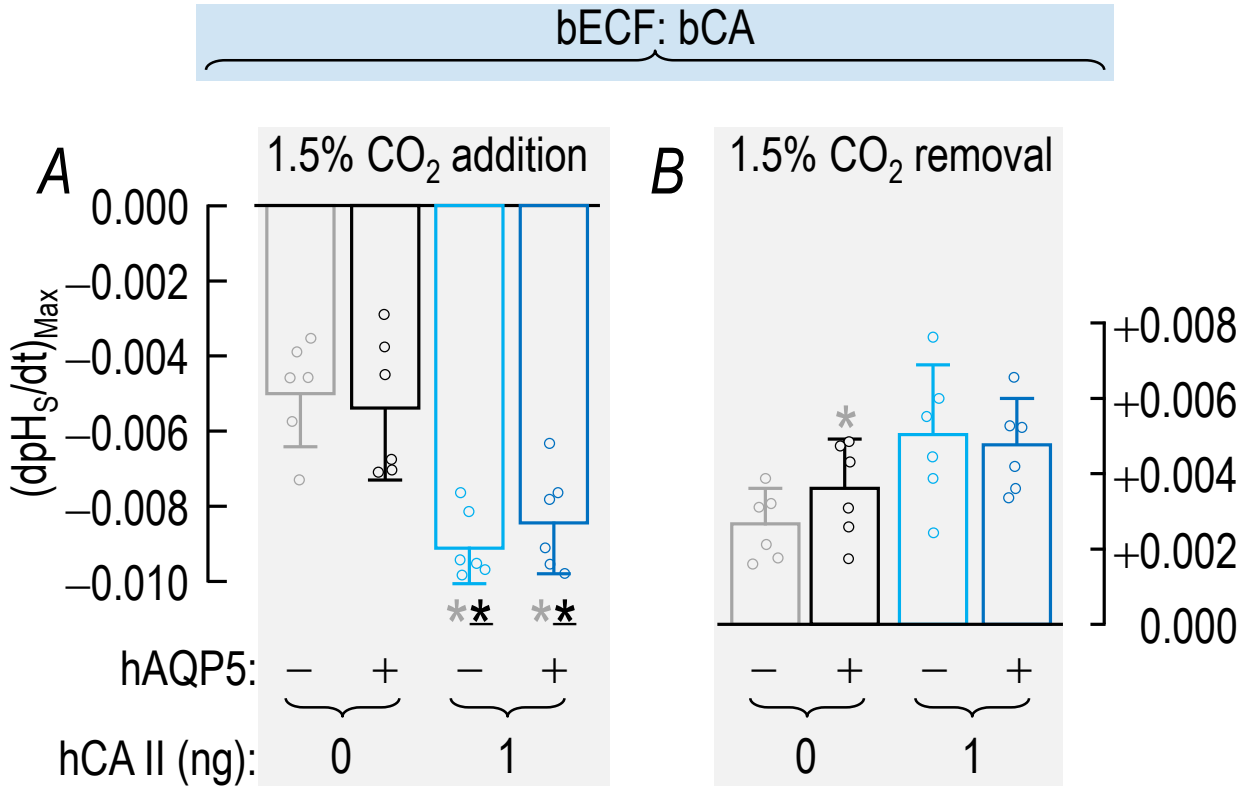

Figure 9 Summary of $(dpH_S/dt)_{Max}$ data from experiments like those in Figure 8: ±hAQP5, ±cytosolic hCA II, all in the presence of extracellular bCA (i.e., +bCA). This figure is analogous to Figure 5, which summarized $(dpH_S/dt)_{Max}$ data obtained from oocytes in the absence of bCA.

A, Summary of $(dpH_S/dt)_{Max}$ upon addition of 1.5% CO_2/10 mM HCO_3^-. We computed individual $(dpH_S/dt)_{Max}$ values as described in Figure 4.

B, Summary of $(dpH_S/dt)_{Max}$ upon removal of 1.5% CO_2/10 mM HCO_3^-.

Data are presented as mean ± SD. "–" and lighter-colored bars indicate that we injected oocytes with H_2O; "+" and darker-colored bars, with cRNA encoding hAQP5 on Day 1. "0" and "1" indicate the amount of hCA II (ng) injected into oocytes on Day 4. Gray/black and light-/dark-blue pairs of bars indicate 4 groups of oocytes. These colors correspond to the colors of the rectangles that surround panel labels (e.g., "H_2O + Tris") in Figure 7. A star associated with a bar indicates

a statistically significant difference when comparing the bar to another bar with the same color as the star. The star/bar combinations are meant to be read right to left; we indicate statistical significance between two bars only once, associating the star with the bar further to the right. Thus, the mean value represented by the dark blue bar in panel *A* differs significantly from the means of the gray and black (underscored to indicate darker than gray) bars. Conversely, the gray bar, which has no stars, differs significantly from the means of the two bars with a gray star. The absence of a star indicates a lack of statistical significance. See Statistics Table 9 for *P*-values.

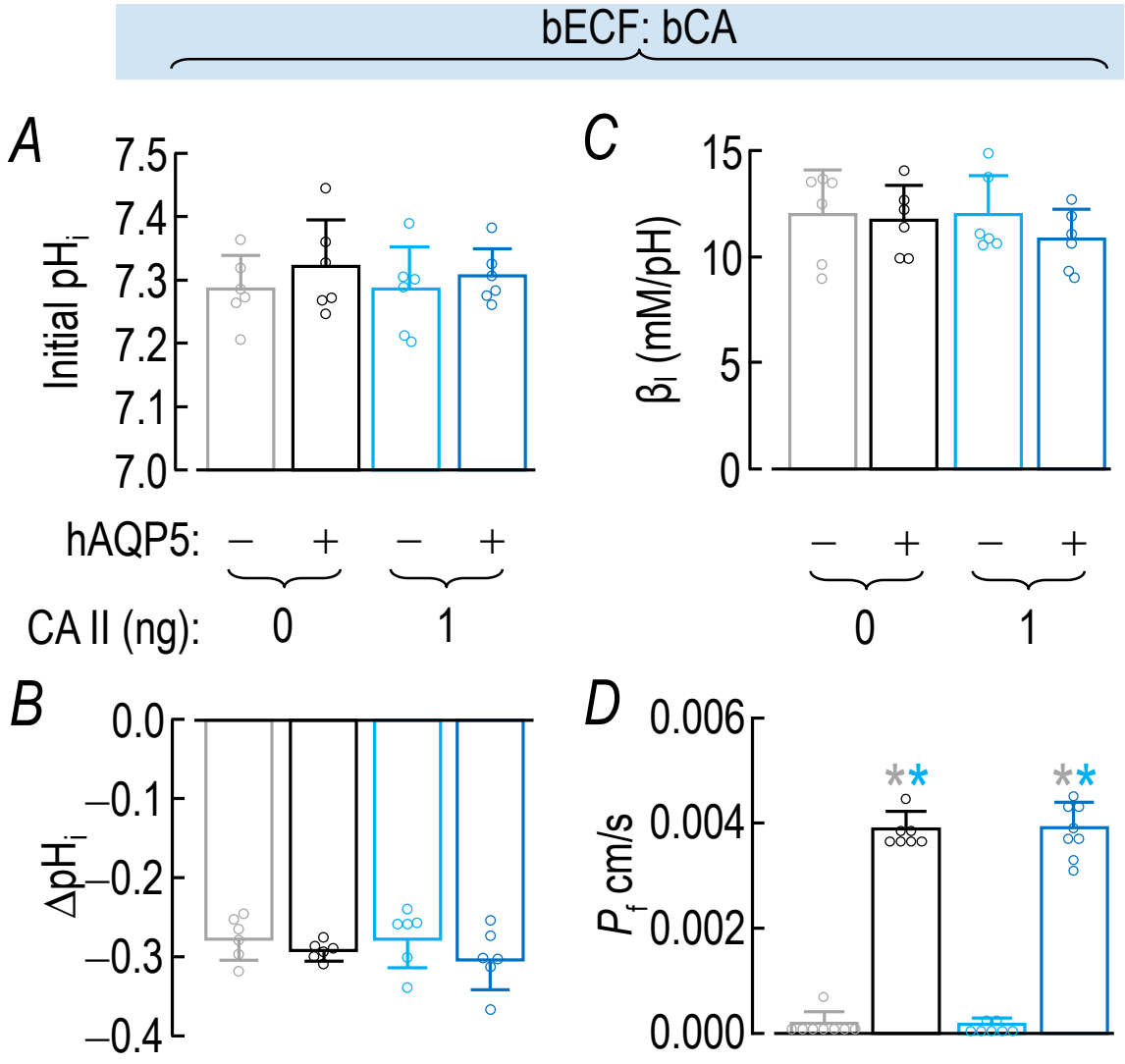

Figure 10 Summary of other oocyte parameters from experiments like those in Figure 7: ±hAQP5, ±cytosolic hCA II, all in the presence of extracellular bCA (i.e., +bCA). This figure is analogous to Figure 6, which summarized comparable data obtained from oocytes in the absence of bCA.

A, Summary of initial pH_i values. We computed individual initial pH_i, ΔpH_i (see panel *B*), and β_I (see panel *C*) values as outlined in "Methods" > "Electrophysiological measurements" > "Calculation of intrinsic intracellular buffering power".

B, Summary of ΔpH_i elicited by addition of 1.5% CO_2/10 mM HCO_3^-.

C, Summary of intrinsic buffering power (β_i).

D, Summary of P_f. We computed individual initial pH_i, ΔpH_i (see panel *B*), and β_I (see panel *C*) values as outlined in "Methods" > "Electrophysiological measurements" > "Measurement of P_f".

Data are presented as mean ± SD. "–" and lighter-colored bars indicate that we injected oocytes injected with H_2O; "+" and darker-colored bars, with cRNA encoding hAQP5 on Day 1. "0" and "1", indicate the amount of hCA II (ng) injected into oocytes on Day 4. Gray/black and light-/dark-blue pairs of bars indicate 8 groups of oocytes. These colors correspond to the colors of the rectangles that surround panel labels (e.g., "H_2O + Tris") in Figure 7. A star associated with a bar indicates a statistically significant difference when comparing the bar to another bar with the same color as the star. A star associated with a bar indicates statistical significance when compared to the bar with the same color as the star. The star/bar combinations are meant to be read right to left; we indicate statistical significance between two bars only once, associating the star with the bar further to the right. Thus, the mean value represented by the dark blue bar in panel *D* differs significantly from the means of the gray and light-blue bars. Conversely, the gray bar, which has no stars, differs significantly from the means of the black and dark-blue bars. The absence of a star indicates a lack of statistical significance. See Statistics Table 10 for *P*-values.

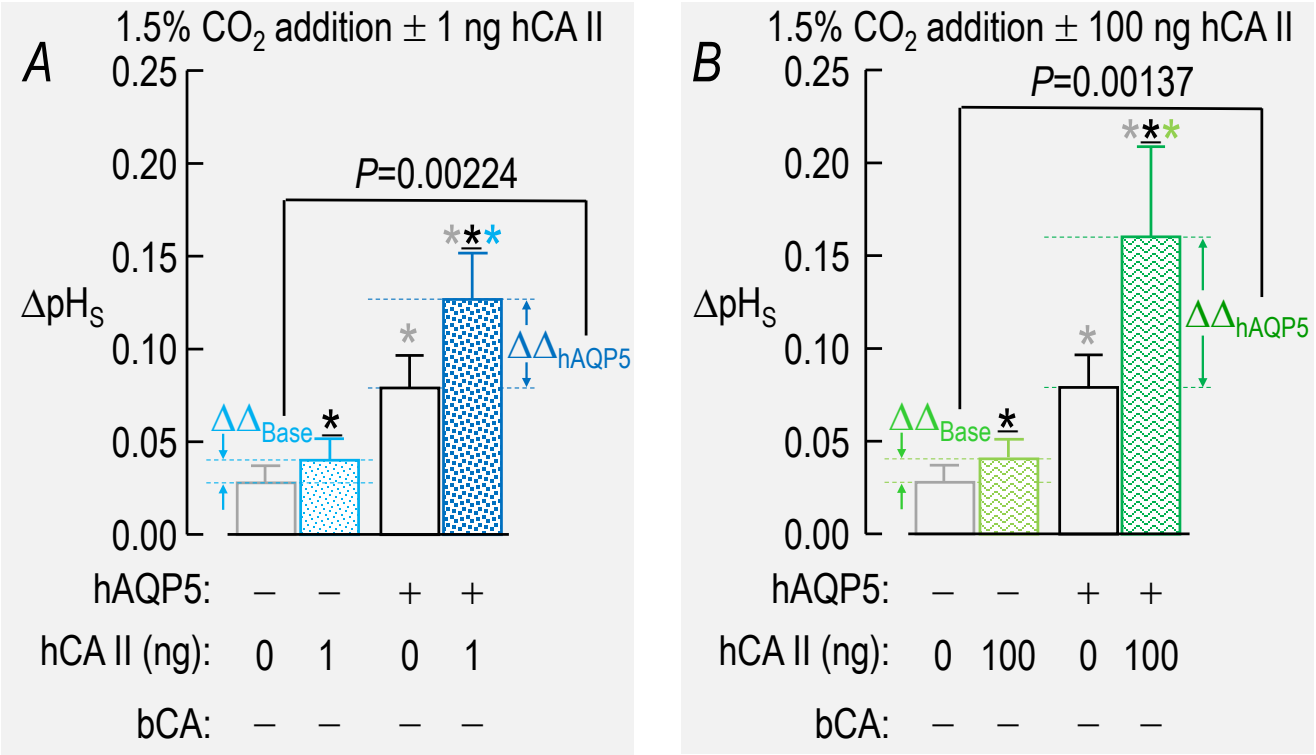

Figure 11 Effect of expressing hAQP5 on ΔΔpHs: comparison of selected ΔpHs bars extracted from Figure 3*A* (–bCA). Here we rearrange bars from Figure 3*A* to juxtapose two bars representing the same hAQP5 status ("–", absent; "+", heterologously expressed), the left bar in a pair representing the absence of hCA II, and the right bar representing the presence of injected hCA II.

A, ΔΔpHs determined with ±1 ng of injected hCA II, during addition of CO_2/HCO_3^-.

B, ΔΔpHs determined with ±100 ng of injected hCA II, during addition of CO_2/HCO_3^-.

For a pair of bars, the difference between ΔpHs values is ΔΔpHs. Thus, $\Delta\Delta_{Base}$ is difference between ΔpHs values under baseline conditions (i.e., no hAQP5), induced by the addition of the trans-side CA (i.e., CA II); $\Delta\Delta_{hAQP5}$ is the corresponding difference between ΔpHs values in AQP5-expressing oocytes. Comparing two pairs of bars, the difference between $\Delta\Delta_{hAQP5}$ and $\Delta\Delta_{Base}$ values is $\Delta\Delta\Delta pH_{S,hAQP5}$.

Although no bCA is present in any of these experiments, we include bCA status ("–", absent from bECF) to facilitate comparisons with Figure 12. The stars, which indicate statistical significance among the individual bars, have the same meanings as in Figure 3*A*. The *P*-values indicate statistical significance between the respective $\Delta\Delta_{Base}$ and $\Delta\Delta_{hAQP5}$ bar pairs, and reflect the statistical significance of the adding 1 ng hCA II (panel *A*) or 100 ng hCA II (Panel *B*), on the "trans" side of the membrane to the pH_S measurement. See Supplemental Table 11*A* and *B* for the statistics summary (including all *P*-values reported by the stars).

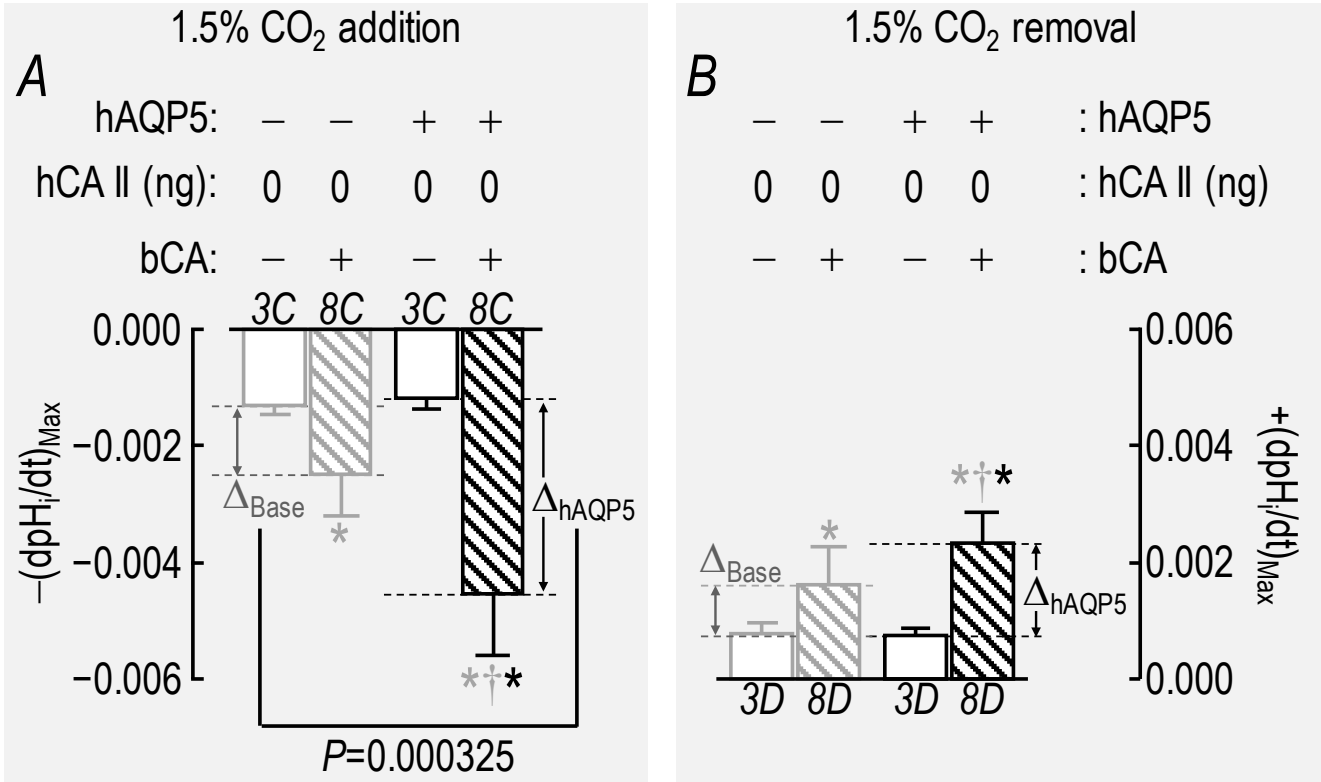

Figure 12 Effect of expressing hAQP5 on $\Delta(dpH_i/dt)_{Max}$: comparison of selected $(dpH_i/dt)_{Max}$ bars extracted from Figure 3*C* vs. Figure 8*C* and from Figure 3*D vs.* Figure 8*D.* Here we rearrange the gray and black bars from Figure 3*C* (–bCA) and the gray and black bars from Figure 8*C* (+bCA) to juxtapose two bars representing the same hAQP5 status ("–", absent; "+", heterologously expressed), the left bar in a pair representing the absence of bCA, and the right bar in a pair representing the presence of bCA in the bECF.

A, Summary of $\Delta(dpH_i/dt)_{Max}$ ±bCA, upon addition of CO_2/HCO_3^-.

B, Summary of $\Delta(dpH_i/dt)_{Max}$ ±bCA, upon removal of CO_2/HCO_3^-.

For a pair of bars, the difference between $(dpH_i/dt)_{Max}$ values is $\Delta(dpH_i/dt)_{Max}$. Thus, Δ_{Base} is difference between $(dpH_i/dt)_{Max}$ values under baseline conditions (i.e., no hAQP5), induced by the addition of the trans-side CA (i.e., bCA); Δ_{hAQP5} is the corresponding difference between $(dpH_i/dt)_{Max}$ values in hAQP5-expressing oocytes. Comparing two pairs of bars, the difference between Δ_{hAQP5} and Δ_{Base} values is $\Delta\Delta(dpH_i/dt)_{Max,hAQP5}$.

Although no hCA II is present in any of these experiments, we include hCA II status ("0 ng", not injected) to facilitate comparisons with Figure 11. The stars, indicate statistical significance among individual bars; the gray star associated with the gray- and black-hatched bars indicates a significant difference compared to the open gray bar (–hAQP5, –bCA); the black star associated with the black-hatched bars (+AQP5, +bCA) indicates a significant difference compared to the open black bar (+hAQP5, –bCA); the gray dagger symbol associated with the black-hatched bars (+AQP5, +bCA) indicates a significant difference compared to the open gray-hatched bar (–hAQP5, +bCA). See Supplemental Table 12*A* and *B* for the statistics summary (including the all *P*-values reported by the stars).

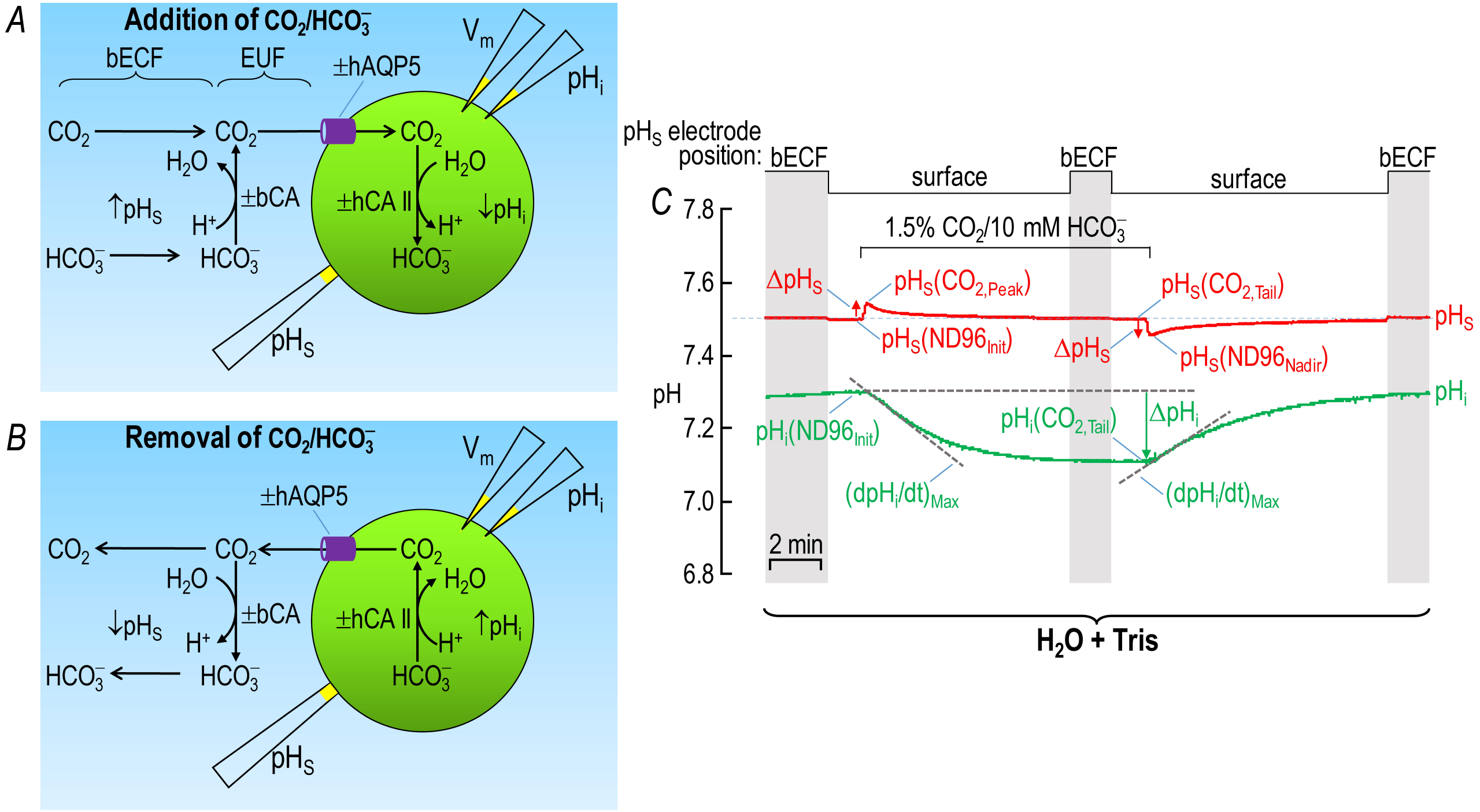
A
Addition of CO_2/HCO_3^-
bECF
EUF
±hAQP5
V_m
pH_i
CO_2
CO_2
CO_2
H_2O
H_2O
↑pH_S
±bCA
±hCA II
↓pH_i
H^+
H^+
HCO_3^-
HCO_3^-
HCO_3^-
pH_S
B
Removal of CO_2/HCO_3^-
V_m
±hAQP5
pH_i
CO_2
CO_2
CO_2
H_2O
H_2O
↓pH_S
±bCA
±hCA II
↑pH_i
H^+
H^+
HCO_3^-
HCO_3^-
HCO_3^-
pH_S
C
pH_S electrode position:
bECF
surface
bECF
surface
bECF
7.8
7.6
7.4
7.2
7.0
6.8
pH
1.5% CO_2/10 mM HCO_3^-
ΔpH_S
$pH_S(CO_{2,Peak})$
$pH_S(CO_{2,Tail})$
pH_S
$pH_S(ND96_{Init})$
ΔpH_S
$pH_S(ND96_{Nadir})$
pH_i
$pH_i(ND96_{Init})$
$pH_i(CO_{2,Tail})$
ΔpH_i
$(dpH_i/dt)_{Max}$
$(dpH_i/dt)_{Max}$
2 min
H_2O + Tris

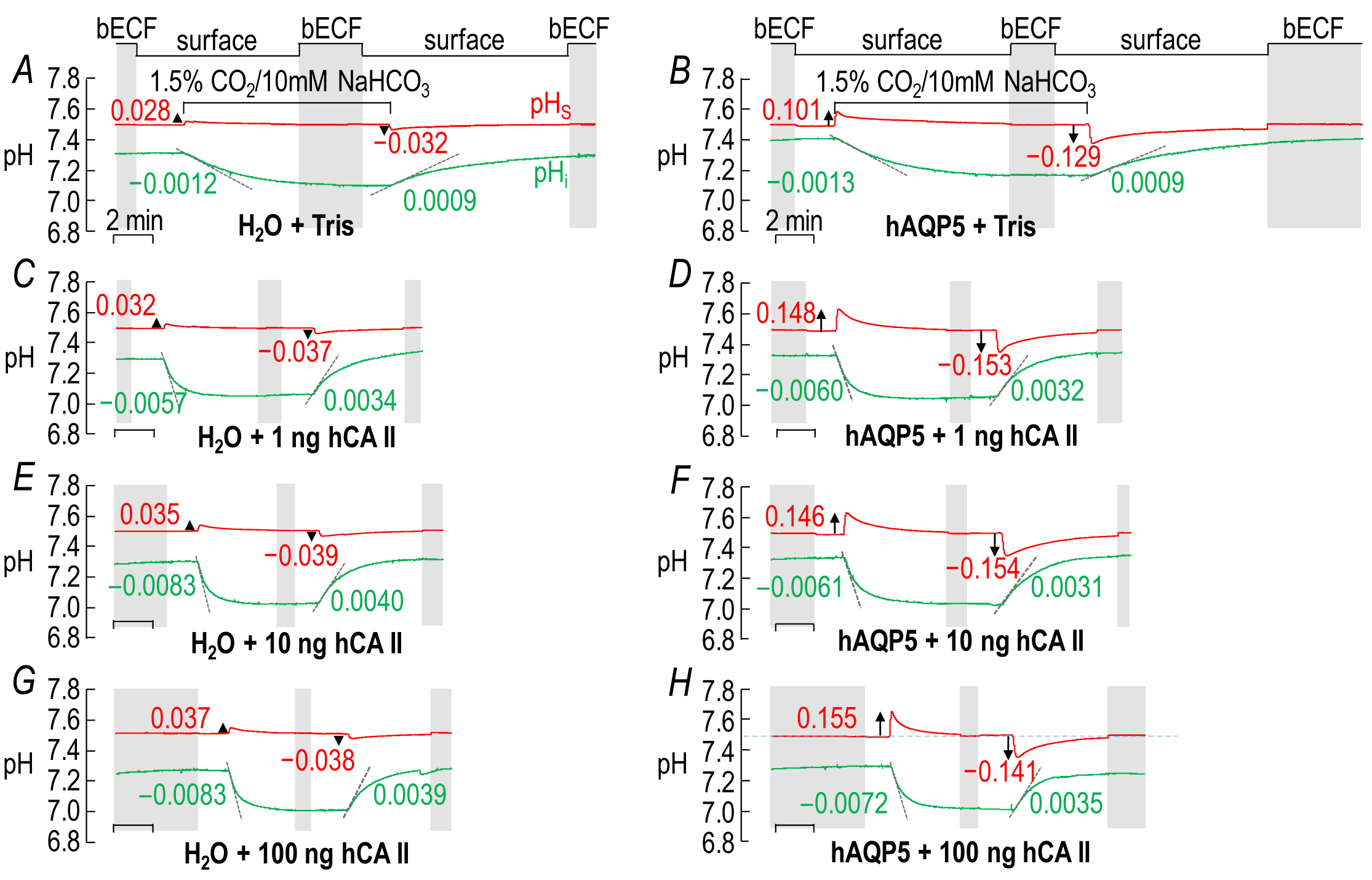
A
bECF
surface
bECF
surface
bECF
1.5% CO2/10mM NaHCO3
pH
7.8
7.6
7.4
7.2
7.0
6.8
0.028
−0.032
pHS
pHi
−0.0012
0.0009
2 min
H2O + Tris
B
bECF
surface
bECF
surface
bECF
1.5% CO2/10mM NaHCO3
0.101
−0.129
−0.0013
0.0009
2 min
hAQP5 + Tris
C
0.032
−0.037
−0.0057
0.0034
H2O + 1 ng hCA II
D
0.148
−0.153
−0.0060
0.0032
hAQP5 + 1 ng hCA II
E
0.035
−0.039
−0.0083
0.0040
H2O + 10 ng hCA II
F
0.146
−0.154
−0.0061
0.0031
hAQP5 + 10 ng hCA II
G
0.037
−0.038
−0.0083
0.0039
H2O + 100 ng hCA II
H
0.155
−0.141
−0.0072
0.0035
hAQP5 + 100 ng hCA II

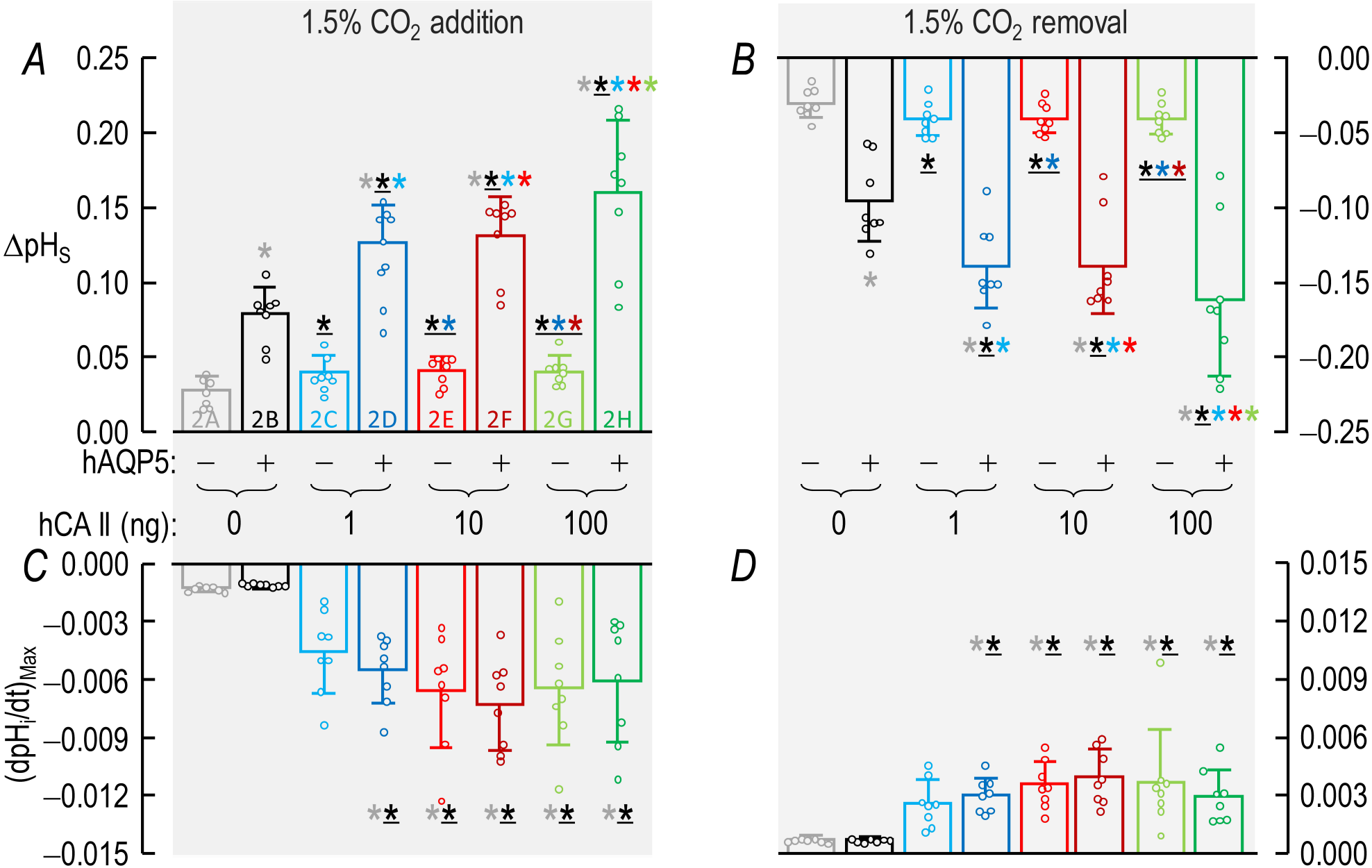
1.5% CO_2 addition
1.5% CO_2 removal
A
B
C
D
ΔpH_S
$(dpH_i/dt)_{Max}$
0.25
0.20
0.15
0.10
0.05
0.00
−0.05
−0.10
−0.15
−0.20
−0.25
0.000
−0.003
−0.006
−0.009
−0.012
−0.015
0.015
0.012
0.009
0.006
0.003
0.000
2A
2B
2C
2D
2E
2F
2G
2H
hAQP5: − + − + − + − +
hCA II (ng): 0 1 10 100

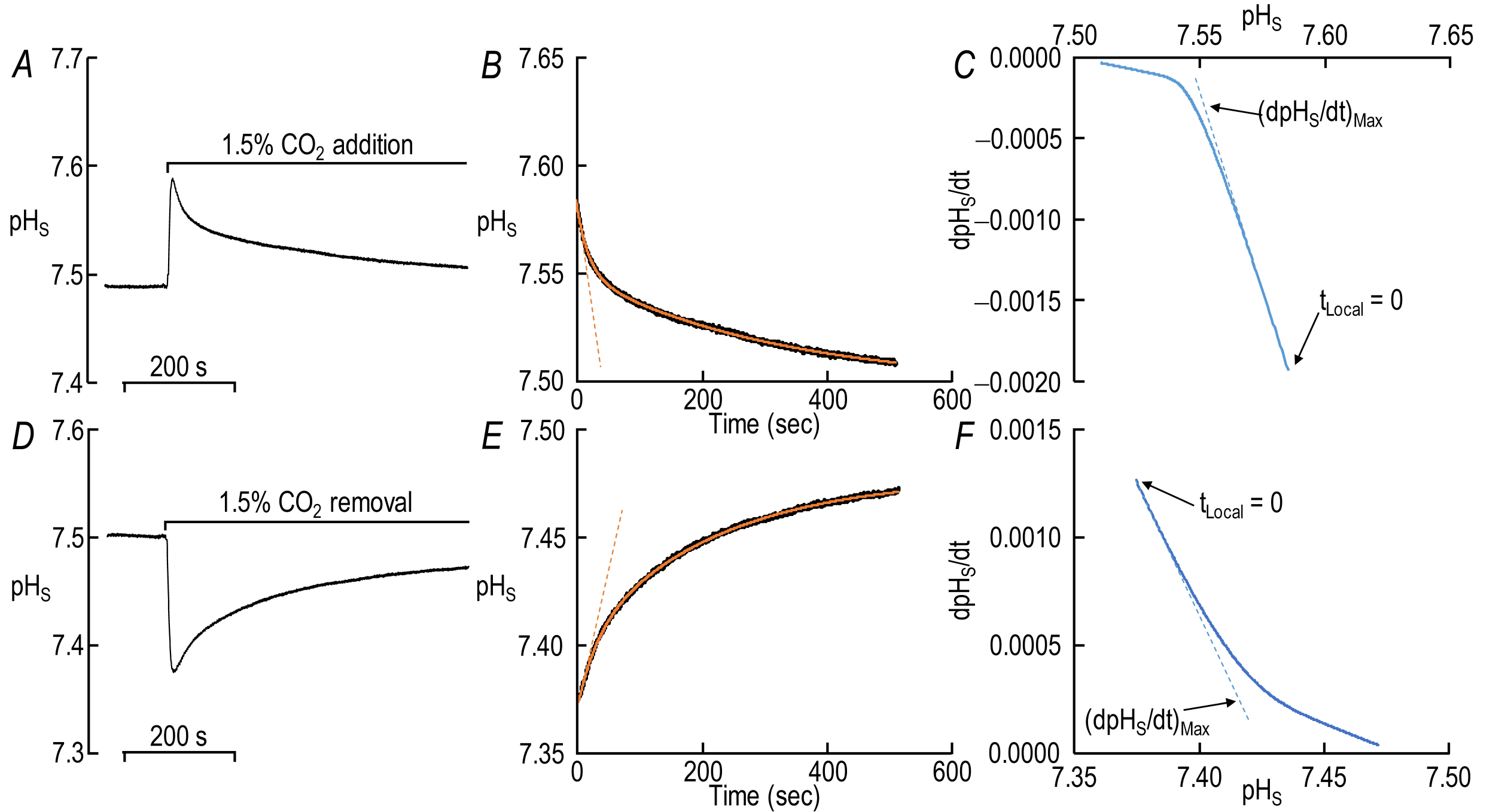
A
7.7
7.6
7.5
7.4
pHS
1.5% CO2 addition
200 s
B
7.65
7.60
7.55
7.50
pHS
0
200
400
600
Time (sec)
C
7.50
7.55
7.60
7.65
pHS
0.0000
–0.0005
–0.0010
–0.0015
–0.0020
dpHS/dt
(dpHS/dt)Max
tLocal = 0
D
7.6
7.5
7.4
7.3
pHS
1.5% CO2 removal
200 s
E
7.50
7.45
7.40
7.35
pHS
0
200
400
600
Time (sec)
F
0.0015
0.0010
0.0005
0.0000
dpHS/dt
tLocal = 0
(dpHS/dt)Max
7.35
7.40
7.45
7.50
pHS

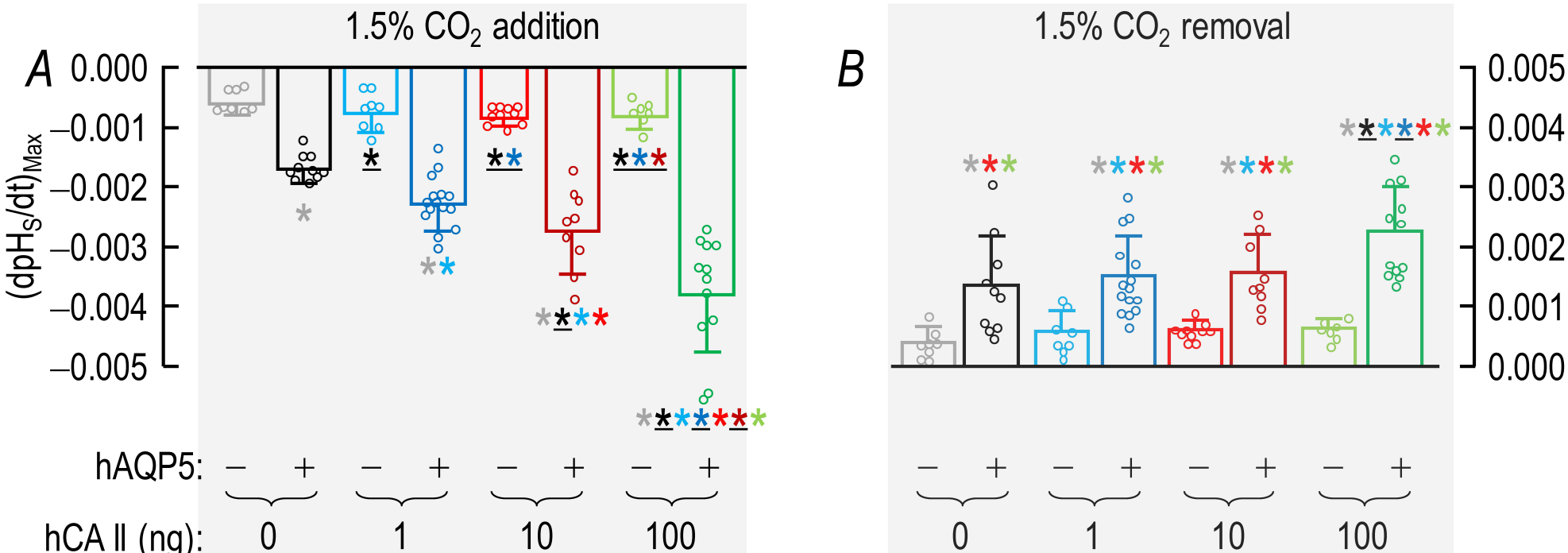
A
1.5% CO_2 addition
$(dpH_S/dt)_{Max}$
0.000
−0.001
−0.002
−0.003
−0.004
−0.005
hAQP5: − + − + − + − +
hCA II (ng): 0 1 10 100
B
1.5% CO_2 removal
0.005
0.004
0.003
0.002
0.001
0.000
− + − + − + − +
0 1 10 100

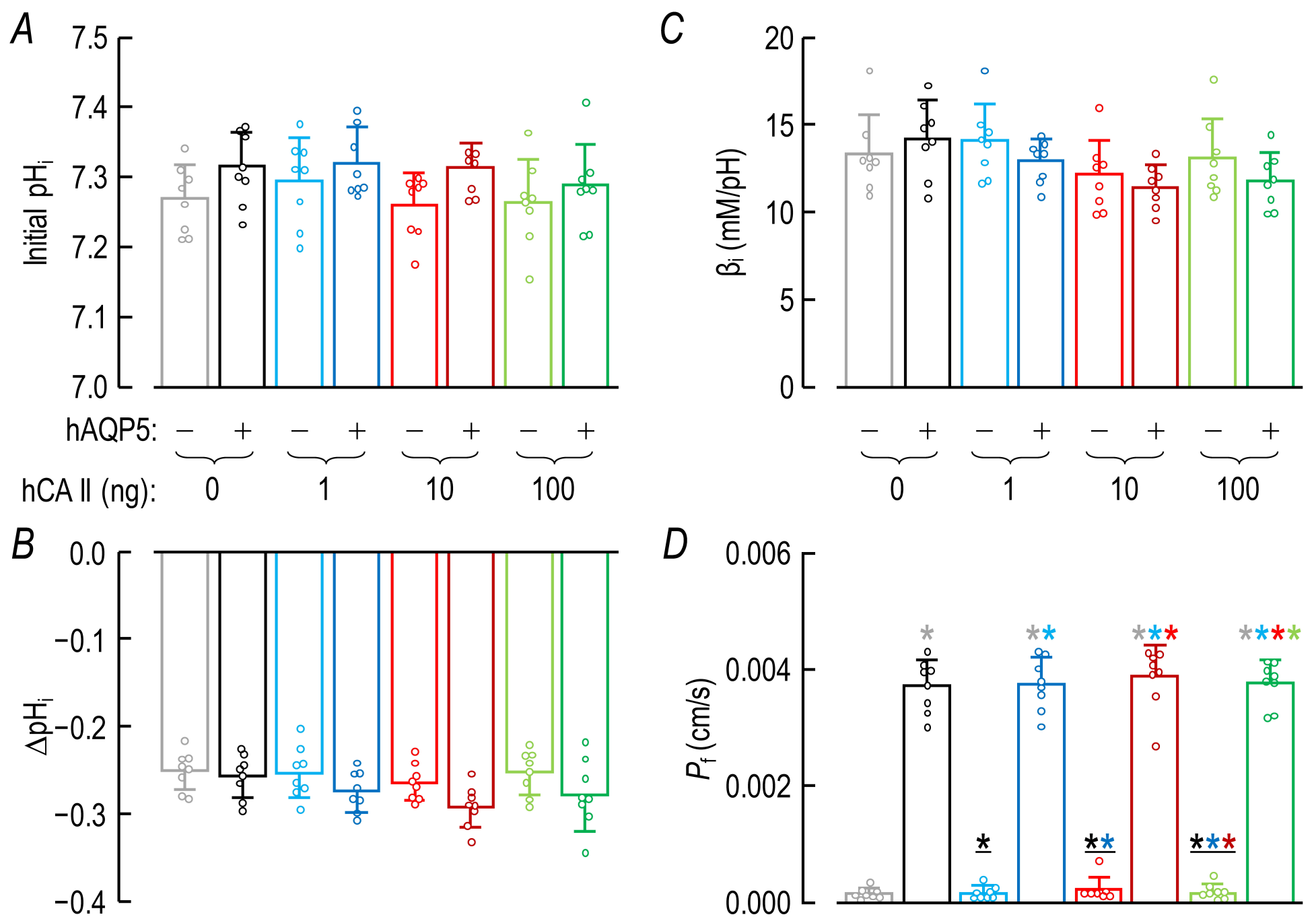
A
Initial pHi
7.5
7.4
7.3
7.2
7.1
7.0
hAQP5: − + − + − + − +
hCA II (ng): 0 1 10 100
B
ΔpHi
0.0
−0.1
−0.2
−0.3
−0.4
C
βi (mM/pH)
20
15
10
5
0
− + − + − + − +
0 1 10 100
D
Pf (cm/s)
0.006
0.004
0.002
0.000

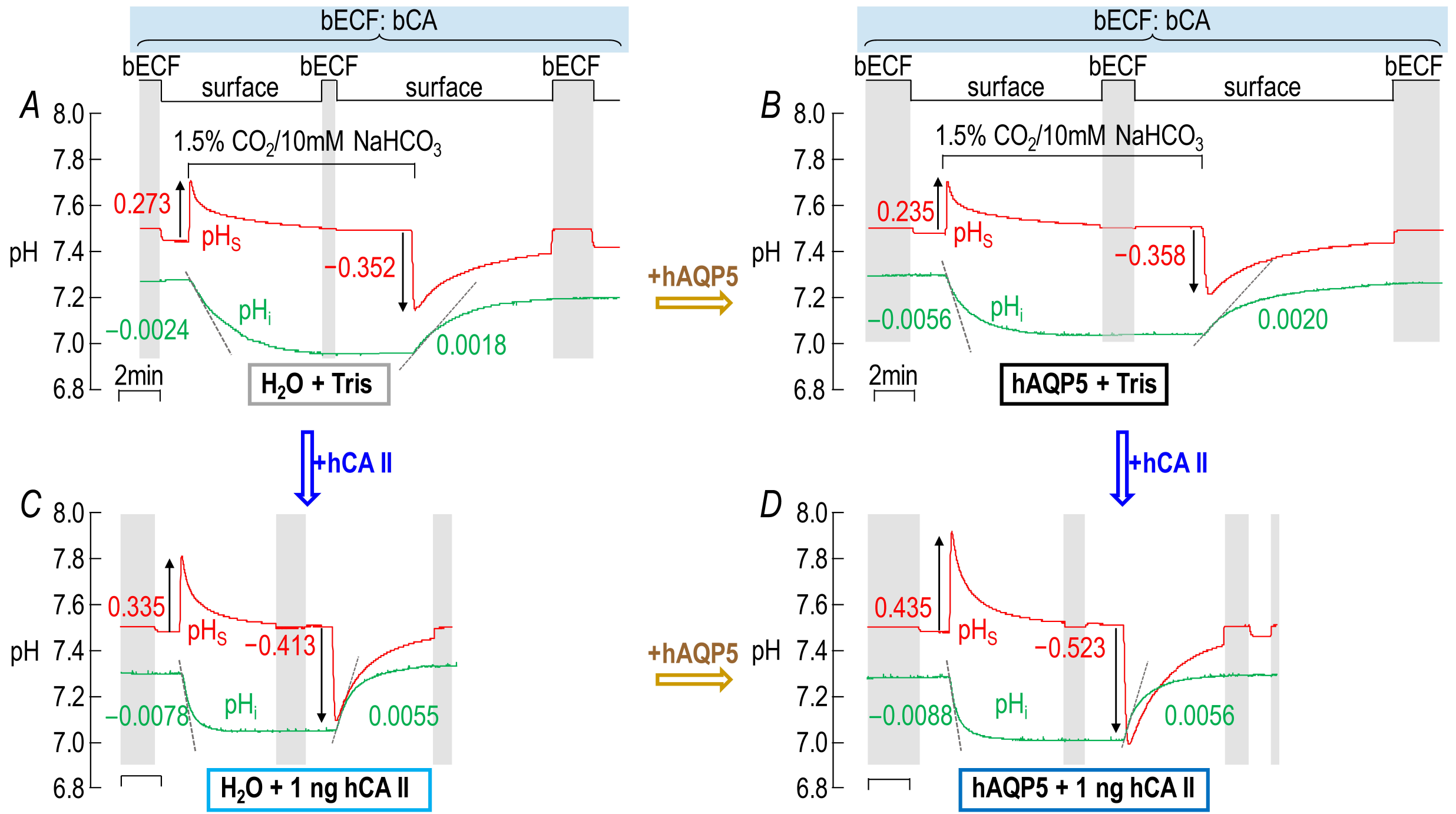
bECF: bCA
bECF
surface
bECF
surface
bECF
A
B
C
D
8.0
7.8
7.6
7.4
7.2
7.0
6.8
pH
1.5% CO2/10mM NaHCO3
0.273
pHS
−0.352
pHi
−0.0024
0.0018
2min
H2O + Tris
0.235
−0.358
−0.0056
0.0020
hAQP5 + Tris
+hAQP5
+hCA II
0.335
−0.413
−0.0078
0.0055
H2O + 1 ng hCA II
0.435
−0.523
−0.0088
0.0056
hAQP5 + 1 ng hCA II

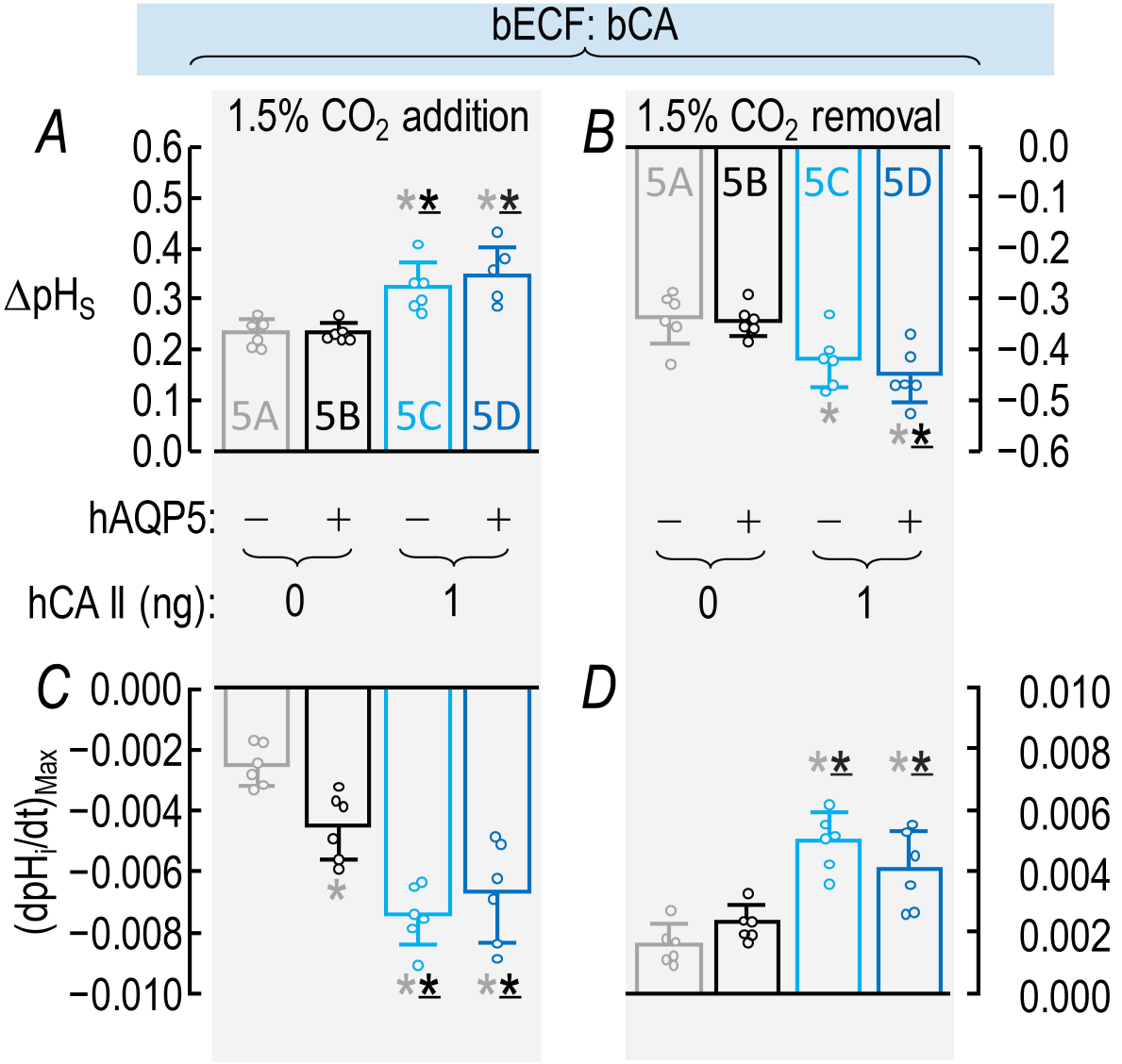
bECF: bCA
A
1.5% CO2 addition
B
1.5% CO2 removal
ΔpHS
0.6
0.5
0.4
0.3
0.2
0.1
0.0
0.0
−0.1
−0.2
−0.3
−0.4
−0.5
−0.6
5A
5B
5C
5D
hAQP5:
−
+
hCA II (ng):
0
1
C
D
(dpHi/dt)Max
0.000
−0.002
−0.004
−0.006
−0.008
−0.010
0.010
0.008
0.006
0.004
0.002
0.000

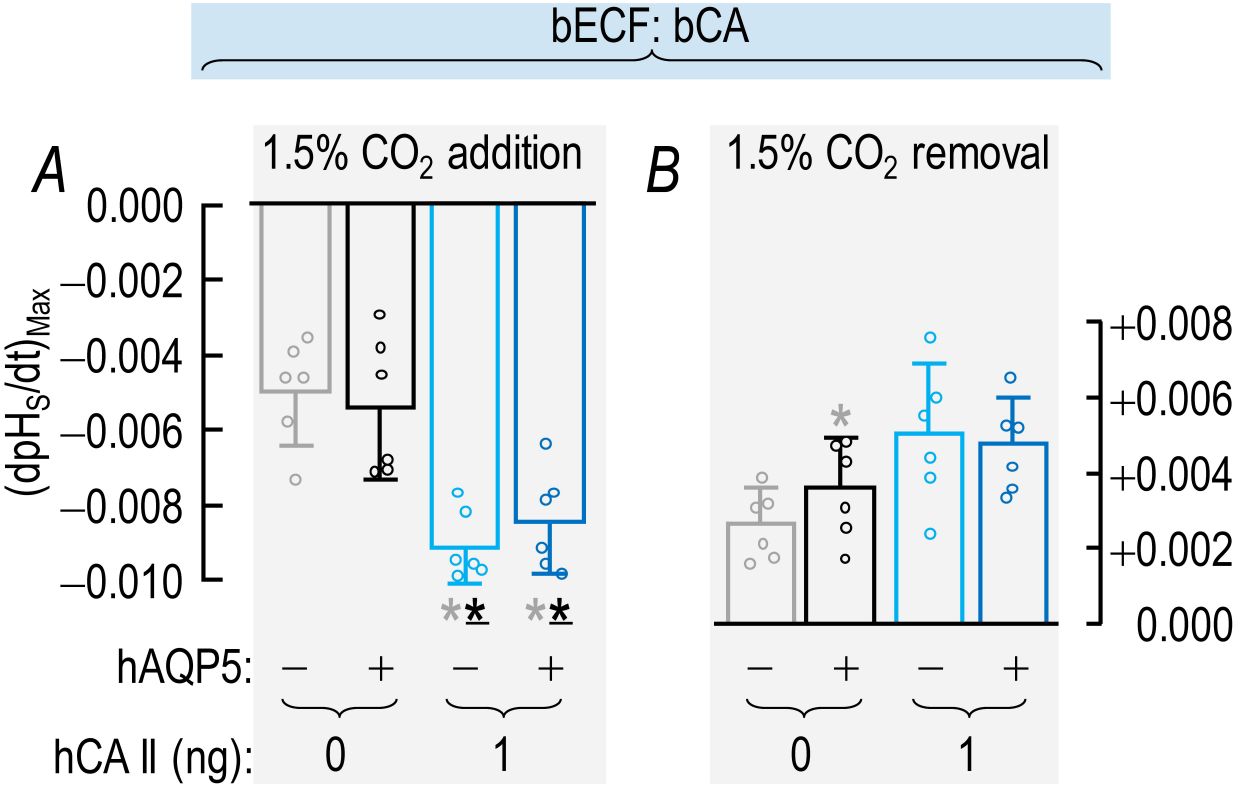
bECF: bCA
A
1.5% CO_2 addition
B
1.5% CO_2 removal
$(dpH_S/dt)_{Max}$
0.000
−0.002
−0.004
−0.006
−0.008
−0.010
+0.008
+0.006
+0.004
+0.002
0.000
*
*
*
*
*
hAQP5:
−
+
−
+
−
+
−
+
hCA II (ng):
0
1
0
1

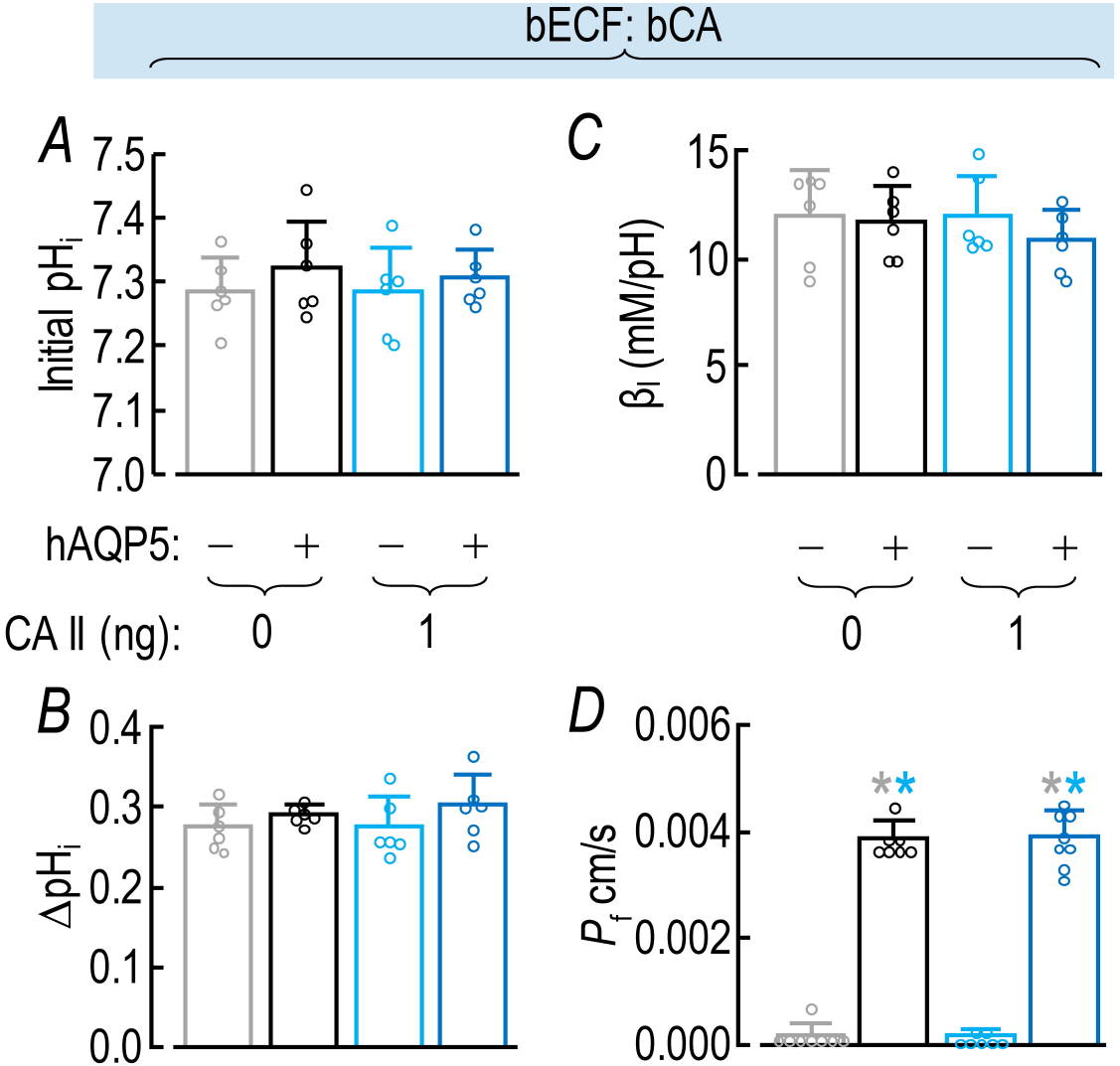
bECF: bCA
A
Initial pHi
7.5
7.4
7.3
7.2
7.1
7.0
C
βI (mM/pH)
15
10
5
0
hAQP5: − + − +
CA II (ng): 0 1
− + − +
0 1
B
ΔpHi
0.4
0.3
0.2
0.1
0.0
D
Pf cm/s
0.006
0.004
0.002
0.000
**
**

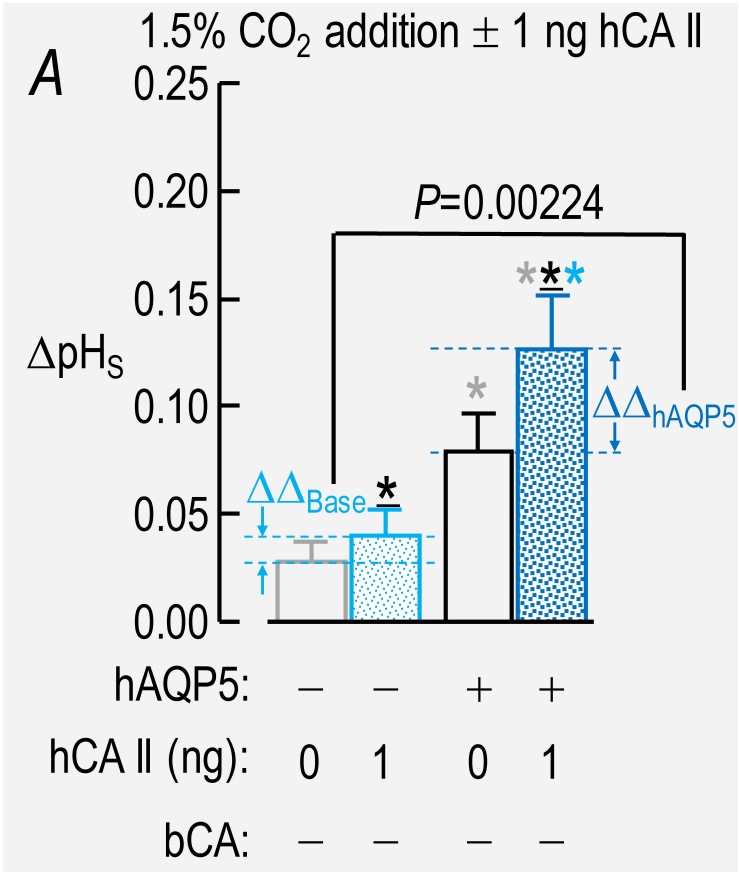
A
1.5% CO2 addition ± 1 ng hCA II
0.25
0.20
0.15
0.10
0.05
0.00
ΔpHS
P=0.00224
ΔΔBase
ΔΔhAQP5
hAQP5: – – + +
hCA II (ng): 0 1 0 1
bCA: – – – –

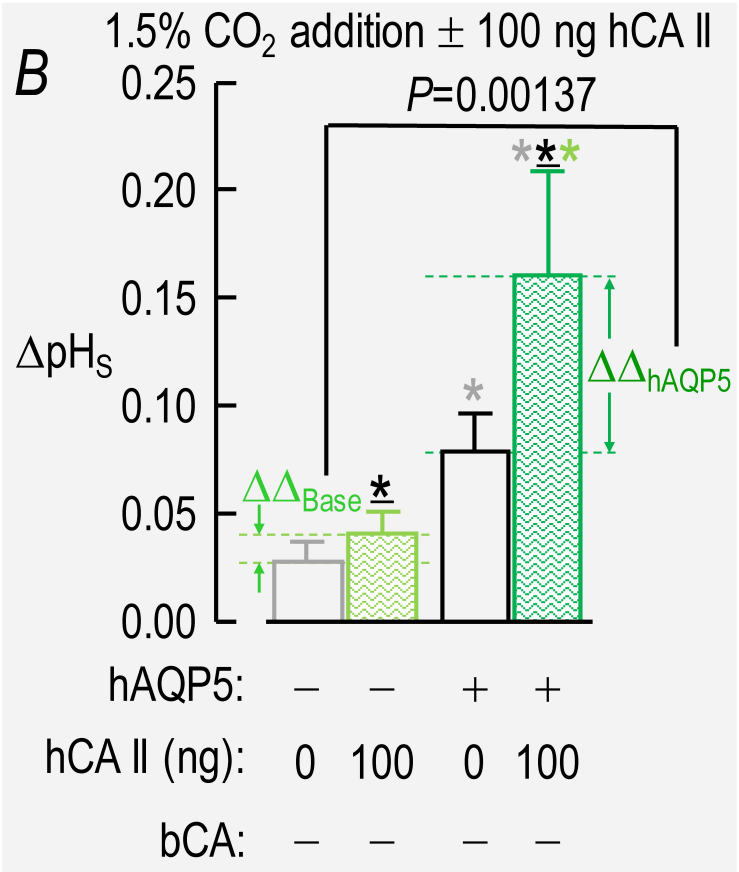
B
1.5% CO2 addition ± 100 ng hCA II
0.25
0.20
0.15
0.10
0.05
0.00
ΔpHS
P=0.00137
ΔΔBase
ΔΔhAQP5
hAQP5: – – + +
hCA II (ng): 0 100 0 100
bCA: – – – –

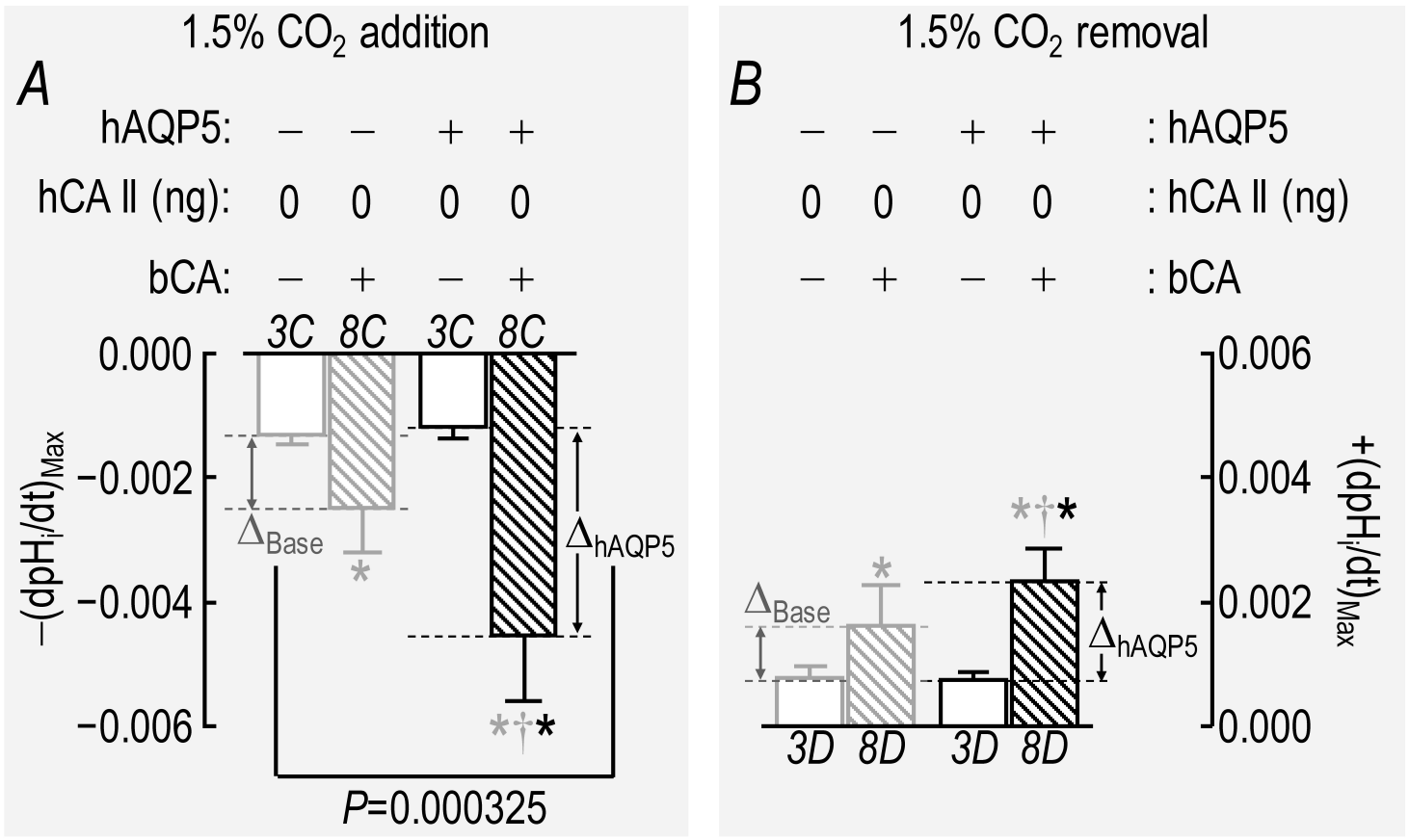
1.5% CO2 addition
A
hAQP5: − − + +
hCA II (ng): 0 0 0 0
bCA: − + − +
3C 8C 3C 8C
0.000
−0.002
−0.004
−0.006
−(dpHi/dt)Max
ΔBase
ΔhAQP5
*
†
P=0.000325
1.5% CO2 removal
B
− − + + : hAQP5
0 0 0 0 : hCA II (ng)
− + − + : bCA
0.006
0.004
0.002
0.000
+(dpHi/dt)Max
ΔBase
ΔhAQP5
*
†
3D 8D 3D 8D